Chemical Consequences of Long-Range Orbital Interactions in Perhydronaphthalene-1,4-diol Monosulfonate Esters

Romano V. A. Orrū

Promotor: dr. Ae. de Groot, hoogleraar in de bio-organische chemie
Co-promotor: dr. J. B. P. A. Wijnberg, universitair hoofddocent organische chemie

Romano V. A. Orrù

Chemical Consequences of Long-Range Orbital Interactions in Perhydronaphthalene-1,4-diol Monosulfonate Esters

Proefschrift
ter verkrijging van de graad van doctor
in de landbouw- en milieuwetenschappen
op gezag van de rector magnificus,
dr. C. M. Karssen
in het openbaar te verdedigen
op maandag 17 oktober 1994
des namiddags te vier uur in de aula
van de Landbouwuniversiteit te Wageningen

CIP-gegevens Koninklijke Bibliotheek, Den Haag

ISBN 90-5485-299-2

Het onderzoek dat beschreven staat in dit proefschrift werd uitgevoerd onder auspiciën van de stichting Scheikundig Onderzoek Nederland (SON) met financiële steun van de Nederlandse organisatie voor Wetenschappelijk onderzoek (NWO).

Stellingen

1. De mate van mechanische breuk die optreedt in Glutenine MacroPolymeer (GMP) na sonificeren wordt door Singh et al. sterk gebagatelliseerd.

Singh, N. K.; Donovan, G. R.; Batey, I. L.; MaCritchie, F. *Cereal Chemistry* 1990, 67, 150–161.

2. De conclusie van Kim et al. dat 2-hydroxypropylering van aardappelzetmeelkorrels voornamelijk in de centrale regio van de bolletjes plaatsvindt, wordt niet door de experimenten van de auteurs aangetoond.

Kim, H. R.; Hermansson, A. M.; Eriksson, C. E. *Starch/Stärke* 1992, 44, 111–116.

3. Bij het verklaren van chemische verschijnselen met behulp van delocalisatie van σ-electronen over meerdere enkelvoudige bindingen, wordt regelmatig ten onrechte voorbij gegaan aan de "*trans* rule".

Bijv. zie : Adcock, W.; Trout, N. A. *Journal of Organic Chemistry* 1991, 56, 3229–3238 en Lambert, J. B.; Salvador, L. A.; Stern, C. L. *Journal of Organic Chemistry* 1993, 58, 5428–5433.
Zie ook: dit proefschrift

4. De door Appendino et al. geïsoleerde verbindingen 5 en 6 hebben waarschijnlijk een omgelegd taxaanskelet en niet het door de auteurs vermelde gewone taxaanskelet.

Appendino, G.; Tagliapietra, S.; Ozen, H. S.; Garibaldi, P. Gabetta, B.; Bombardelli, E. *Journal of Natural Products* 1993, 56, 514–520.

5. Dat het chloorperoxidase uit C. fumago en het broomperoxidase uit C. officinalis regioselectief zijn in de vorming van halohydrines uit (E)-α-methylcinnamyl alcohol wordt door Coughlin et al. niet bewezen.

Coughlin, P.; Roberts, S.; Rush, C.; Willets, A. *Biotechnology Letters* 1993, 15, 907–912.

6. Burgeot et al. gaan er ten onrechte van uit dat meting van de EROD-activiteit in de lever van rode poon voldoende is om vervuiling van de zee met PCB's en PAK's aan te tonen.

Burgeot, T.; Bocquéné, G.; Truquet, P.; Le Dean, L.; Galgani, F. *The Science of the Total Environment* 1994, 142, 213–220.

7. Het feit dat het normaliter somber gestemde CPB ineens positief bericht over de plannen van het nieuwe kabinet geeft te denken over de (on)partijdigheid van dit instituut.

8. In grote delen van Afrika is niet overbevolking maar juist "onder"-bevolking de oorzaak van veel armoede en honger.

9. Het gedwongen overstappen op de consumptie van kip zou een belangrijke bijdrage kunnen leveren aan het oplossen van het voedsel probleem in de wereld.

10. Uitgebreid organoleptisch onderzoek kan de consumptie van haantjes sterk stimuleren.

Stellingen behorende bij het proefschrift: "The Chemical Consequences of Long-Range Orbital Interactions in Perhydronaphthalene-1,4-diol Monosulfonate Esters".

Te verdedigen op 17 oktober 1994 door Romano V. A. Orru.

(Bedankt Roel Orsel, Ron Kesselmans, Wiet Jenniskens, Maurice Franssen, Hedwig Sleiderink en Peter Knippels)

Voorwoord

Voordat u vol overgave en met veel interesse dit proefschrift gaat doorbladeren moet u weten dat de auteur niet de enige geweest is die aan de totstandkoming ervan gewerkt heeft. Ik overdrijf niet door te zeggen dat minstens de hele vakgroep Organische Chemie in Wageningen heeft meegewerkt, van de glasblazers tot de schoonmaaksters. U zult begrijpen dat deze bladzijde niet groot genoeg is om al deze mensen persoonlijk te noemen. Enkelen wil ik echter niet onvermeld laten.

Als eerste wil ik Hannie bedanken, zij heeft mij behoed voor vele enge ziekten door regelmatig mijn koffiemok schoon te maken en het tafelkleedje te wassen.

Verder, Hugo, Kees en Rien bedankt voor de snelle en nauwkeurige massa- en element analyses van mijn stofjes. Bep, jou wil ik bedanken voor de geduldige en bekwame hulp bij het bedienen van de NMR apparatuur. Voor de vele handige tips bij de GC en HPLC analyses ben ik Pim zeer erkentelijk.

Aede, jij bood mij vier jaar geleden de mogelijkheid om aan dit promotie-onderzoek te beginnen. Je was zelfs bereid om te wachten met de aanstelling, omdat ik nog per se een stage wilde doen. De vrijheid die je me vervolgens gegeven hebt om dit onderzoek uit te voeren was van groot belang. Jouw vertrouwen in mij heb ik dan ook zeer gewaardeerd.

De hulp van jou, Sies, bij al het rekenwerk was onontbeerlijk. In een tropisch verhitte kamer die blauw stond van de sigaretterook, trachtte jij onder het genot van thee-met-vijf-klontjes-suiker mij de beginselen van de "compu-chemie" bij te brengen. De vele middagen die ik daar heb doorgebracht zullen me nog lang bijblijven. Speciaal wil ik je bedanken voor de hulp en begeleiding bij het totstandkomen van hoofdstuk 5.

Er zaten nog heel wat foutjes en onvolmaaktheden in het manuscript. Wiet, ik wil je bedanken voor de nauwkeurige wijze waarop je ze allemaal opgespoord hebt. Het zal niet makkelijk geweest zijn in de afgelopen lange hete zomer.

Hans, zonder jouw bekwame en intensieve begeleiding was het me waarschijnlijk niet gelukt. Ik heb veel van je geleerd. Over chemie in de praktijk en in theorie. Over het schrijven van een wetenschappelijke tekst. En over hoe moeilijk het is voor jou als rasechte Amsterdammer te moeten werken met boerse Wageningers. Hans, het was mij een waar genoegen bij jouw werkgroep te mogen horen.

Minstens 700 keer heb ik een "kolom" gedaan in de afgelopen jaren. Stilzitten achter een druppelend kraantje was niet mijn grootste hobby. Maar gelukkig waren daar mijn zaalgenoten Ron en Wiet. Al snel werd duidelijk dat je tijdens het "kolommen" genoeg tijd over hebt om allerlei streken uit te halen met elkaar, de buren en natuurlijk het liefst met argeloze voorbijgangers. Ron en Wiet jullie waren (en zijn) onverbeterlijk.
Ook wil ik Henk, Harrie en Anja niet vergeten, bij wie ik vaak ging "buurten" en die aangename congresmaatjes waren. Met Henk vormde ik samen de borrelcommissie en in verband hiermee bedank ik de rest van de vakgroep voor het feit dat ze toch steeds weer bereid waren om naar onze onzinnige borrels te komen (Bart bedankt voor de volledige medewerking bij sommige van deze borrels).
Marijke, bedankt voor het geduld en de vriendschap. Zonder jou zou het allemaal een stuk moeilijker geweest zijn.
Als laatste wil ik André bedanken. Voor de dropjes.

Romano

Augustus 1994

Aan mijn vader en moeder

Contents

Chapter 1

Chemical Consequences of Through-Bond and Through-Space Orbital Interactions

1.1 Introduction

About 25 years ago Hoffmann, Imamura, and Hehre[1] have delineated two distinct mechanisms to designate long-range intramolecular interactions between non-conjugatively connected functional groups: orbital interactions through-bond (TBI) and orbital interactions through-space (TSI).[1,2]
The best description of through-bond interaction is to take into account that σ-electrons are delocalized, just as π-electrons. However, the energy effects concomitant with σ-conjugation are considerably smaller than those for the much more familiar π-conjugation. The localized bond model is therefore very successful in explaining the vast majority of phenomena in the chemistry of saturated organic compounds. However, in certain cases it can be illuminating to consider the concept of delocalization of σ-electrons to understand some of the underlying principles of these phenomena, as will become clear from this thesis.
The TBI mechanism involves an interaction in which the orbitals of the substituents interact with each other *via* their mutual coupling with the σ- and σ*-orbitals of the intervening saturated bridge.[3-13] Thus, the σ-bonds are essential and participate in this kind of electronic interaction. They simply cannot be regarded as an inert framework. TSI between two functional groups is the result of the direct spatial overlap of the orbitals associated with the two functional groups. It is obvious that the geometry of the molecule determines directly the extent of TSI. For TSI the σ-bonds can be considered as the "backbone" of the molecule which holds the molecule together and merely allows the necessary close approach for the functional groups needed for the interaction.

Based on model calculations Hoffmann *et al.*[1,2] found some general "rules" for the interaction between two orbitals separated by n σ-bonds.
The strength of TSI should be attenuated fairly strongly with the increasing number of orbital separations n, and is relatively unimportant for direct interorbital distances greater than 3Å.[4,14]

The magnitude of TBI decreases with increasing n, but to a much lesser extent than TSI does. TBI should be significant even for n=8, corresponding to an interorbital distance of about 10Å.[8,15] The extent of TBI depends both on the degree of coupling (effectiveness of overlap) between the orbitals of each interacting functional group with those of the adjoining σ-bonds, and on the strength of the coupling of the σ-bridge orbitals with each other[16,17]. So for a given value of n, TBI depends on the conformation of the σ-relay and on the orientation of the interacting orbitals of the substituents with respect to this σ-relay. It should be noted that these factors are fully analogous to the geometrical requirements that determine the extent of π-conjugation. However, due to the fundamental differences between the symmetries of s and p orbitals, visualization of the geometrical factors influencing the effectiveness of σ-conjugation is far less straightforward. Generally, a *trans* orientation of these orbitals with the vicinal σ-bonds, together with an "all *trans*" or "W" arrangement of the σ-bonds between the donor- and acceptor group, is optimal for TBI. For example, the interaction of two lone-pairs over four σ-bonds *via* TBI should diminish along the series I>II>III, since II and III have one and two *cis*oid (or gauche) arrangements of σ-bonds, respectively (Figure 1.1). This is generally referred to as the "*trans* rule".[4]

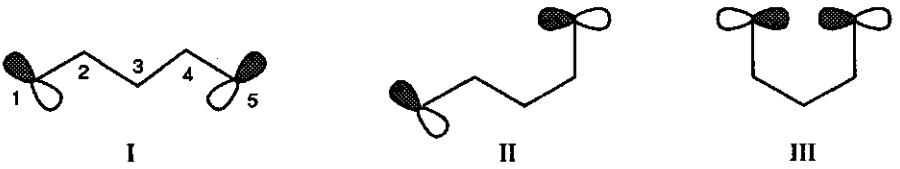

Figure 1.1: I = "all trans" geometry; II = "sickle" geometry; III = "U" geometry.

Even if the direct coupling between the orbitals of the functional groups appears to be through-space (as in Figure 1, III), the *relative* signs of the interacting orbitals may -*via* TBI- be critically dependent on the parity (odd or even) of n. TBI and TSI are "in phase" for an even number of intervening σ-bonds (n) and reinforce each other.[7] For an odd number of n they are "out of phase" and oppose each other. This through-bond correlation of the signs of the functional group orbitals is called the "parity rule".[4] In a way this can be compared with the alternating bond effect, which is so familiar in the organic chemistry of aromatic and olefinic compounds. In σ-systems, it can be shown that the withdrawal of electron density from a certain bond has most of its mesomeric effect not on the neigboring bond(s) but one bond further on.

Since 1968 an overwhelming amount of experimental[18-24] and theoretical[25-29] evidence for the occurrence of TBI and TSI between two functional groups in organic compounds is produced. Most experimental studies have focussed on the spectroscopic manifestations of TBI and TSI and are -mostly- in accordance with the above-mentioned ideas put forward by Hoffmann. The main subject of this chapter will be the chemical manifestations of TBI and TSI. Special attention will be focussed on their applicability in organic synthesis.

1.2 Chemical Consequences of Through-Bond Orbital Interactions

1.2.1 General

Whereas spectroscopic studies directed towards detection of TBI have been highly successful, there are relatively few examples of the chemical consequences of through-bond orbital interactions.[5] Many multifunctionalized molecules whose spectral properties are markedly affected by TBI between the substituents, show little or no effects of these interactions in their chemical behavior. There are several reasons for this chemical passivity.

(1) In most cases these orbital interactions occur between two filled orbitals. This means that the total energy does not change very much. Reactions involving closed-shell molecules are therefore quite insensitive to the presence of orbital interactions between a donor and an acceptor substituent.

(2) The energy effects accompanying TBI are usually small. Interactions between the orbitals of functional groups, mediated through the intervening σ-bonds, can only lower or heighten the activation enthalpy of a reaction, although small enthalpy differences can have profound effects on the rate of reaction.[29]

(3) Since most (linear) σ-systems are highly flexible with great rotational freedom, the dihedral angles have to be interpreted in terms of time averages. Only in compounds possessing a fixed geometry in which the conditions for maximum TBI ("*trans* rule") can be maintained throughout the reaction, the chemical consequences of σ-effects can be expected.

These arguments may give rise to the feeling that TBI is of little importance in everyday organic chemistry. However, neglecting TBI is perhaps permissible for many intermolecular reactions, for intramolecular reactions this is often not the case. In the next sections a number of examples of chemical reactions, in which TBI (and TSI) is believed to play an essential role, will be discussed.

1.2.2 The Grob Fragmentation

The best-known example of participation of the σ-framework in an intramolecular chemical reaction is the heterolytic Grob fragmentation.[30,31] This fragmentation reaction can, in principle, take place in either a concerted manner or *via* a two-step mechanism (Scheme 1.1). In the concerted mechanism both the C_α–X and C_β–C_γ bond are broken synchronously utilizing the transition state **A**. Grob concluded that the concerted process should operate if both the C_α–X bond and the orbital of the nitrogen lone-pair are *anti* and parallel (= antiperiplanar) to the C_β–C_γ bond, and that the lone-pair of nitrogen accelerates the dissociation of the C_α–X bond.

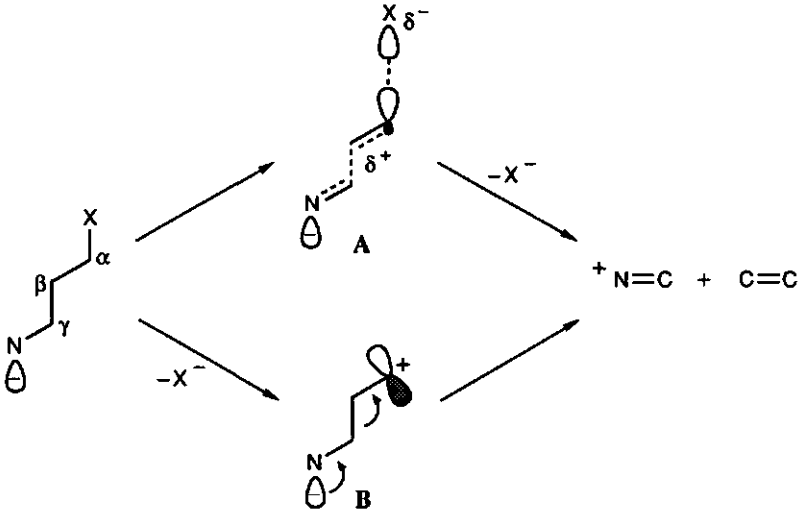

Scheme 1.1

The two-step mechanism begins with a rate-determining loss of the nucleofugal group X leading to the intermediate **B**. This carbocationic intermediate may undergo typical cationic reactions suchs as interception by nucleophiles, β-elimination, and/or ring closure in addition to, or instead of, fragmentation.

The high stereospecificity of the concerted fragmentation is clearly demonstrated with the solvolysis of three stereoisomeric N-methyldecahydroquinolin-5-ol tosylate esters **1**, **2**, and **3**.[32] Of these only the isomers **1** and **2** with equatorial tosylate groups exhibit the necessary antiperiplanarity of the orbitals involved and are found to undergo exclusive fragmentation to give the iminium ions **4** and **5** (or their hydrolysis products), respectively (Scheme 1.2). That these processes are concerted is apparent

from the fact that the reaction rates are much higher for these compounds than for their homomorphous 1-decalol tosylate esters.

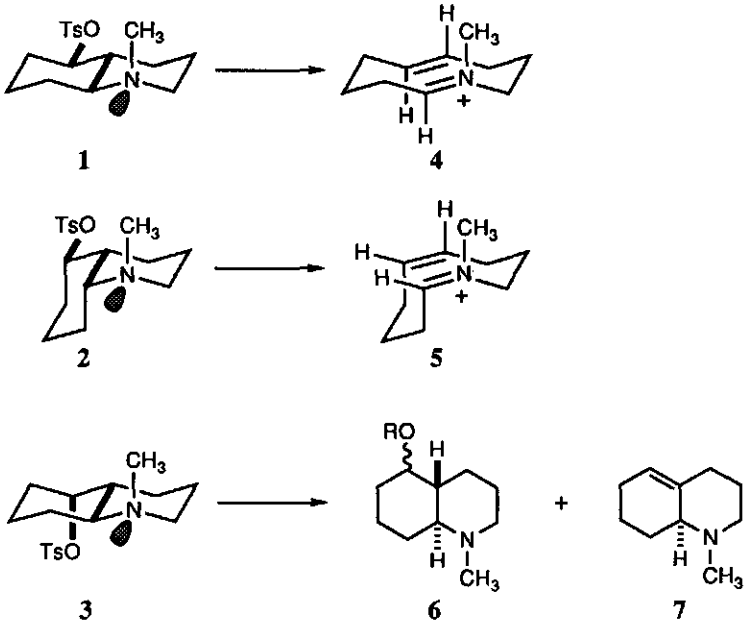

Scheme 1.2

Isomer **3** with an axial tosylate group, on the other hand, reacts more slowly than its homomorph. Since only substitution (**6**) and elimination (**7**) products are formed, this reaction must proceed *via* the two-step mechanism.

The influence of the orientation of the nitrogen lone-pair becomes apparent from solvolysis experiments with the epimeric N-methyldecahydroquinolin-7-ol tosylate esters **8** and **9** (Scheme 1.3).[32] Neither **8** nor **9** undergoes fragmentation. Both compounds exhibit only substitution (**10**) and elimination (**11**). In these compounds the nitrogen lone-pair is not oriented antiperiplanarly to the C_8–C_{8a} bond. Thus in **8** fragmentation *via* the concerted mechanism is not possible even though the C_7–OTs and the C_8–C_{8a} bond are antiperiplanar. The two-step fragmentation of **8** or **9** *via* an intermediate carbocation is also impossible for the same reasons. The non-participation of the lone-pair of nitrogen also follows from a comparison of the rate constants with those of the homomorphous 2-decalol tosylate esters. As a result of the inductive withdrawing effect of the nitrogen atom, the reaction rates of **8** and **9** are reduced appreciably with respect to their homomorphs.

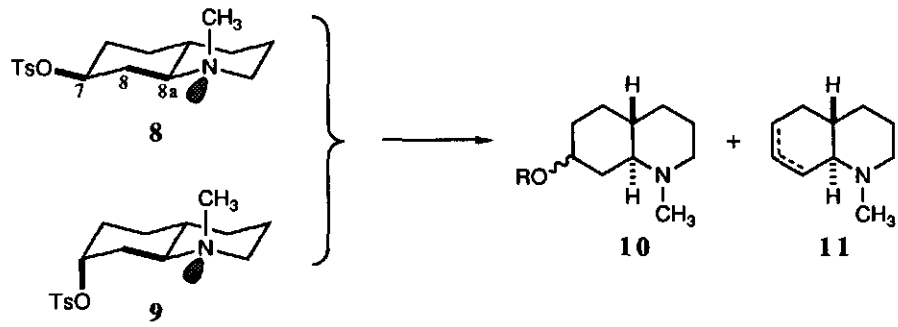

Scheme 1.3

Quantum mechanical calculations show that the heterolytic fragmentation corresponds with the concept of through-bond coupling.[9,33] The conformational requirements and orbital rules for the concerted fragmentation process are the same for the two-step fragmentation. When both mechanisms are possible the concerted reaction path will be followed and accelerated.

1.2.3 *Electrophilic Additions to Double Bonds*

As described in section 1.2.2, an incipient carbocation can be stabilized by the lone-pair of an amino group on the γ-C. A similar stabilizing effect of a (developing) carbocation has been found for the carbonyl oxygen (Figure 1.2).[34,35] This effect is somewhat surprising since a carbonyl group normally acts as an electron withdrawing substituent.

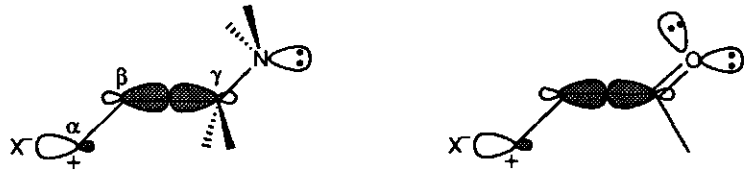

Figure 1.2: The stabilizing effect of nitrogen and carbonyl lone-pairs on an incipient carbocationic center.

Quantum chemical calculations confirm this stabilizing effect of a carbonyl group.[36] These calculations show that, for instance, the carbocation **12a** is more stable than its isomer **12b** (Scheme 1.4). The relative long C_β–C_γ bond and the short C_α–C_β bond calculated for **12a** are in agreement with a through-bond stabilizing interaction

between the oxygen lone-pair and the empty p orbital at C_α. This interaction can be depicted by the mesomeric structures **12a** ↔ **12a'**.

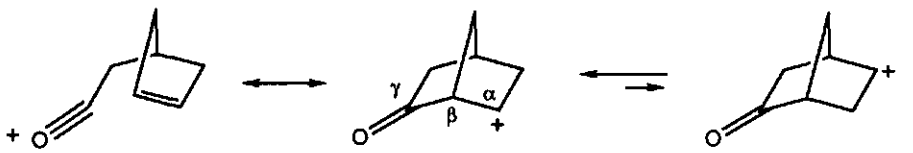

12a' **12a** **12b**

Scheme 1.4

Experimental support for this mechanism comes from electrophilic additions to norbornenone **13** which give exclusively the adducts **14** (Scheme 1.5).[34c] Also the formation of the carboxylic acid **15** after treatment of **13** with aqueous acid corresponds with the TBI stabilizing effect of a carbonyl oxygen on carbocations.[37]

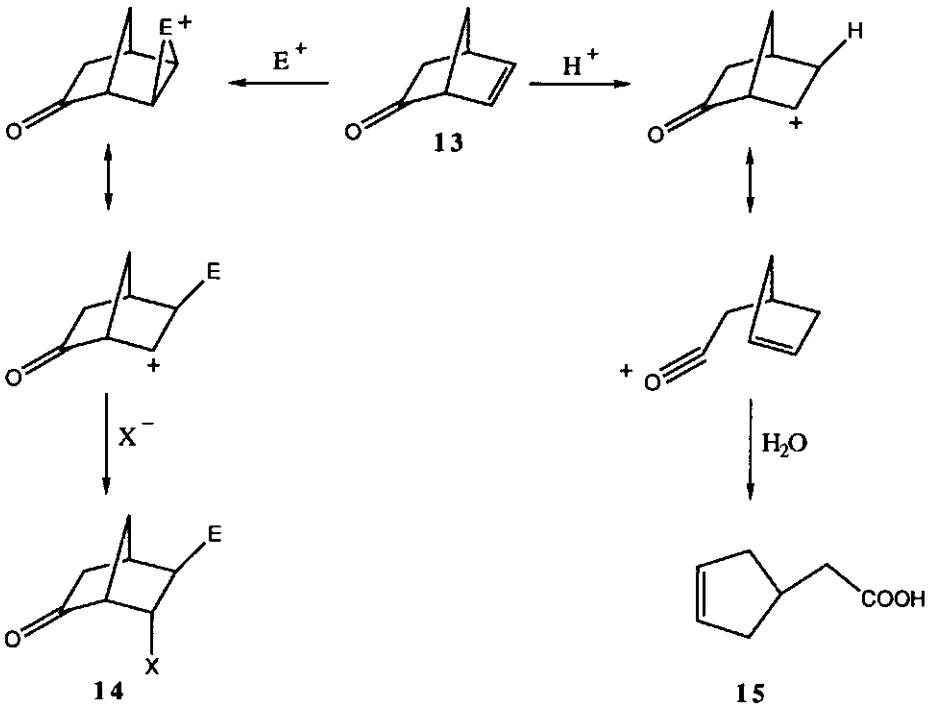

Scheme 1.5

1.2.4 Addition Reactions to Trigonal Carbon

Substituents at the 5-position of adamantane derivatives with a trigonal carbon atom at the 2-position have a profound influence on the stereoselectivity of addition reactions to the trigonal carbon of these compounds (*face selection*).[38] Because the basic skeleton of adamantanes is rigid, and the distant substituent in the equatorial 5-position does not affect the chemistry at the trigonal center C_2 in any steric way, the stereoselectivity is only directed by the electronic nature of the substituent. Electron withdrawing substituents X at C_5 of adamantan-2-one **16** cause preferentially a *syn* approach of the nucleophile, while electron donating substituents favor an *anti* attack.[39-41]

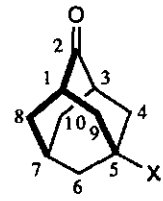

16

It has been shown that the addition always takes place *anti* to the more electron-rich pairs of vicinal C–C bonds (Figure 1.3), and that the substituent X serves to polarize the flanking β C–C bonds into two electronic distinct pairs (C_1–C_9; C_3–C_4 vs C_1–C_8; C_3–C_{10}).[42,43,44] Transition-state *hyperconjugation*[45] (β- or σ-participation) is believed to account for the distinct polarization of the flanking C–C bonds.[46]

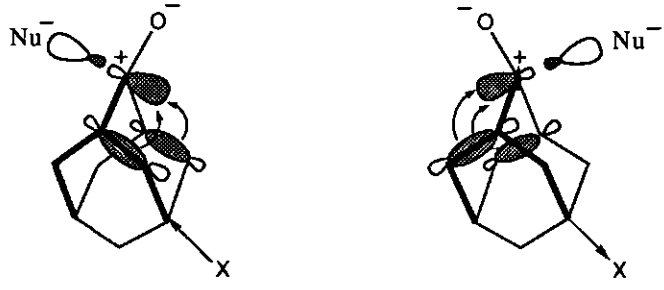

Figure 1.3: An electron donating substituent X on the δ-position causes anti addition of the nucleophile (A), whereas an electron withdrawing substituent results in syn approach of the nucleophile (B).

1.2.5 *Long-Range Electronic Effects of Group IV(14) Elements*

The elements silicon (Si), germanium (Ge), tin (Sn), and lead (Pb) have a remarkable ability to stabilize a positive charge on bordering carbon atoms. The stabilizing effect increases going from Si to Pb.[47] The ability of these metals to stabilize a positive charge is undoubtedly related to their high polarizability and low electronegativity. However, as the following examples demonstrate, only a very effective electronic effect that couples the metal donor atom with the (developing) p orbital through the intervening σ-bonds can explain the strong stabilizing influence of these elements on a positive charge.

The best-known example is the so-called β-effect,[48] which is almost certainly the result of orbital interactions through one C–C single bond (Scheme 1.6).

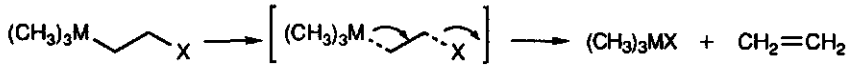

Scheme 1.6

In most studies the positive charge is produced solvolytically. The presence of a β-metal atom accelerates the solvolysis process. For tin this acceleration can amount to a factor of 10^{15} compared with hydrogen.[49] This β-effect has been discussed in terms of two possible mechanisms: *nonvertical* and *vertical (hyperconjugative) stabilization* (Figure 1.4).[47a] Nonvertical stabilization can be regarded as an internal, S_N2-like, stabilization of the developing carbocation on C_α (mechanism **a**). In contrast, vertical stabilization involves donation of the M–C σ-electrons to the empty p orbital on C_α without significant movement of atomic positions (mechanism **b**). In addition the positive charge may be stabilized by simple induction, but its range will not extend beyond the neighboring bond(s) significantly.

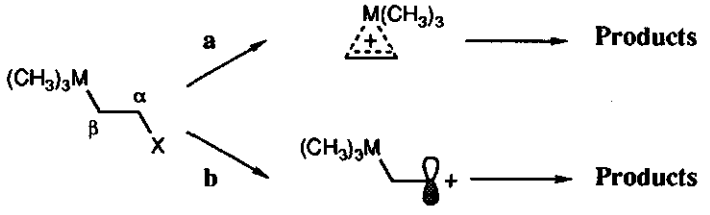

Figure 1.4: Nonvertical (a) and vertical (b) stabilization.

Exhaustive studies (theoretical[50] as well as chemical[48,51]) on the β-effect of silicon have revealed that the majority of the kinetic accelerations observed in solvolysis is caused by vertical stabilization with little or no movement of the Si–C bond, corresponding to a transition state resembling the open carbocation in Figure 1.4. These studies also showed the dependence of the magnitude of the stabilizing effect on the stereochemical relationship between silicon and the leaving group X. It was found that an antiperiplanar arrangement of the Si–C bond and the leaving group gave maximum orbital overlap in the transition state and hence maximum stabilization.

The accelerating effect of group IV(14) metals on the departure of nucleofugal groups at γ-carbons is considerably smaller than the β-effect, albeit significantly.[52-54] The γ-effect, which takes place through two C–C single bonds, has been studied for the greater part with silicon as donor atom. For example, the solvolysis of compound **17**, in which the trimethylsilyl and leaving group both have an equatorial orientation, was accelerated by a factor 452 compared with the solvolysis of a corresponding compound in which the trimethylsilyl group is replaced by a *tert*-butyl group.[53] On the other hand, the solvolysis of the *trans* isomer **18**, in which the leaving group is axially oriented, was only accelerated by a factor of 1.2. Upon reaction of compound **17**, the cyclopropane compound **19** was formed in 16% yield, apart from the expected substitution and elimination products.

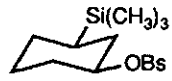

17

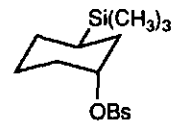

18

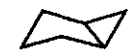

19

It was concluded that two different mechanisms are operative here and that the mechanisms are determined by the different configurations of **17** and **18**. The latter compound reacts by solvolytic ionization of the sulfonate ester bond followed by nucleophilic substitution or proton elimination. On the other hand, the solvolysis of compound **17** is assisted by silicon. This σ-assistance of silicon has been attributed to normal hyperconjugation and/or silicon promoted carbon participation through the back lobe of the Si–C_α bond to the incipient empty p orbital of the carbocationic center at C_γ (Scheme 1.7).[53b] This latter effect, referred to as *homohyperconjugation*,[54,55] is only possible in a "W" (zigzag) arrangement of the intervening σ-bonds.

Scheme 1.7

It should be noted that the cyclopropane product **19** resembles the homohyperconjugatively stabilized transition state (or intermediate) in Scheme 1.7. It is also noteworthy that replacement of silicon by tin in compound **17** led to the selective formation of **19**.[56]

Little or no accelerating effect was observed during the solvolysis of organosilicon compounds in which the silicon atom is placed at the δ-position of the leaving group.[57] On the other hand, the existence of the δ-effect of tin has been demonstrated (Scheme 1.8).[58]

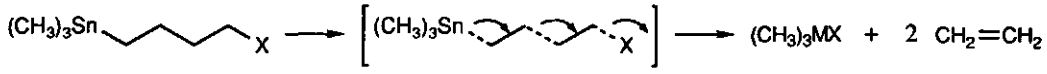

Scheme 1.8

Large δ-effects of tin have been found with compounds possessing a rigid adamantyl framework.[59] From solvolysis experiments with the adamantyl compounds **20** and **21**, together with the formation of the fragmentation product **22** (only from **20**), it is concluded that both the donor trimethylstannyl substituent and the sulfonate ester group must be antiperiplanar to the central C–C bond(s) for a maximum δ-effect. A TBI over three C–C single bonds (*double hyperconjugation*) can explain these results.[44]

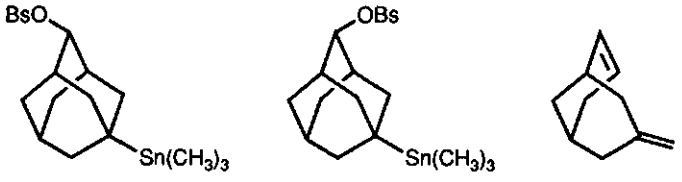

20 **21** **22**

Another illustrative example of the δ-effect of tin is found during the solvolysis of the cyclohexyl stannyltosylates **23** and **24**.[56,60] The *trans* isomer **23** has an *anti-gauche-anti* arrangement of the Sn–C–C–C–C–OTs moiety that permits double hyperconjugation as shown in Scheme 1.8. This double hyperconjugative interaction finds expression in

the formation of 1,5-hexadiene (60%) and a fast reaction time (40 times faster than the solvolysis rate of cyclohexyl tosylate). The *cis* isomer **24** has an *anti-gauche-gauche* arrangement which precludes such an interaction. As a result, **24** reacts only 6 times faster than cyclohexyl tosylate, and mainly substitution and elimination products are formed.

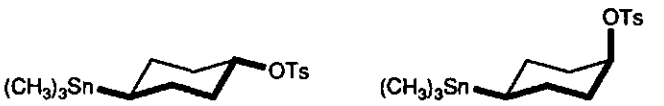

23 **24**

In an attempt to define the limits of σ-delocalization the ζ-effect (interaction over five C–C single atoms) was investigated, using tin as the donor atom.[60] The solvolysis rate of the stannyltosylate **25** was compared with its parent compound lacking the tin substituent. It was found that the presence of the tin substituent in this system does not enhance the solvolysis rate. However, one can ask if compound **25** has the proper structure to study long-range TBI effects. It is known that an "all *trans*" arrangement of the σ-bonds between the donor and the leaving group is required to optimize long-range orbital interactions. As shown in Figure 1.5, compound **25** does not fulfil this condition. To investigate the limits of σ-delocalization additional research is required. A more suitable substrate for this purpose might be a compound like **26** which does possess the optimal "all *trans*" arrangement of C–C single bonds.

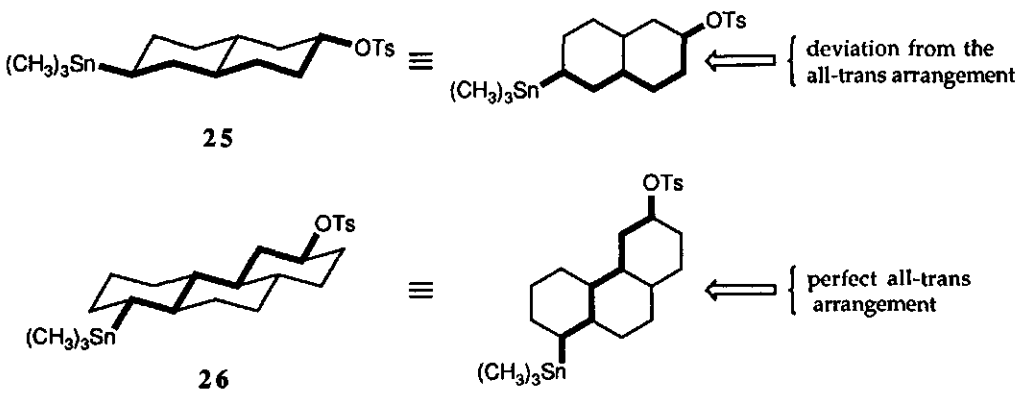

Figure 1.5: Compound 26 possesses an optimal "all trans" arrangement of the σ-relay, but 25 not.

In summary, the accelerating effects of β-, γ-, or δ-group IV(14) elements on the departure of a leaving group X in solvolysis reactions, with respect to the corresponding compounds lacking the metal donor, fits very well the concept of through-bond coupling.[44,56,61] Furthermore, the products formed in these reactions are easily explained with through-bond and through-space orbital interactions. The stabilizing effect decreases with an increasing number of intervening σ-bonds and is optimized for an "all *trans*" arrangement of the σ-relay.

1.2.6 Other Long-Range Electronic Effects

Remarkable long-range substituent effects have been reported in geometrically constraint systems.[62] Under solvolytic conditions the dibromides **27** and **28** react much slower (625- and 50-fold, respectively) than the corresponding monobromides **29** and **30**.

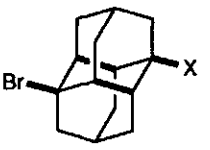

27 : X = Br
29 : X = H

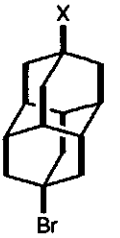

28 : X = Br
30 : X = H

A through-bond inductive effect over three and five σ-bonds, respectively, has been proposed to explain these results. Multiple pathways (thick lines) are thought to be responsible for these remarkably large effects.

Other striking examples of long-range interactions through σ-bonds have been found during studies on the Birch reduction of various conformationally fixed molecules containing aromatic and ethylenic functions separated by three, four, five, and six σ-bonds.[63]

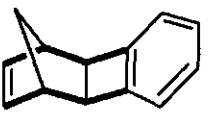

31

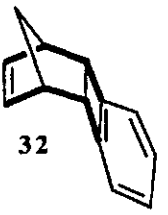

32

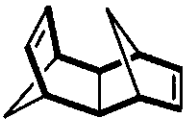

33

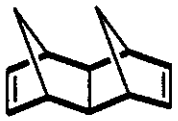

34

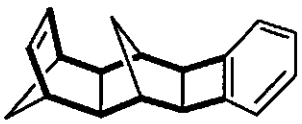

35

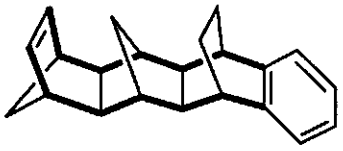

36

For example, the compounds **31–36** are all reduced considerably faster than norbornene under Birch conditions. Furthermore, it was found that a "W" arrangement (**31** and **34**) of relaying σ-bonds optimizes the rate of reduction, as is predicted by the "*trans* rule".

1.2.7 Base-Induced and -Directed Rearrangement and Elimination of Perhydronaphthalene-1,4-diol Monosulfonate Esters

From recent work of Jenniskens *et al.* on the total synthesis of sesquiterpenes,[64,65] it is known that cyclic 1,4-diol monosulfonate esters react very smoothly upon treatment with sodium *tert*-amylate in refluxing apolar solvents like benzene or toluene to give rearrangement and/or elimination products. For example, treatment of the tosylate **37** with sodium *tert*-amylate in refluxing benzene leads to an almost quantitative formation of the rearrangement product **38** (Scheme 1.9).[64] This selective skeletal rearrangement has been rationalized by assuming that deprotonation of the tertiary hydroxyl group induces intramolecularly the heterolysis of the tosylate group, just as in the Wharton reaction (*vide infra*). The oxygen anion donates electrons to both the β C–C bonds by a through-bond inductive mechanism, thus enlarging the electron density of these bonds and their ability to participate in the ionization process.[66] Both the β bonds are antiperiplanar to the developing carbocationic p orbital, which is essential for an effective stabilizing effect (Scheme 1.9). The dipolar intermediate **A** rapidly rearranges to the thermodynamically more stable intermediate **B**. In the latter intermediate the original angular methyl group and the alkoxide function are close together, which leads to a selective formation of **38**.

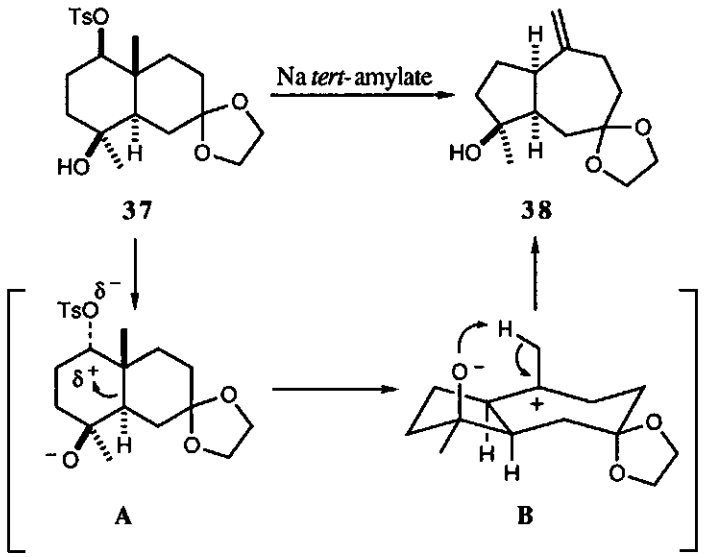

Scheme 1.9

The elimination of the sulfonate ester group in the mesylates **39** and **40** probably follows the same reaction principles.[65] Both compounds give the olefin **41** as the main product upon treatment with sodium *tert*-amylate in refluxing toluene (Scheme 1.10).

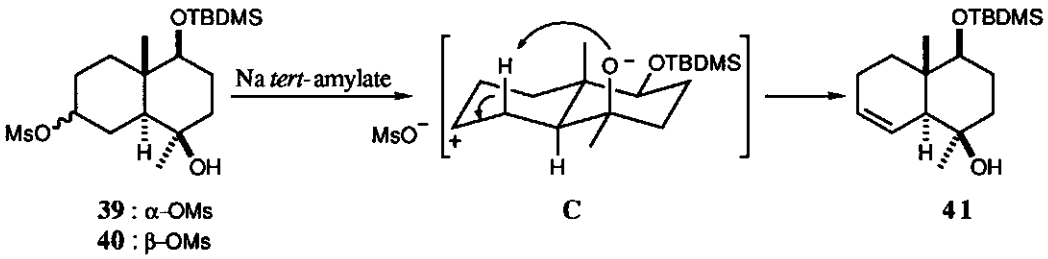

Scheme 1.10

A concerted intramolecular alkoxide-induced *anti* elimination mechanism might explain the fast and almost selective formation of **41** from **39**.[67,68] On the other hand, the preferential formation of **41** from **40** must proceed *via* a *syn* elimination. Normally, *anti* elimination is much faster than *syn* elimination in fixed six-membered ring systems. The elimination rates of **39** and **40**, however, are practically the same. These observations have led to the conclusion that both the *anti* and *syn* elimination probably proceed *via* an identical mechanism in which the deprotonation of the hydroxyl group is the crucial factor. Just as proposed for the

rearrangement reactions, deprotonation of the tertiary hydroxyl group is thought to be attended with ionization of the sulfonate ester bond. In the resulting dipolar intermediate **C** the carbocationic center will facilitate elimination[69] with the intramolecular process as the most favorable one. Once again, the ionization of the sulfonate ester bond, induced by deprotonation of the hydroxyl group, can only be rationalized by assuming a long-range orbital interaction that couples the alkoxide group and the nucleofugal sulfonate ester group through the intervening C–C single bonds.

1.2.8 Applications in Organic Synthesis

There are relatively many examples of the chemical manifestations of orbital interactions over two or three σ-bonds. On the other hand, reports on the synthetic utility of reactions in which long-range orbital interactions (over more than three σ bonds) play a role are scarce. For example, β-functionalized organosilicon compounds have found general application in the synthesis of alkenes.[70] The γ-effect of silicon or tin is also used in synthesis, although less frequently.[71] The high yield conversion (87%) of the γ-silyl nitro compound **42** into the corresponding ketone **43** (Nef reaction) under mild conditions is a typical example of the γ-effect of silicon (Scheme 1.11).[72] Without the silyl substituent this reaction proceeds only in poor yield (8%).

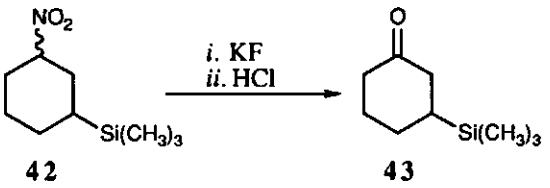

42 **43**

Scheme 1.11

Another synthetic application of the γ-effect of group IV(14) elements is found in the conversion of the epoxy stannane **44** into the cyclopropane adduct **45** (Scheme 1.12).[73] This conversion only proceeds if a "W" arrangement is present.

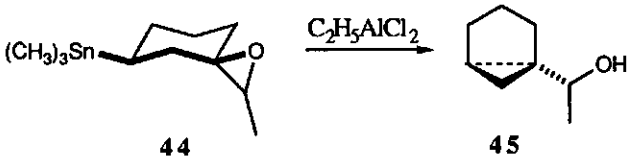

44 **45**

Scheme 1.12

Next to the group IV(14) elements, the directing effect of a carbonyl group on addition to double bonds has been used in organic synthesis.[74] However, the most important synthetic application of reactions that involve orbital interactions is the heterolytic (Grob) fragmentation.[75] Especially, the base-induced fragmentation of cyclic 1,3-diol monosulfonate esters, known as the Wharton fragmentation,[75b,76] must be mentioned in this connection. In the Wharton reaction the compounds can undergo olefin-forming fragmentation with formation of an electrofugal carbonyl fragment. In this instance the base does not play its usual role in elimination reactions but instead serves to remove a proton from the hydroxyl group, which enables the sulfonate ester group to come off more easily since O^- is a powerful electron donor.
Three striking examples of the usefulness of the Wharton reaction in the synthesis of macrocycles are given in Scheme 1.13.

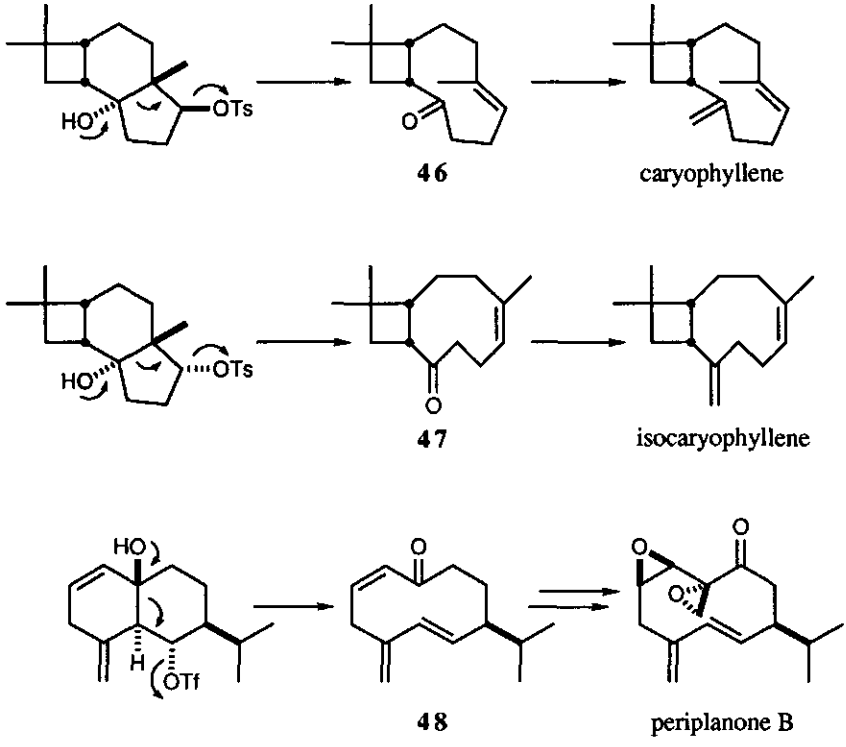

Scheme 1.13

The magnificent approach to caryophyllene and isocaryophyllene *via* the (*E*)- and (*Z*)-cyclononenes **46** and **47**, respectively, exemplifies the solution to stereoselective access of macrocyclic alkenes.[77]

The stereospecific C–C bond scission provides an exceptionally concise route to the trienone **48**,[78] a known intermediate for the synthesis of periplanone B which is a sex attractant of the American cockroach.[79,80]

Another way to induce fragmentation in the Wharton reaction is the desilylation of trimethylsilylethers as is exemplified in the synthesis of the *cis*-fused hexahydroazulenone **50** from the silylether **49** (Scheme 1.14). Treatment of the hydroxyl analogue of **49** with strong base gives, *via* epimerization, mainly the *trans*-fused isomer of **50**.[81]

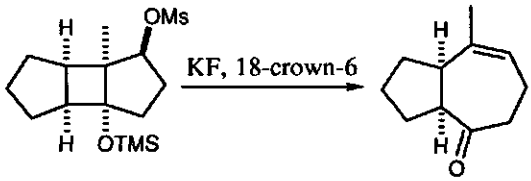

49 **50**

Scheme 1.14

One of the very few examples of the synthetic utility of longer-range orbital interactions (over more than three σ-bonds) are the base-induced and -directed rearrangement and elimination reactions of perhydronaphthalene-1,4-diol monosulfonate esters. The generation of an oxygen anion is thought to be attended with the ionization of the sulfonate ester group three C–C bonds away. Note the analogy with the Wharton reaction.

The rearrangement reaction has been successfully applied in the synthesis of the unnatural sesquiterpene (±)-*epi*-nardol (**52**). Treatment of the tosylate **51** with sodium *tert*-amylate in refluxing benzene afforded **52** in 90% yield (Scheme 1.15).[64]

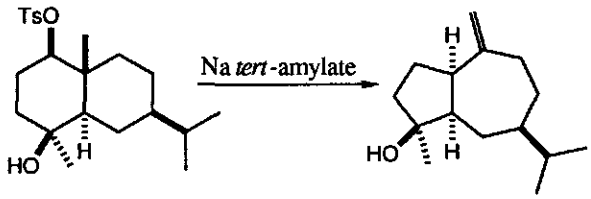

51 **52**

Scheme 1.15

In combination with the base-induced and -directed elimination of perhydronaphthalene-1,4-diol monosulfonate esters (**39** and/or **40** → **41**) the above-mentioned rearrangement has been used in the total synthesis of the natural sesquiterpene (±)-alloaromadendrane-4α,10α-diol (**55**).[65] In this total synthesis the axial tertiary hydroxyl group plays a central role in the two key steps: (i) the selective formation of **41** and (ii) the skeletal rearrangement of **53** to **54** (Scheme 1.16).

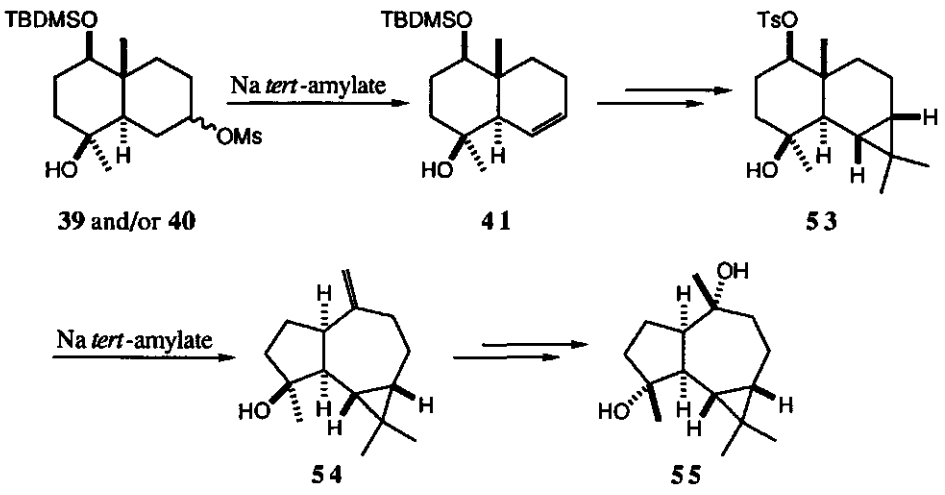

Scheme 1.16

1.2.9 Related Reactions

Long-range orbital interactions might also play an important role in reactions of compounds in which the bridge that connects the two interacting functionalities contains unsaturated bond(s) and/or hetero atom(s). Many of such reactions have been reported. However, only a few have been scrutinized in a mechanistic and a stereochemical context. For a detailed summary of these reactions and their synthetic applications see reference 82. It should be noted that in this thesis attention will be focussed on reactions of compounds in which a saturated carbon bridge connects the electron donor and electron acceptor substituent. However, one example might be illustrative.

Compound **56** reacts fast upon treatment with excess NaOMe to give almost exclusively **57** (Scheme 1.17).[83] This fragmentation process might involve long-range interactions over six bonds between the electron donating O^- group and the tosylate function. In the transition state (**a**) of this process, in which seven atoms are

involved, three σ-bonds are broken synchronously.[83a] The oxygen lone-pair as well as the participating bonds are properly aligned for maximum orbital overlap and fulfil the stereoelectronic requirements for a concerted fragmentation process.

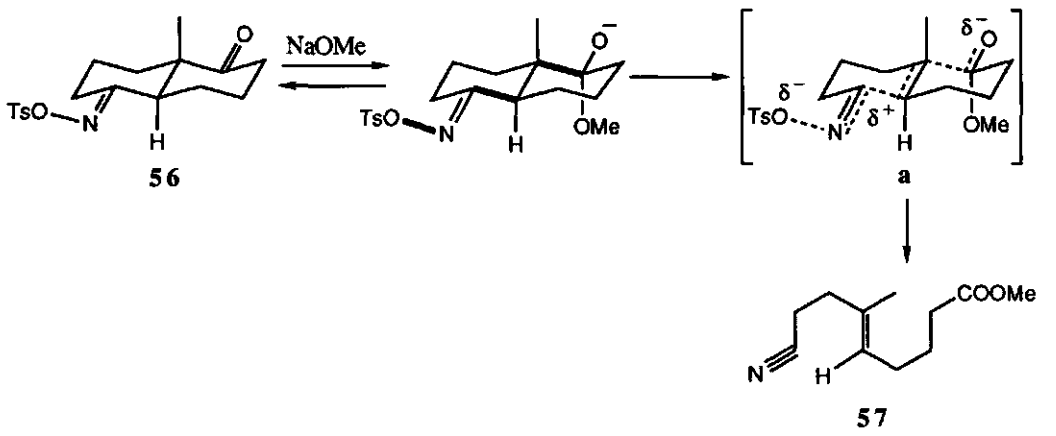

56 a 57

Scheme 1.17

1.3 Scope of this Thesis

From the section 1.2.8 it is clear that stereochemical and stereoelectronic factors are important in the Wharton reaction. A fast concerted fragmentation process requires the antiperiplanarity of the bonds undergoing cleavage. A stepwise pathway involving an intermediate carbocation may occur if a *gauche* relationship exists between these bonds.

The observations of Jenniskens *et al.* raised the question whether the same or different stereochemical and stereoelectronic principles as found for the Wharton reaction are applicable to the base-induced reactions of cyclic *1,4-diol* monosulfonate esters. It should be emphasized that in the latter reactions four σ-bonds separate the tertiary hydroxyl group and the mesylate group.

The aim of the present investigation is to explore the mechanistic aspects of the base-induced reaction of 1,4-diol monosulfonate esters and to define its stereochemical and stereoelectronic principles.

In chapter 2, the syntheses of the compounds studied in this thesis are described.

In chapter 3, the importance of initial deprotonation of the tertiary hydroxyl group is discussed. Furthermore, it is described how the orientation of the sulfonate ester group in combination with the orientation of the deprotonated hydroxyl group

determines the product outcome of the reaction. The way in which the electron donating ability of the oxygen anion affects the reaction rate and reaction outcome is also described in this chapter.
The influence of the geometry of the σ-bridge connecting the electron donor substituent and the electron acceptor substituent on the product outcome and rate of the reaction will be the main subject of chapter 4.
In order to explore the underlying principle features of the rearrangement- and homofragmentation reactions, described in chapter 4, a semi-empirical MNDO study on model compounds was undertaken. In chapter 5, the results will be presented.
The extent of the coupling between the alkoxide and the sulfonate ester is not only determined by the orientation of these substituents and/or the geometry of the σ-relay but also by the order of substitution of the carbon atom next to the carbon atom to which the mesylate group is connected. This will be discussed in chapter 6.
Finally in chapter 7, the influence of TBI on the desilylation reaction of the silylated analogs of 1,4-diol monosulfonate esters will be reported.

1.4 References and Notes

(1) Hoffmann, R.; Imamura, A.; Hehre, W. J. *J. Am. Chem. Soc.* **1968**, *90*, 1499-1509.
(2) Hoffmann, R. *Acc. Chem. Res.* **1971**, *4*, 1-9.
(3) For excellent reviews see references 4-13.
(4) Paddon-Row, M. N. *Acc. Chem. Res.* **1982**, *15*, 245-251.
(5) Paddon-Row, M. N.; Jordan, K. D. In *Modern Models of Bonding and Delocalization*; J. F. Liebman and A. Greenberg, Ed.; VCH publishers: New York, **1988**; chapter 3.
(6) Jordan, K. D.; Paddon-Row, M. N. *Chem. Rev.* **1992**, *92*, 395-410.
(7) Verhoeven, J. W. *Recl. Trav. Chim. Pays-Bas* **1980**, *99*, 369-379.
(8) Paddon-Row, M. N.; Verhoeven, J. W. *New J. Chem.* **1991**, *15*, 107-116.
(9) Gleiter, R. *Angew. Chem., Int. Ed. Engl.* **1974**, *13*, 696-701.
(10) Gleiter, R. *Pure Appl. Chem.* **1987**, *59*, 1585-1594.
(11) Gleiter, R.; Schäfer, W. *Acc. Chem. Res.* **1990**, *23*, 369-375.
(12) Martin, H.-D.; Mayer, B. *Angew. Chem.* **1983**, *95*, 281-313.
(13) Closs, G. L.; Miller, J. R. *Science* **1988**, *240*, 440-447.
(14) However, TSI over 5Å have been reported. See references 5 and 6.
(15) Much larger distances have been reported also. See for example references 16 and 17.
(16) Paddon-Row, M. N.; Jordan, K. D. *J. Am. Chem. Soc.* **1993**, *115*, 2952-2960.

(17) Zhu, Y.; Schuster, G. B. *J. Am. Chem. Soc.* **1993**, *115*, 2190-2199.
(18) Pasman, P.; Rob, F.; Verhoeven, J. W. *J. Am. Chem. Soc.* **1982**, *104*, 5127-5133.
(19) Krijnen, B.; Beverloo, H. B.; Verhoeven, J. W.; Reiss, C. A.; K., G.; Heijdenrijk, D. *J. Am. Chem. Soc.* **1989**, *111*, 4433-4440.
(20) Kroon, J.; Oliver, A. M.; Paddon-Row, M. N.; Verhoeven, J. W. *J. Am. Chem. Soc.* **1990**, *112*, 4868-4873.
(21) Bartetzko, R.; Gleiter, R.; Muthard, J. L.; Paquette, L. A. *J. Am. Chem. Soc.* **1978**, *100*, 5589-5594 .
(22) Closs, G. L.; Calcaterra, L. T.; Green, N. J.; Penfield, K. W.; Miller, J. R. *J. Phys. Chem.* **1986**, *90*, 3673-3683.
(23) Snow, L. D.; Williams, F. *J. Chem. Soc., Chem. Commun.* **1983**, 1090-1092.
(24) Schneider, H. J.; Wiegand, E. F.; Becker, N. *J. Org. Chem.* **1988**, *53*, 3361-3364.
(25) Hush, N. S.; Paddon-Row, M. N.; Cotsaris, E.; Oevering, H.; Verhoeven, J. W.; Heppener, M. *Chem. Phys. Lett.* **1987**, *117*, 8-11.
(26) Hush, N. S.; Wong, A. T.; Bacskay, G. B.; Reimers, J. R. *J. Am. Chem. Soc.* **1990**, *112*, 4192-4197.
(27) Heilbronner, E.; Schmelzer, A. *Helv. Chim. Acta* **1975**, *58*, 936-967.
(28) Brunck, T. K.; Weinhold, F. *J. Am. Chem. Soc.* **1976**, *98*, 4392-4393.
(29) van der Kerk, S. M.; Verhoeven, J. W.; Stirling, C. J. M. *J. Chem. Soc., Perkin Trans. II* **1985**, 1355-1360.
(30) Grob, C. A. *Helv. Chim. Acta* **1955**, *38*, 594-610.
(31) Grob, C. A. *Angew. Chem., Int. Ed. Engl.* **1969**, *8*, 535-622.
(32) Grob, C. A.; Kiefer, H. R.; Lutz, H. J.; Wilkens, H. J. *Helv. Chim. Acta* **1967**, *50*, 416-431.
(33) Gleiter, R.; Stohrer, W.; Hoffmann, R. *Helv. Chim. Acta* **1972**, *55*, 893-906.
(34) (a) Carrupt, P.-A.; Avenati, M.; Quarroz, D.; Vogel, P. *Tetrahedron Lett.* **1978**, 4413-4416.
(b) Avenati, M.; Carrupt, P.-A.; Quarroz, D.; Vogel, P. *Helv. Chim. Acta* **1982**, *65*, 178-203.
(c) Carrupt, P.-A.; Vogel, P. *Helv. Chim. Acta* **1989**, *72*, 1008-1028.
(35) (a) Takeuchi, K.; Yoshida, M. *J. Org. Chem.* **1989**, *54*, 3772-3773.
(b) Yoshida, M.; Takeuchi, K. *J. Org. Chem.* **1993**, *58*, 2566-2572.
(36) (a) Carrupt, P.-A.; Vogel, P. *Tetrahedron Lett.* **1984**, *25*, 2879-2882.
(b) Carrupt, P.-A.; Vogel, P. *J. Phys. Org. Chem.* **1988**, *1*, 287-298.
(c) Carrupt, P.-A.; Vogel, P. *J. Org. Chem.* **1990**, *55*, 5696-5700.
(37) (a) Lajunen, M. *Acc. Chem. Res.* **1985**, *18*, 254-258.
(b) Lajunen, M.; Lahti, M.; Heimo, S. *Acta Chem. Scand.* **1989**, *43*, 771-776.

(38) For a summary and references, see: Bodepudi, V. R.; le Noble, W. J. *J. Org. Chem.* **1991**, *56*, 2001-2006.

(39) Cheung, C. K.; Tseng, L. T.; Lin, M.-H.; Srivastava, S.; le Noble, W. J. *J. Am. Chem. Soc.* **1986**, *108*, 1598-1605.

(40) Lin, M.; Silver, J. E.; le Noble, W. J. *J. Org. Chem.* **1988**, 53, 5155-5158.

(41) Li, H.; le Noble, W. J. *Tetrahedron Lett.* **1990**, *31*, 4391-4392.

(42) Srivastava, S.; le Noble, W. J. *J. Am. Chem. Soc.* **1987**, *109*, 5874-5875.

(43) Lin, M.; Cheung, C. K.; le Noble, W. J. *J. Am. Chem. Soc.* **1988**, *110*, 6562-6563.

(44) Adcock, W.; Trout, N. A. *J. Org. Chem.* **1991**, *56*, 3229-3238.

(45) Cieplak, A. S. *J. Am. Chem. Soc.* **1981**, *103*, 4540-4552.

(46) Hahn, J. M.; le Noble, W. J. *J. Am. Chem. Soc.* **1992**, *114*, 1916-1917.

(47) (a) Traylor, T. G.; Hanstein, W.; Berwin, H. J.; Clinton, N. A.; Brown, R. S. *J. Am. Chem. Soc.* **1971**, *93*, 5715-5725.
(b) Hannon, S. J.; Traylor, T. G. *J. Org. Chem.* **1981**, *46*, 3645-3650.
(c) Traylor, T. G.; Koermer, G. S. *J. Org. Chem.* **1981**, *46*, 3651-3657.

(48) Lambert, J. B. *Tertrahedron* **1990**, *46*, 2677-2689.

(49) Lambert, J. B.; Wang, G.; Teramura, D. H. *J. Org. Chem.* **1988**, *53*, 5422-5428.

(50) (a) Lambert, J. B.; Wang, G.-T. *J. Phys. Org. Chem.* **1988**, *1*, 169-178.
(b) Wang, G.; Li, D.; Chelius, E. C.; Lambert, J. B. *J. Chem. Soc., Perkin Trans. 2* **1990**, 331-334.
(c) White, J. M.; Robertson, G. B. *J. Org. Chem.* **1992**, *57*, 4638-4644.
(d) Wierschke, S. G.; Chandrasekhar, J.; Jorgensen, W. L. *J. Am. Chem. Soc.* **1985**, *107*, 1496-1500.

(51) Lambert, J. B.; Emblidge, R. W.; Malany, S. *J. Am. Chem. Soc.* **1993**, *115*, 1317-1320.

(52) (a) Fischer, W.; Grob, C. A. *Helv. Chim. Acta* **1978**, 1588-1608.
(b) Grob, C. A.; Gründel, M.; Sawlewicz, P. *Helv. Chim. Acta* **1988**, *71*, 1502-1507.

(53) (a) Shiner, V. J., Jr.; Ensinger, M. W.; Kriz, G. S. *J. Am. Chem. Soc.* **1986**, *108*, 842-844.
(b) Shiner, V. J., Jr.; Ensinger, M. W.; Rutkowske, R. D. *J. Am. Chem. Soc.* **1987**, *109*, 804-809.
(c) Shiner, V. J., Jr.; Ensinger, M. W.; Huffman, J. C. *J. Am. Chem. Soc.* **1989**, *111*, 7199-7205.
(d) Shiner, V. J., Jr.; Ensinger, M. W.; Kriz, G. S.; Halley, K. A. *J. Org. Chem.* **1990**, *55*, 653-661.

(54) Bentley, T. W.; Kirmse, W.; Llewellyn, G.; Söllenböhmer, F. *J. Org. Chem.* **1990**, *55*, 1536-1540.

(55) Adcock, W.; Kok, G. B. *J. Org. Chem.* **1987**, 52, 356-364.

(56) Lambert, J. B.; Salvador, L. A.; So, J.-H. *Organometallics* **1993**, *12*, 697-703.
(57) Fessenden, R. J.; Seeler, K.; Dagani, M. *J. Org. Chem.* **1966**, *31*, 2483-2487.
(58) Davis, D. D.; Black, R. H. *J. Organomet. Chem.* **1974**, *82*, C30-C34.
(59) (a) Adcock, W.; Coope, J.; Shiner, V. J., Jr.; Trout, N. A. *J. Org. Chem.* **1990**, *55*, 1411-1412.
(b) Adcock, W.; Krstic, A. R.; Duggan, P. J.; Shiner, V. J., Jr.; Coope, J.; Ensinger, M. W. *J. Am. Chem. Soc.* **1990**, *112*, 3140-3145.
(60) Lambert, J. B.; So, J.-H.; Salvador, L. A. *Tetrahedron Lett.* **1990**, *31*, 3841-3844.
(61) Lambert, J. B.; Salvador, L. A. *J. Org. Chem.* **1993**, *58*, 5428-5433.
(62) Gund, T. M.; Schleyer, P. v. R.; Unruh, G. D.; Gleicher, G. J. *J. Org. Chem.* **1974**, *39*, 2995-3003.
(63) (a) Paddon-Row, M. N.; Hartcher, R. *J. Am. Chem. Soc.* **1980**, *102*, 662-670.
(b) Paddon-Row, M. N.; Hartcher, R. *J. Am. Chem. Soc.* **1980**, *102*, 671-678.
(c) Paddon-Row, M. N.; Hartcher, R. *Aust. J. Chem.* **1980**, *33*, 785-794.
(d) Chau, D. D.; Paddon-Row, M. N.; Patney, H. K. *Aust. J. Chem.* **1983**, *36*, 2423-2446.
(64) Wijnberg, J. B. P. A.; Jenniskens, L. H. D.; Brunekreef, G. A.; de Groot, A. *J. Org. Chem.* **1990**, *55*, 941-948.
(65) Jenniskens, L. H. D.; Wijnberg, J. B. P. A.; de Groot, A. *J. Org. Chem.* **1991**, *56*, 6585-6591.
(66) Lenoir, D.; Apeloig, Y.; Arad, D.; Schleyer, P. v. R. *J. Org. Chem.* **1988**, *53*, 661-675
(67) Menger, F. M.; Chow, J. F.; Kaiserman, H.; Vasquez, P. C. *J. Am. Chem. Soc.* **1983**, *105*, 4996-5002.
(68) Lansbury, P. T.; Mojica, C. A. *Tetrahedron Lett.* **1986**, *27*, 3967-3970.
(69) Bordwell, F. G. *Acc. Chem. Res.* **1972**, *5*, 374-381.
(70) Chan, T.-H. *Acc. Chem. Res.* **1977**, 442-448.
(71) Fleming, I.; Urch, C. J. *J. Organomet. Chem* **1985**, *285*, 173-191.
(72) Hwu, J. R.; Gilbert, B. A. *J. Am. Chem. Soc.* **1991**, *113*, 5917-5918.
(73) (a) Plamondon, L.; Wuest, J. D. *J. Org. Chem.* **1991**, *56*, 2066-2075.
(b) Plamondon, L.; Wuest, J. D. *J. Org. Chem.* **1991**, *56*, 2076-2081.
(74) Vogel, P.; Fattori, D.; Gasparini, F.; Le Drian, C. *Synlett* **1990**, 173-185.
(75) (a) Becker, K. B.; Grob, C. A. In *The Chemistry of Functional Groups. Supplement A: The Chemistry of Double-Bonded Functional Groups. Part 2*; S. Patai, Ed.; John Wiley & Sons: London, 1977; chapter 8.
(b) Caine, D. *Org. Prep. Proced. Int.* **1988**, *20*, 1-51.
(76) (a) Wharton, P. S. *J. Org. Chem.* **1961**, *26*, 4781-4782.
(b) Wharton, P. S.; Hiegel, G. A. *J. Org. Chem.* **1965**, *30*, 3254-3257.
(c) Wharton, P. S.; Baird, M. D. *J. Org. Chem.* **1971**, *36*, 2932-2937.

(77) Corey, E. J.; Mitra, R. B.; Uda, H. *J. Am. Chem. Soc.* **1964**, *86*, 485-492.
(78) Cauwberghs, S. G.; DeClercq, P. J. *Tetrahedron Lett.* **1988**, *29*, 6501-6504.
(79) Schreiber, S.; Santini, C. *J. Am. Chem. Soc.* **1984**, *106*, 4038-4044.
(80) Kitahara, T.; Mori, M.; Mori, K. *Tetrahedron* **1987**, *43*, 2689-2699.
(81) Tietze, L.-F.; Reichert, U. *Angew. Chem* **1980**, *92*, 832-833.
(82) Ho, T.-L. In *Heterolytic Fragmentation of Organic Molecules;* Wiley-Interscience: New York, **1993**.
(83) (a) Eisele, W.; Grob, C. A.; Renk, E.; von Tschammer, H. *Helv. Chim. Acta* **1968**, *51*, 816-828.
(b) Grob, C. A.; von Tschammer, H. *Helv. Chim. Acta* **1968**, *51*, 1082.

Chapter 2

Synthesis of Monosulfonate Esters of Perhydronaphthalene-1,4-diols*

2.1 Introduction

Suitably functionalized perhydronaphthalenes are frequently used in the synthesis of eudesmane[1,2] and *cis*-fused guaiane[3,4] sesquiterpenes. Starting from the Wieland-Miescher ketone or its derivatives, successful methods have been developed for the synthesis of appropriately functionalized *trans*-fused perhydronaphthalenes.[5,6] Together with the highly developed understanding of the stereochemistry and conformational analysis, their rigid structure makes these compounds very attractive to study long-range orbital interactions.

In this chapter the syntheses of mesylates **39**, **40**, and **58–67** are described. The numbering system of the carbon framework follows the system depicted in Figure 2.1 throughout the text of this chapter.[7]

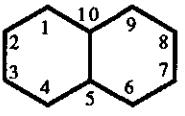

Figure 2.1: Numbering of naphthalene skeleton

The structures of the mesylates studied in this thesis are compiled in Charts 2.1–2.3. The six-membered rings are all *trans*-fused. This means that the naphthalene framework of these compounds possesses a chair-chair conformation with a rigid *trans* fusion. Furthermore, in all cases a mesylate leaving group is employed for reasons of uniformity, and because mesylates are easy to prepare. Finally, all the sulfonate esters studied in this thesis have a tertiary hydroxyl group, because secondary alcohols can undergo oxidation under the influence of strong bases.[3]

The compounds depicted in Chart 2.1 were synthesized in order to investigate how the orientation of the sulfonate ester group in combination with the orientation of

* Parts of this chapter have been published: Orrū, R. V. A.; Wijnberg, J. B. P. A.; Jenniskens, L. H. D.; de Groot, A. *J. Org. Chem.* **1993**, *58*, 1199 and Orrū, R. V. A.; Wijnberg, J. B. P. A.; Bouwman, C. T.; de Groot, A. *J. Org. Chem.* **1994**, *59*, 374.

the tertiary hydroxyl group determines the outcome and rate of their reactions with sodium *tert*-amylate (Chapter 3). The mesylates **60–65** (Chart 2.2) were prepared to determine the influence of the geometry of the relaying σ-bonds on the reactions with sodium *tert*-amylate (Chapter 4). Finally, in order to explore the effects of the order of substitution (Chapter 6) of the carbon atom that borders the carbon atom to which the mesylate group is attached, the compounds **40**, **66**, and **67** (Chart 2.3) were prepared.

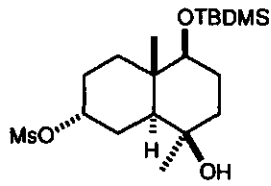

39

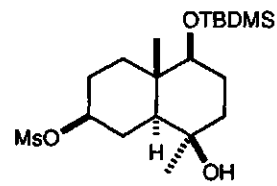

40

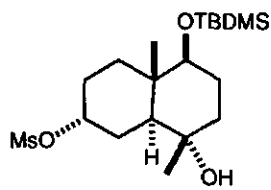

58

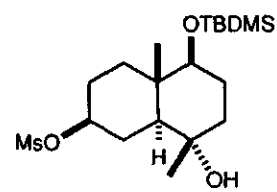

59

Chart 2.1

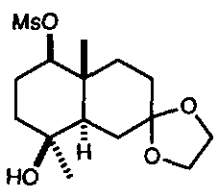

60

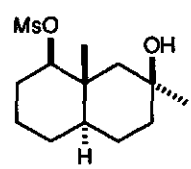

62

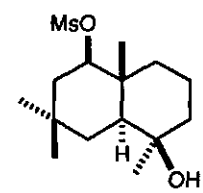

64

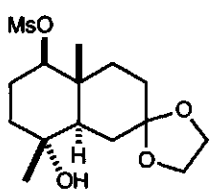

61

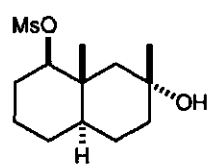

63

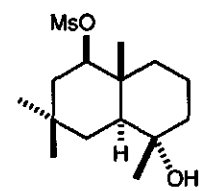

65

Chart 2.2

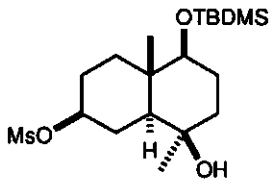

40

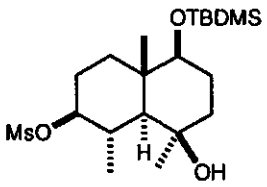

66

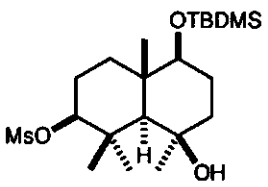

67

Chart 2.3

2.2 Synthesis of the Mesylates 39, 40, 58, and 59

The mesylates **39** and **40** were prepared from the readily available monoacetalized TBDMS-ether **68** as described.[4] For the synthesis of the mesylates **58** and **59** compound **68** was converted into **69** *via* a Wittig condensation with $Ph_3P{=}CH_2$ in DMSO (Scheme 2.1). Epoxidation of **69** with magnesium monoperoxyphthalate (MMPP) in a mixture of trimethyl orthoformate and MeOH[1] gave the epoxy acetal **70**. After reduction of **70** with $LiAlH_4$ in refluxing THF and subsequent hydrolysis of the dimethyl acetal function, the ketone **71** was obtained. Reduction of **71** with L-Selectride in THF at –78 °C[8] afforded exclusively the secondary 3α-alcohol **72**. For the preparation of the 3β-alcohol **73**, the ketone **71** was reduced selectively with $LiAlH_4$ in THF at room temperature. Treatment of the alcohols **72** and **73** with MsCl in pyridine provided the mesylates **58** and **59** respectively, in high yield.

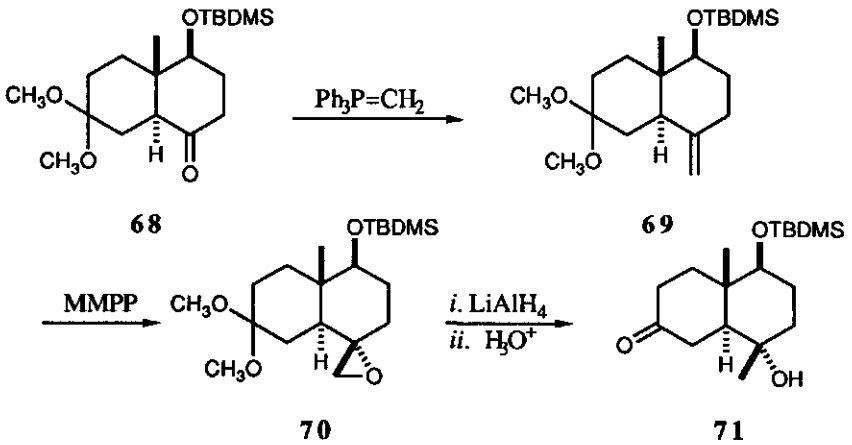

Scheme 2.1

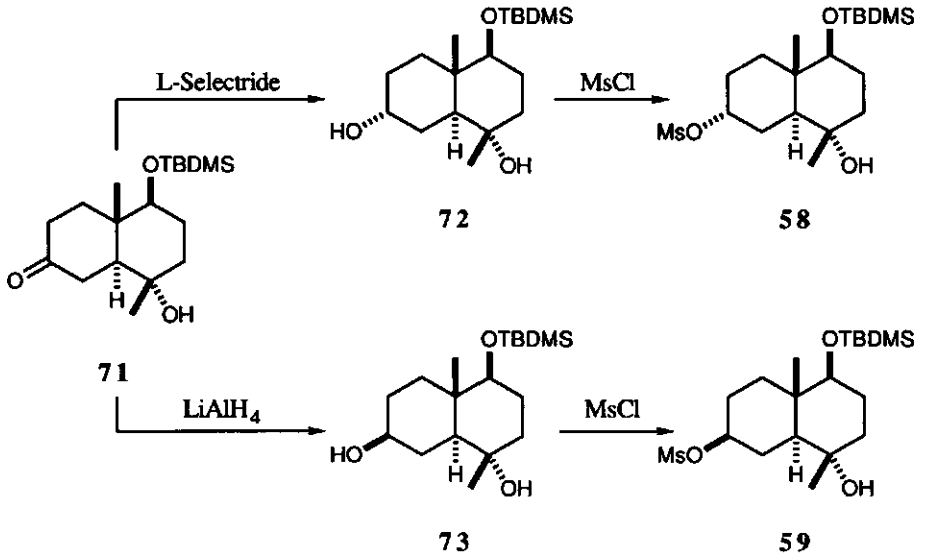

Scheme 2.1 continued

2.3 Synthesis of the Mesylates 60-65

The mesylates **60** and **61** were prepared from the known compounds **74**[3] and **71**, respectively, *via* intermediates **75** and **76**, according to standard procedures (Scheme 2.2).

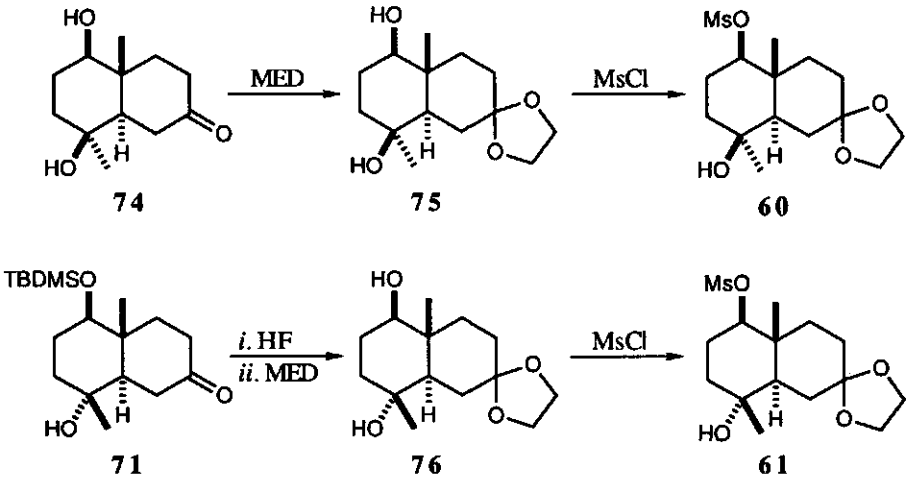

Scheme 2.2

The readily available ketone **77**[9] was the starting material for the synthesis of the mesylates **62** and **63** (Scheme 2.3). Bromination of **77** with dibromobarbituric acid (DBBA)[10] yielded the bromide **78** which upon treatment with $Li(t\text{-}BuO)_3AlH$ in THF at –78 °C afforded exclusively the 7β-alcohol **79**. An internal S_N2 reaction under the influence of *t*-BuOK in *t*-BuOH (**79** → **80**) went smoothly. Regioselective opening of the oxirane ring with $LiAlH_4$ in refluxing THF and subsequent oxidation with PDC converted **80** into the ketone **81**. The TBDMS ether bond of **81** was then cleaved with HF in aqueous acetonitrile, and the resulting hydroxy ketone was treated with an excess of MeMgI to afford the diol **82**. For the preparation of diol **84**, the ketone **81** was subjected to a Wittig reaction with $Ph_3P{=}CH_2$ in DMSO to yield the olefinic TBDMS-ether **83**. Cleavage of the TBDMS ether bond of **83** followed by epoxidation with *in situ* generated dimethyldioxirane[11] and reduction with $LiAlH_4$ led to the diol **84** as the sole product. Treatment of the diols **82** and **84** with MsCl in pyridine provided the mesylates **62** and **63** in yields of 47% and 39%, respectively, overall from **77**.

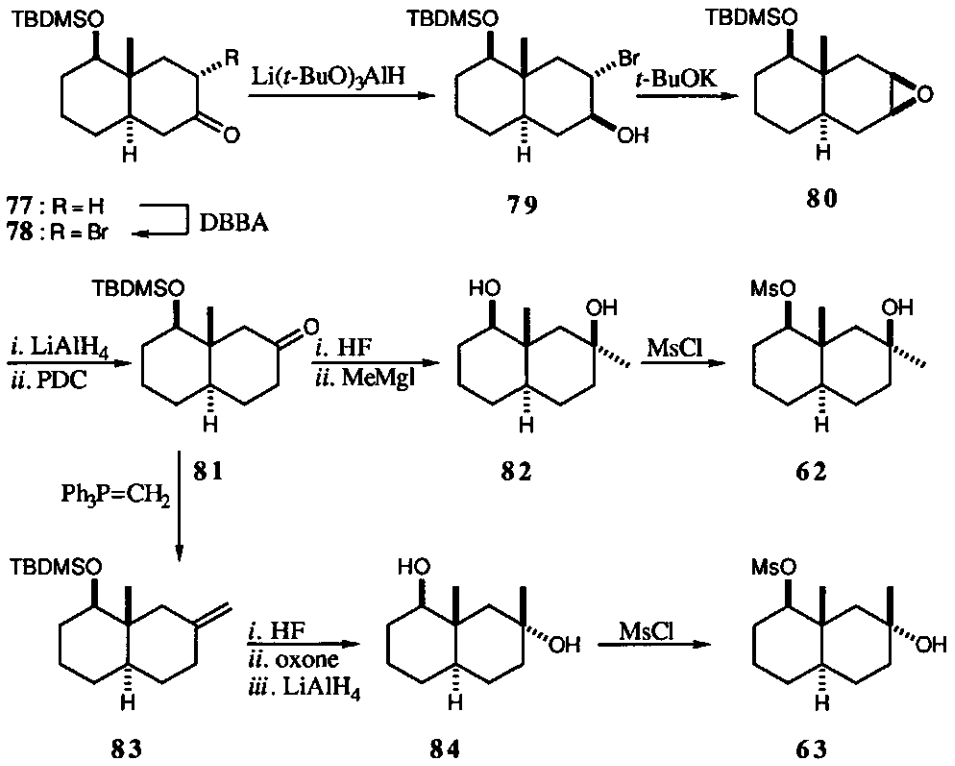

Scheme 2.3

For the synthesis of the mesylates **64** and **65** the known Robinson annulation product **85**[12] was converted into its cyclic thioacetal **86** by a known procedure[13] (Scheme 2.4). Upon treatment with sodium metal in liquid NH_3 at reflux temperature **86** was desulfurized, and at the same time its carbonyl function was reduced. In this way an easily separable 1:10 mixture of the alcohols **87a** and **87b**, respectively, was produced. Protection of the alcohol group as its TBDMS-ether[14] (**87b** → **88**) was successively followed by oxidative hydroboration (BH_3•THF; NaOH, H_2O_2), oxidation (PDC), and equilibration (NaOMe, MeOH) to give the *trans*-fused ketone **89**.

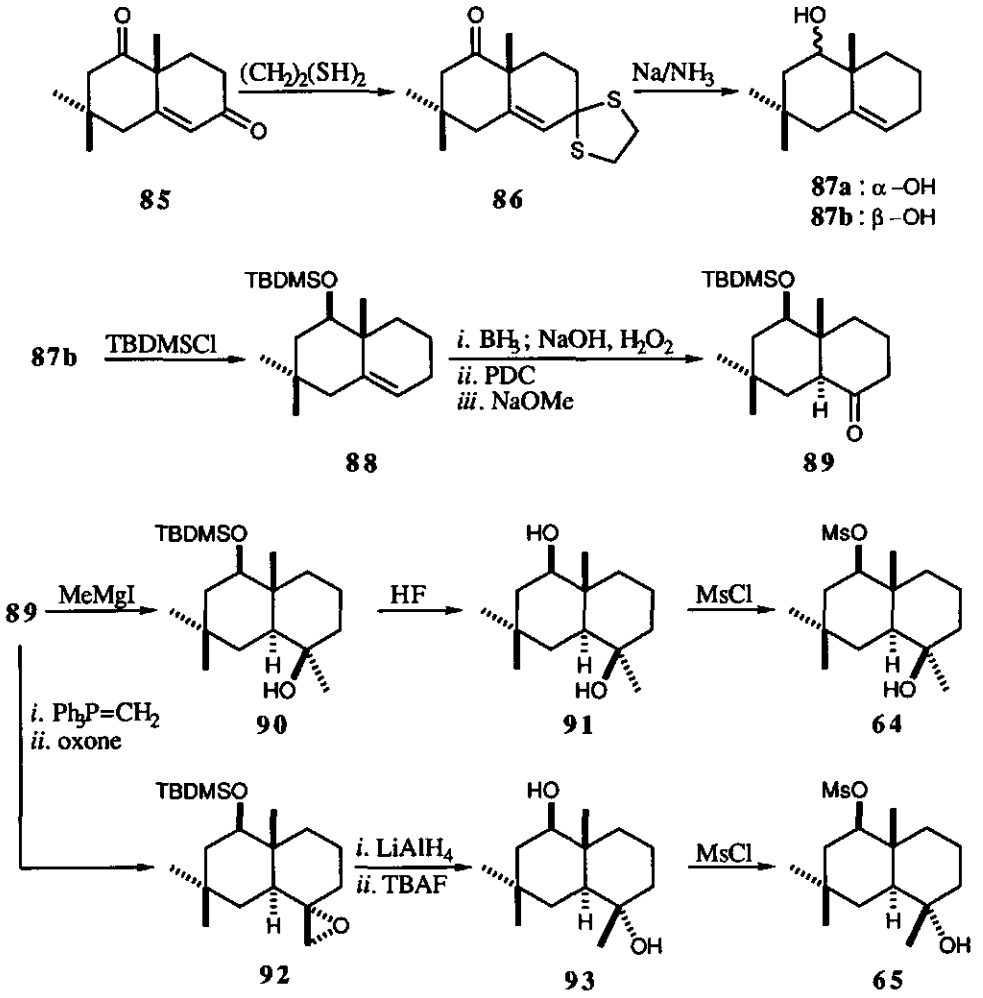

Scheme 2.4

This ketone could be used for the synthesis of both the mesylates **64** and **65**. Treatment of **89** with MeMgI in dry ether afforded the monoprotected diol **90**. Cleavage of the TBDMS ether bond (**90** → **91**) and mesylation produced the mesylate **64** in an overall yield of 32% from **85**. A Wittig condensation of ketone **89** with $Ph_3P{=}CH_2$ in DMSO and subsequent epoxidation of the resulting exocyclic double bond with dimethyldioxirane afforded exclusively the epoxide **92**. Reduction of the oxirane ring with $LiAlH_4$ in refluxing THF, and removal of the TBDMS protecting group with tetrabutylammonium fluoride (TBAF) afforded the desired diol **93**. Finally, treatment of **93** with MsCl in pyridine provided the mesylate **65** in 44% overall yield from **86**.

2.4 Synthesis of the Mesylates 66 and 67

For the synthesis of the mesylates **66** and **67** the readily available enedione acetate **94**[5] was converted into the enedione TBDMS-ether **95** by succesive deacetylation (NaOMe, MeOH) and protection (TBDMSCl, DMF)(Scheme 2.5).

For the synthesis of the mesylate **66** the C_4–C_5 double bond of **95** was reduced with metallic lithium in a 2:1 mixture of liquid NH_3 and THF, respectively, at reflux temperature. In this way three compounds were obtained: 3β-hydroxy ketone **96** (17%) and an inseparable 3:5 mixture of two isomeric diketones **97** (69%). Equilibration of the two isomers **97** with NaOMe in dry MeOH for 48 h, followed by treatment with 2-butanone dioxolane (MED) gave a 7:2 mixture of the C_3 mono-acetalized compounds **98a** and **98b**, respectively.[15,16] No bis-acetals or C_6-acetalized products were formed.[5] This mixture could be separated by column chromatography and in this manner pure **98a** was obtained.

The stereochemistry and the conformation of the compounds **98a** and **98b** was revealed from their NMR spectra. The ^{13}C shielding data for the angular methyl group of **98a** and **98b** were 11.29 and 20.98 ppm, respectively. These data imply a *trans* ring junction for compound **98a** and a *cis* ring junction for compound **98b**.[17] Additionally, in the ^1H-NMR spectrum of **98a** a doublet at 2.32 ppm (J = 11.6 Hz) was observed. From ^{13}C-^1H correlated 2D-NMR spectra it was concluded that this doublet must arise from the proton at C_5. The large coupling constant (J = 11.6 Hz) together with a fairly large NOE observed for the proton at C_5 upon irradiation of the proton at C_9 confirmed our stereochemical assignments concerning the ring junction and the orientation of the C_4 methyl group.

A Grignard reaction of **98a** with MeMgI in dry ether followed by hydrolysis of the ethylene acetal function gave the 6β-hydroxy ketone **99**. For the preparation of the 3β-alcohol **100**, ketone **99** was reduced with $LiAlH_4$ in THF at room temperature. It

should be noted that treatment of **96** with an excess of MeMgI also gave the diol **100**. Treatment of the alcohol **100** with MsCl in pyridine provided the mesylate **66** in 28% overall yield from **94**.

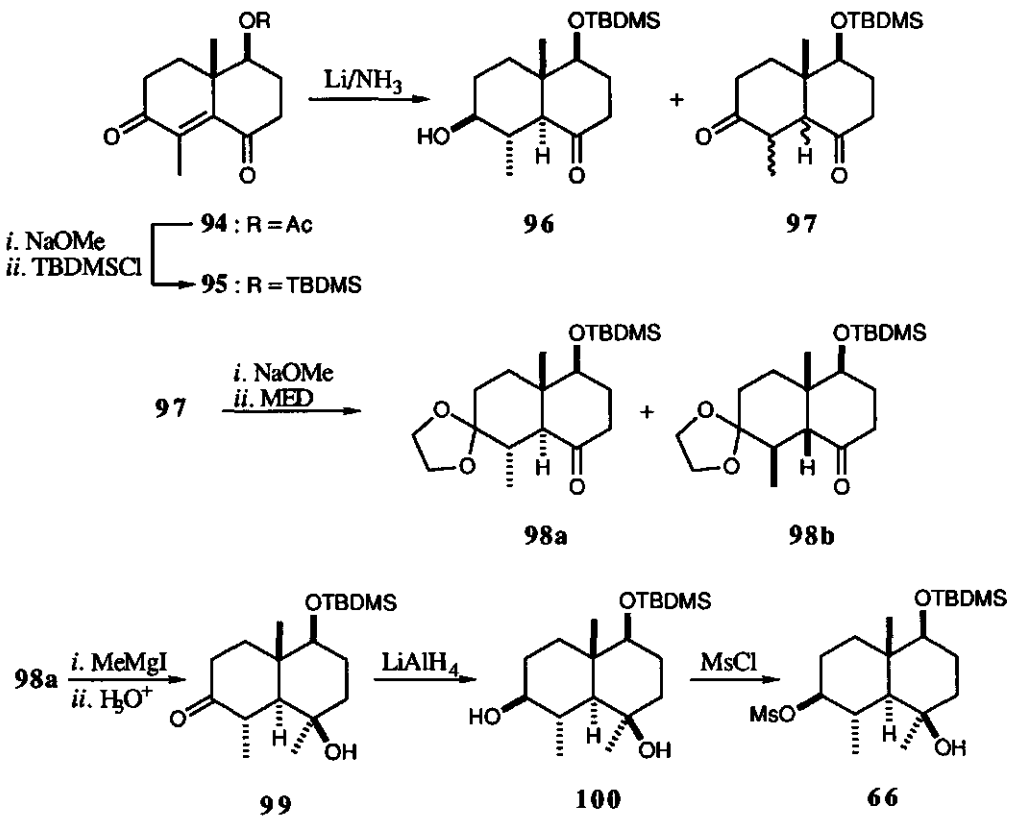

Scheme 2.5

The synthesis of the mesylate **67** (Scheme 2.6) started with the TBDMS-ether **95**. Reductive alkylation[18,19] of **95** and subsequent quenching of the enolate anion with MeI was employed to introduce the *gem*-dimethyl group at C_4. In this way a mixture of the *gem*-dimethyl dione **101** (25%) and the corresponding hydroxy ketone **102** (47%) was formed. The ^1H spectrum of **102** showed two double doublets at 3.07 ppm (J = 5.1, 10.5 Hz) and at 3.58 ppm (J = 5.2, 10.6 Hz). This is characteristic for the presence of a secondary hydroxyl group with an equatorial orientation. Additional information for the structure of **102** came from the ^{13}C-^1H correlated 2D-NMR measurements, which revealed that the signal of the proton at C_5 appears as a singlet at δ 1.97. This is only possible with a C_3 hydroxyl and a C_6 carbonyl group. Finally, the *trans* ring junction of compound **102** was established with NOE-difference experiments. Both the protons at

C_3 and C_9 are in close proximity of the proton at C_5. These NMR data unequivocally establish the structure of **102**. The structural assignments for **101** were much less straightforward due to severe overlap of signals in its ^{1}H-NMR spectrum. However, after conversion of **101** into **103**, this problem could be solved. ^{13}C-^{1}H correlated 2D-NMR experiments to determine the chemical shift of the C_5 proton, and irradiation of the C_9 proton which gave a NOE with the C_5 proton led to the conclusion that **103** has a *trans* ring junction. Hence, assuming that no epimerization took place during the acetalization, compound **101** is also *trans*-fused.

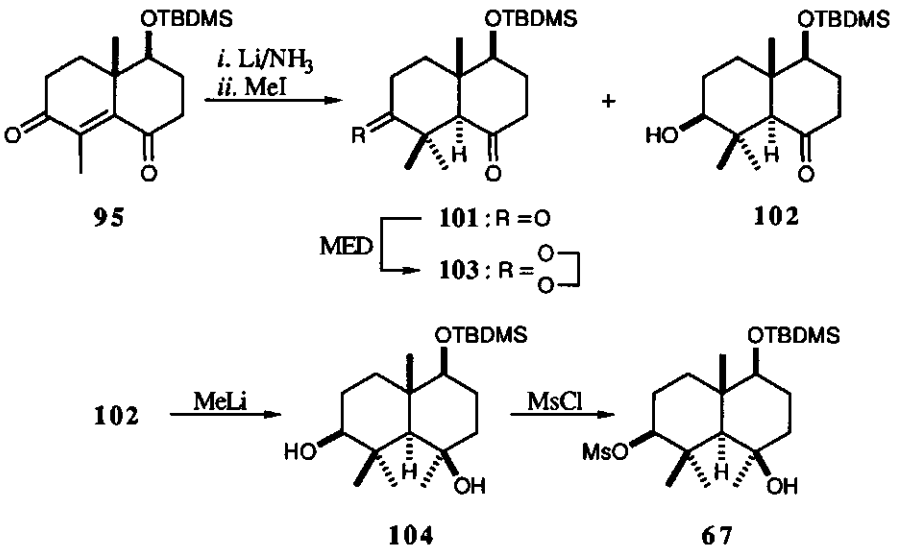

Scheme 2.6

When the ketone **102** was treated with MeMgI in dry ether, no addition products could be detected. Apparently, the carbonyl group in **102** was converted into its enolate which upon hydrolysis gave the starting material back. However, treatment of **102** with MeLi in THF at –78 °C, under which conditions enolization is much less important,[20] gave the desired diol **104**. The mesylate **67** was obtained after reaction of **104** with MsCl in pyridine in 18% overall yield from **95**.

2.5 Experimental Section

General. Melting points are uncorrected. NMR spectra are recorded in $CDCl_3$ unless otherwise noted. Chemical shifts are relative to TMS (δ 0.00) with $CHCl_3$ as internal standard (δ 7.23 (^{1}H) and δ 76.90 (^{13}C)). ^{13}C NMR multiplicities were determined by using a DEPT pulse sequence. ^{1}H–^{13}C

heteronuclear shift correlation spectra were performed at 200 MHz, using delay times in the pulse sequence of 3.3 and 2.2 ms. ^{1}H NOE difference experiments were done at 200 MHz, using a τ_m of 2 s. MS data were determined at 70 eV on either an AEI MS 902 spectrometer or a Hewlett Packard 5970B series Mass Selective Detector, coupled with a DB-17 fused silica capillary column, 30 m X 0.25 mm i.d., film thickness 0.25 μm. GC analyses were carried out with FID and a DB-17 fused silica capillary column, 30 m X 0.25 mm i.d., film thickness 0.25 μm, and H_2 as carrier gas. Peak areas were integrated electronically. Flash chromatography was performed on Merck silica gel 60 (230–400 mesh).

Solvents were dried and freshly distilled by common practice. For all dry reactions, flasks were dried at 150 °C and flushed with dry N_2, just before use, and reactions were carried out under N_2 unless otherwise reported. Product solutions were dried over $MgSO_4$, unless otherwise noted, and then the solvent was evaporated under reduced pressure.

The starting materials **68**[4], **74**[3], **77**[9], **85**[13] and **94**[5] were prepared following previously described procedures.

(4aα,5α,8aβ)-5-[(*tert*-Butyldimethylsilyl)oxy]decahydro-2,2-dimethoxy-4a-methyl-8-methylenenaphthalene (69). To a stirred solution of 200 mL of 0.275 M (dimethylsulfinyl)sodium in dry DMSO was added 22.0 g (60 mmol) of Ph_3PCH_3Br in small portions at rt. The reaction mixture was stirred at 40 °C for 1 h, after which time a solution of 9.00 g (25.3 mmol) of **68** in 150 mL of dry DMSO was added dropwise. Stirring was continued at 50 °C for 2 h. After cooling to rt, the reaction mixture was diluted with 500 mL of water and extracted with ten 100-mL portions of petroleum ether (bp 40–60 °C). The combined organic layers were washed with 250 mL of brine and dried. After evaporation, the remaining residue was flash chromatographed on silica gel (petroleum ether (bp 40–60 °C)) to give 8.21 g (92%) of **69** as a colorless oil: ^{1}H NMR (90 MHz) δ –0.21 (s, 6 H), 0.53 (s, 3 H), 0.79 (s, 9 H), 1.00–2.33 (m, 11 H), 3.00 (s, 3 H), 3.10 (s, 3 H), 3.26 (dd, J = 5, 11 Hz, 1 H), 4.33 (br s, 1 H), 4.64 (br s, 1 H); MS, *m*/*z* (relative intensity) 354 (M^+, 2.5), 322 (23), 297 (14), 265 (100), 167 (33), 107 (10), 75 (45); calcd for $C_{20}H_{38}O_3Si$ (M^+) *m*/*z* 354.2590, found *m*/*z* 354.2580.

(1α,4β,4aβ,8aα)-4-[(*tert*-Butyldimethylsilyl)oxy]octahydro-7,7-dimethoxy-4a-methylspiro-[naphthalene-1(2*H*),2′-oxirane] (70). A solution of 8.21 g (23.2 mmol) of **69**, 30 mL of $CH(OMe)_3$, and 0.315 g of *p*-TsOH in 300 mL of MeOH was stirred at rt for 45 min, after which time 16.5 g (26.7 mmol) of MMPP was added. The reaction mixture was stirred at rt for 40 h and then concentrated under reduced pressure. The resulting residue was taken up in a mixture of 200 mL of 10% aqueous $Na_2S_2O_3$ and 400 mL of saturated aqueous $NaHCO_3$, and then extracted with six 100-mL portions of CH_2Cl_2. The combined organic layers were dried over a 1:1 mixture of anhyd K_2CO_3 and Na_2SO_4. After evaporation, the resulting product was flash chromatographed on silica gel (10:1 petroleum ether (bp 40–60 °C)/EtOAc) to give 7.49 g (87%) of **70** as a clear oil: ^{1}H NMR (90 MHz) δ –0.13 (s, 6 H), 0.70 (s, 12 H), 0.91–1.87 (m, 11 H), 2.31 (d, J = 4.5 Hz, 1 H), 2.49 (d, J = 4.5 Hz, 1 H), 2.96 (s, 3 H), 3.01 (s, 3 H), 3.19 (m, $W_{1/2}$ = 15 Hz, 1 H); MS, *m*/*z* (relative

intensity) 370 (M^+, 3.5), 338 (19), 313 (39), 281 (91), 265 (10), 175 (20), 101 (35), 75 (100), 55 (19); calcd for $C_{20}H_{38}O_4Si$ (M^+) *m/z* 370.2539, found *m/z* 370.2529.

(4aα,5α,8β,8aβ)-5-[(*tert*-Butyldimethylsilyl)oxy]octahydro-8-hydroxy-4a,8-dimethyl-2(1*H*)-naphthalenone (71). To a solution of 2.49 g (6.73 mmol) of **70** in 300 mL of dry THF was added 1.20 g (32 mmol) of $LiAlH_4$ at 0 °C. The reaction mixture was refluxed for 1 h and then, after cooling to 0 °C, carefully quenched with a small amount of saturated aqueous Na_2SO_4. After addition of 200 mL of EtOAc, the reaction mixture was dried and evaporated to yield 2.48 g (99%) of a crude hydroxy dimethylacetal [^1H NMR (90 MHz) δ –0.12 (s, 3 H), –0.10 (s, 3 H), 0.73 (s, 9 H), 0.90 (s, 3 H), 1.00 (s, 3 H), 1.03-2.50 (m, 12 H), 3.17 (m, 1 H), 3.21 (s, 3 H), 3.27 (s, 3 H)]. This crude product was dissolved in 75 mL of acetone and 10 mL of 10% HCl was added. The reaction mixture was stirred at rt for 15 min and neutralized with 10 mL of saturated aqueous $NaHCO_3$. The reaction mixture was concentrated under reduced pressure, taken up in 50 mL of water, and extracted with three 25-mL portions of CH_2Cl_2. The combined organic layers were dried and evaporated. The resulting product was crystallized from petroleum ether (bp 40–60 °C) to give 1.68 g (77%) of **71** as white crystals: mp 135–137 °C; ^1H NMR (90 MHz) δ –0.15 (s, 6 H), 0.80 (s, 9 H), 0.90–2.40 (m, 12 H), 1.00 (s, 3 H), 1.11 (s, 3 H), 3.21 (dd, J = 4.8, 9.0 Hz, 1 H); MS, *m/z* (relative intensity) 326 (M^+, 2), 311 (2), 269 (100), 251 (25), 193 (17), 159 (24), 133 (10), 119 (17), 75 (85), 43 (38); calcd for $C_{14}H_{25}O_3Si$ (M^+–57) *m/z* 269.1573, found *m/z* 269.1571. Anal. Calcd for $C_{18}H_{34}O_3Si$: C, 66.20; H, 10.49. Found: C, 65.93; H, 10.46.

(1α,4β,4aβ,7α,8aα)-4-[(*tert*-Butyldimethylsilyl)oxy]decahydro-1,4a-dimethyl-1,7-naphthalenediol (72). To a solution of 1.15 g (3.50 mmol) of hydroxy ketone **71** in 100 mL of dry THF was added dropwise 5 mL of 1 M L-Selectride in THF at –78 °C. The solution was stirred at –78 °C for 30 min, allowed to warm to rt over a 30-min period, and then a mixture of 100 mL of C_2H_5OH and 25 mL of water was added. After stirring at rt for 2 h, 70 mL of 6 M aqueous NaOH and 85 mL of 30% H_2O_2 were added at –20 °C and stirring was continued at 0 °C for an additional 16 h. The organic solvents were distilled off under reduced pressure and the remaining aqueous layer was extracted with ten 50-mL portions of CH_2Cl_2. The combined organic layers were washed with three 50-mL portions of water, dried, and then evaporated. The resulting residue was flash chromatographed on silica gel (1:1 petroleum ether (bp 40–60 °C)/EtOAc) to yield 1.075 g (93%) of **72** as white crystals: mp 174–175 °C (from diisopropyl ether); ^1H NMR (200 MHz) δ 0.01 (s, 6 H), 0.83 (s, 3 H), 0.85 (s, 9 H), 1.06 (s, 3 H), 1.21–2.35 (m, 13 H), 3.62 (dd, J = 7.0, 8.0 Hz, 1 H), 4.14 (br s, $W_{1/2}$ = 7 Hz, 1 H); MS, *m/z* (relative intensity) 328 (M^+, 0.5), 313 (3), 271 (100), 253 (12), 195 (4), 161 (70), 119 (40), 105 (40), 75 (70), 43 (44); calcd for $C_{14}H_{27}O_3Si$ (M^+-57) *m/z* 271.1729; found *m/z* 271.1725. Anal. Calcd for $C_{18}H_{36}O_3Si$: C, 65.80; H, 11.04. Found: C, 65.72; H, 11.05.

(1α,4β,4aβ,7β,8aα)-4-[(*tert*-Butyldimethylsilyl)oxy]decahydro-1,4a-dimethyl-1,7-naphthalenediol (73). To a solution of 1.120 g (3.44 mmol) of hydroxy ketone **72** in 150 mL of dry THF was added 1.4 g (36 mmol) of $LiAlH_4$. The reaction mixture was allowed to stir at rt for 15 min and then quenched by the careful addition of a small amount of saturated aqueous Na_2SO_4. The reaction mixture was dried and

evaporated. The resulting product was crystallized from diisopropyl ether to afford 1.069 g (95%) of diol **73** as white crystals: mp 184–187 °C; ^{1}H NMR (200 MHz) δ 0.00 (s, 3 H), 0.01 (s, 3 H), 0.73–1.88 (m, 12 H), 0.85 (s, 12 H), 1.11 (s, 3 H), 2.03 (m, 1 H), 3.19 (dd, J = 6.0, 7.5 Hz, 1 H), 3.58 (m, $W_{1/2}$ = 24 Hz, 1 H); MS, m/z (relative intensity) 271 (M^+–57, 65), 253 (19), 235 (77), 161 (76), 133 (22), 119 (44), 105 (51), 93 (37), 75 (100), 43 (59); calcd for $C_{14}H_{27}O_3Si$ (M^+–57) m/z 271.1729, found m/z 271.1729. Anal. Calcd for $C_{18}H_{36}O_3Si$: C, 65.80; H, 11.04. Found: C, 65.59; H, 11.00.

(4′aα,5′α,8′α,8′aα)-Octahydro-4′a,8′-dimethylspiro[1,3-dioxolane-2,2′(1′*H*)-naphthalene]-5′,8′-diol (75). To a solution of 1.31 g (6.16 mmol) of **74** in a mixture of 30 mL of CH_2Cl_2 and 30 mL of MED were added catalytic amounts of ethylene glycol and camphorsulfonic acid. The reaction mixture was stirred at rt for 24 h, after which time 1.5 mL of Et_3N was added. The reaction mixture was then diluted with 100 mL of CH_2Cl_2 and washed with 50 mL of brine. The organic layer was dried and evaporated to give the crude dioxolane **75**. Recrystallization from MeOH and flash chromatography of the mother liquid (1:2 petroleum ether (bp 40–60 °C)/EtOAc) afforded 1.30 g (82%) of **75**: mp 149–150 °C; ^{1}H NMR (200 MHz) δ 1.04 (s, 3 H), 1.12 (s, 3 H), 1.21–2.02 (m, 13 H), 3.26 (dd, J = 4.0, 11.4 Hz, 1 H), 3.89–3.98 (m, 4 H); ^{13}C NMR (50 MHz) δ 11.47 (q), 26.62 (t), 29.55 (q), 30.34 (2t), 36.26 (t), 38.39 (s), 39.25 (t), 47.30 (d), 63.86 (t), 64.05 (t), 70.96 (s), 78.98 (d), 109.45 (s); MS m/z (relative intensity) 256 (M^+, 2), 238 (2), 206 (2), 198 (6), 167 (3), 139 (2), 99 (100); calcd for $C_{14}H_{24}O_4$ (M^+) m/z 256.1674, found m/z 256.1677. Anal. Calcd for $C_{14}H_{24}O_4$: C, 65.59; H, 9.43. Found: C, 65.31; H, 9.44.

(4′aα,5′α,8′β,8′aβ)-Octahydro-4′a,8′-dimethylspiro[1,3-dioxolane-2,2′(1′*H*)-naphthalene]-5′,8′-diol (76). To a solution of 1.68 g (5.15 mmol) of **71** in 100 mL of acetonitrile was added 3 mL of 40% aqueous HF. The mixture was stirred at rt for 2.5 h and then poured into 250 mL of saturated aqueous $NaHCO_3$. After extraction of the aqueous layer with four 50-mL portions of EtOAc, the combined organic layers were dried and evaporated to give 1.10 g of a dihydroxy ketone [^{1}H NMR (90 MHz) δ 0.89 (s, 3 H), 1.00 (s, 3 H), 1.21–2.59 (m, 13 H), 3.22 (m, 1 H)]. This crude product was treated with MED for 2.5 h as described above for the acetalization of **74**. Workup and flash chromatography (1:2 petroleum ether (bp 40–60 °C)/EtOAc) yielded 0.95 g (72%) of **76**: ^{1}H NMR (200 MHz) δ 0.88 (s, 3 H), 1.06 (s, 3 H), 1.07–1.89 (m, 13 H), 3.32 (dd, J = 4.7, 10.7 Hz, 1 H), 3.83–3.98 (m, 4 H); ^{13}C NMR (50 MHz) δ 11.94 (q), 21.88 (q), 28.47 (t), 30.10 (t), 30.46 (t), 37.57 (t), 38.49 (s), 49.95 (t), 49.73 (d), 63.97 (2t), 70.88 (s), 78.74 (d), 109.25 (s); MS m/z (relative intensity) 256 (M^+, 1.6), 238 (4), 206 (4), 198 (8), 167 (4), 139 (3), 99 (100); calcd for $C_{14}H_{24}O_4$ (M^+) m/z 256.1674, found m/z 256.1678.

(3α,4aβ,5β,8aα)-3-Bromo-5-[(*tert*-butyldimethylsilyl)-oxy]octahydro-4a-methyl-2(1*H*)-naphthalenone (78). To a solution of 2.30 g (8.04 mmol) of DBBA in 95 mL of dry ether was added a solution of 5.10 g (17.0 mmol) of **77** in 40 mL of dry ether. The reaction mixture was allowed to stir at rt for 20 h. After filtration, the reaction mixture was washed with two 100-mL portions of water, dried, and evaporated. The residue was flash chromatographed (50:1 petroleum ether (bp 40–60 °C)/EtOAc) to

give 3.65 g (87%) of a white solid: mp 114–115 °C (from MeOH); ^{1}H NMR (90 MHz) δ –0.11 (s, 6 H), 0.70 (s, 9 H), 0.90 (s, 3 H), 1.12–1.79 (m, 9 H), 2.19 (d, *J* = 8.7 Hz, 1 H), 2.61 (dd, *J* = 7.2, 12.3 Hz, 1 H), 3.11 (m, 1 H), 4.54 (dd, *J* = 7.2, 13.8 Hz, 1 H); MS *m*/*z* (relative intensity) 376 (M^+, 0.2), 374 (M^+, 0.2), 319 (21), 317 (20), 253 (14), 240 (20), 239 (100), 163 (21), 121 (20), 75 (48), 73 (20); calcd for $C_{17}H_{31}Br^{79}O_2Si$ (M^+) *m*/*z* 374.1271, found *m*/*z* 374.1272. Anal. Calcd for $C_{17}H_{31}BrO_2Si$: C, 54.30; H, 8.32. Found: C, 54.70; H, 8.61.

(2α,3β,4aα,5α,8aβ)-3-Bromo-5-[(*tert*-butyldimethyl-silyl)oxy]decahydro-4a-methyl-2-naphthalenol (79). To a stirred solution of 4.42 g (11.8 mmol) of **78** in 150 mL of dry THF was added 7.5 g (30 mmol) of Li(*t*-BuO)$_3$AlH at –78 °C. The reaction mixture was stirred at –78 °C for 3 h and then quenched by dropwise addition of 50 mL of saturated aqueous Na_2SO_4. The two-phase mixture was separated and the aqueous layer was extracted with three 50-mL portions of EtOAc. The combined organic layers were washed with 50 mL of brine, dried, and evaporated. The resulting residue was flash chromatographed (30:1 petroleum ether (bp 40–60 °C)/EtOAc) to yield 4.42 g (99%) of **79** as white crystals: mp 82–85 °C (from petroleum ether (bp 40–60 °C)); ^{1}H NMR (90 MHz), δ –0.18 (s, 6 H), 0.74 (s, 12 H), 0.90–1.80 (m, 10 H), 2.32 (dd, *J* = 12.5, 4.0 Hz, 1 H), 2.45 (br s, 1 H) 3.21 (dd, *J* = 5.0, 10.1 Hz, 1 H), 3.63 (m, 1 H), 4.18 (m, 1 H); MS *m*/*z* (relative intensity) 378 (M^+, 0.3), 376 (M^+, 0.3), 321 (6), 319 (6), 303 (9), 301 (9), 239 (6), 195 (4), 193 (4), 150 (34), 147 (100), 105 (34), 95 (11), 91 (12), 75 (31), 73 (17); calcd for $C_{17}H_{33}Br^{79}O_2Si$ (M^+) *m*/*z* 376.1434, found *m*/*z* 376.1431.

(2α,3β,4aα,5α,8aβ)-5-[(*tert*-Butyldimethylsilyl)oxy]octahydro-4a-methyl[naphthalene-2(1*H*),3(4*H*),2′,3′-oxirane] (80). To a stirred solution of 4.33 g (11.5 mmol) of **79** in 120 mL of dry *t*-BuOH was added 1.74 g (15.5 mmol) of *t*-BuOK. The reaction mixture was heated at reflux for 2 h, allowed to come to rt, and then poured into 150 mL of water. The aqueous solution was extracted with three 100-mL portions of petroleum ether (bp 40–60 °C). The combined organic layers were dried and evaporated. The remaining residue was flash chromatographed (30:1 petroleum ether (bp 40–60 °C)/EtOAc) to give 2.91 g (85%) of **80**: ^{1}H NMR (90 MHz) δ –0.13 (s, 6 H), 0.79 (s, 12 H), 0.88–1.73 (m, 10 H), 2.20 (m, 1 H), 2.91–3.09 (m, 3 H); MS *m*/*z* (relative intensity) 296 (M^+, 1), 281 (1), 239 (46), 221 (67), 147 (67), 119 (20), 105 (47), 93 (15), 91 (29), 81 (15), 79 (20), 75 (100); calcd for $C_{17}H_{32}O_2Si$ (M^+) *m*/*z* 296.2171, found *m*/*z* 296.2169.

(4aα,8β,8aβ)-8-[(*tert*-Butyldimethylsilyl)oxy]octahydro-8a-methyl-2(1*H*)-naphthalenone (81). To a solution of 2.73 g (9.22 mmol) of **80** in 150 mL of dry THF was added 0.85 g (22 mmol) of $LiAlH_4$ at rt. The reaction mixture was refluxed for 90 min and then, after cooling to 0 °C, quenched with 50 mL of saturated aqueous Na_2SO_4. The reaction mixture was extracted with three 100-mL portions of EtOAc. The organic layers were combined and dried. Evaporation yielded 2.66 g of a pale yellow oil [^{1}H NMR (90 MHz) δ 0.10 (s, 6 H), 0.79 (s, 9 H), 0.81–2.33 (m, 14 H), 0.92 (s, 3 H), 3.29 (m, 1 H), 4.07 (br s, 1 H)]. This oil was dissolved in 125 mL of CH_2Cl_2, and then 5.15 g (13.7 mmol) of PDC was added. The reaction mixture was allowed to stir at rt for 20 h and filtered through Celite, and the filter cake was washed with two 100-mL portions of CH_2Cl_2. The solvent was evaporated and the resulting residue was flash

chromatographed (20:1 petroleum ether (bp 40–60 °C)/ EtOAc) to give 2.39 g (88%) of **81** as a white solid: mp 117–119 °C (from diisopropyl ether); ^{1}H NMR (200 MHz) δ –0.02 (s, 3 H), 0.00 (s, 3 H), 0.71 (s, 3 H), 0.84 (s, 9 H), 1.15–2.09 (m, 11 H), 2.29 (m, 1 H), 2.47 (m, 1 H), 3.22 (dd, *J* = 4.7, 9.2 Hz, 1 H); ^{13}C NMR (50 MHz) δ –5.07 (q), –4.26 (q), 10.37 (q), 17.77 (s), 23.68 (t), 25.60 (3q), 27.01 (t), 28.40 (t), 30.17 (t), 41.22 (t), 42.46 (d), 43.21 (s), 53.00 (t), 78.58 (d), 211.73 (s); MS *m/z* (relative intensity), 296 (M^+, 0.4), 281 (4), 239 (100), 181 (62), 157 (10), 147 (30), 115 (11), 107 (11), 75 (40), 73 (14); calcd for $C_{17}H_{32}O_2Si$ (M^+) *m/z* 296.2171, found *m/z* 296.2166. Anal. Calcd for $C_{17}H_{32}O_2Si$: C, 68.88; H, 10.88. Found: C, 68.79; H, 10.99.

(2α,4aβ,8α,8aα)-Decahydro-2,8a-dimethyl-2,8-naphthalenediol (82). The TBDMS-ether **81** (2.61 g, 8.81 mmol) was treated with HF as described for the desilylation of **71**. Workup afforded 1.59 g of a crude keto alcohol [^{1}H NMR (90 MHz) δ 0.75 (s, 3 H), 0.81-1.89 (m, 8 H), 1.90–2.59 (m, 6 H), 3,37 (m, 1 H)]. A solution of this crude product in 100 mL of dry ether was added dropwise to 10 mL of 2.6 M MeMgI in ether. The reaction mixture was stirred at rt for 30 min, after which time the excess MeMgI was destroyed cautiously with saturated aqueous NH_4Cl. After dilution with 100 mL of water, the two-phase mixture was separated and the aqueous layer was extracted with three 100-mL portions of EtOAc. The combined organic layers were washed with 100 mL of brine, dried, and evaporated. The remaining residue was crystallized from *n*-hexane to yield 1.31 g (76%) of **82** as white crystals: mp 158–160 °C; ^{1}H NMR (200 MHz) δ 0.97–2.20 (m, 15 H), 1.02 (s, 3 H), 1.18 (s, 3 H), 3.14 (dd, *J* = 4.6, 10.6 Hz, 1 H); ^{13}C NMR (50 MHz) δ 11.56 (q), 24.09 (t), 24.30 (t), 27.11 (t), 29.71 (t), 33.28 (q), 39.49 (s), 39.52 (t), 44.01 (d), 49.20 (t), 71.10 (s), 80.12 (d); MS *m/z* (relative intensity) 198 (M^+, 11), 183 (96), 180 (100), 162 (37), 147 (54), 122 (57), 107 (88), 95 (41), 85 (46), 81 (52); calcd for $C_{12}H_{22}O_2$ (M^+) *m/z* 198.1620, found *m/z* 198.1624. Anal. Calcd for $C_{12}H_{22}O_2$: C, 72.67; H, 11.18. Found C, 72.40; H, 11.38.

(1α,4aβ,8aα)-1-[(*tert*-Butyldimethylsilyl)oxy]decahydro-8a-methyl-7-methylenenaphthalene (83). The procedure described for the synthesis of **69** was employed by using 125 mL of 0.103 M (dimethylsulfinyl)sodium in dry DMSO, 5.0 g (14 mmol) of Ph_3PCH_3Br, and 3.00 g (10.1 mmol) of **81** in 100 mL of DMSO. When the dropwise addition of the DMSO solution was complete, stirring was continued for 16 h at rt. After the usual workup the remaining residue was flash chromatographed (petroleum ether (bp 40–60 °C)) to give 2.76 g (93%) of **83** as a colorless oil: ^{1}H NMR (90 MHz) δ 0.02 (s, 6 H), 0.72 (s, 3 H), 0.91 (s, 9 H), 1.02–2.49 (m, 13 H), 3.23 (dd, *J* = 5.5, 9.2 Hz, 1 H), 4.56 (br s, 1 H), 4.65 (br s, 1 H); MS *m/z* (relative intensity) 294 (M^+, 0.8), 279 (1), 237 (40), 219 (6), 161 (30), 119 (8), 105 (7), 91 (7), 75 (100), 41 (14); calcd for $C_{14}H_{25}OSi$ (M^+–57) *m/z* 237.1675, found *m/z* 237.1677.

(2α,4aα,8β,8aβ)-Decahydro-2,8a-dimethyl-2,8-naphthalenediol (84). The silyl ether **83** (2.00 g, 6.80 mmol) was treated with HF for 2.5 h as described above for the desilylation of **71**. Workup yielded 1.19 g of an alcohol [^{1}H NMR (90 MHz) δ 0.81 (s, 3 H), 1.01–2.56 (m, 14 H), 3.39 (m, 1 H), 4.65 (br s, 1 H), 4.71 (br s, 1 H)]. To a solution of this crude product in 150 mL of CH_2Cl_2 were added 150 mL of acetone, 50 mL of water, 0.075 g of 18-crown-6, and 8.5 g of $NaHCO_3$. The mixture was stirred vigorously and then 50

mL of 0.29 M oxone[11] (29 mmol of $KHSO_5$) in water was added dropwise at 0 °C. Stirring was continued for an additional 30 min, after which time 100 mL of 10% aqueous $Na_2S_2O_3$ and 150 mL of saturated aqueous $NaHCO_3$ were added. The two-phase mixture was separated and the aqueous layer was extracted with seven 25-mL portions of CH_2Cl_2. The combined organic layers were dried and evaporated. The remaining residue was flash chromatographed (10:1 petroleum ether (bp 40–60 °C)/EtOAc) to yield 0.90 g of a single epoxide [^{1}H NMR (200 MHz) δ 0.85 (s, 3 H), 1.01–1.85 (m, 14 H), 2.52–2.72 (m, 2 H), 3.28 (m, 1 H)]. This epoxide was treated with $LiAlH_4$ (0.75 g, 19 mmol) as described above for the reduction of the epoxide **70**. The usual workup resulted in a crude product that was crystallized from *n*-hexane to afford 0.90 g (64%) of diol **84** as white crystals: mp 141–143 °C; ^{1}H NMR (200 MHz) δ 0.74 (s, 3 H), 0.76–1.74 (m, 13 H), 1.34 (s, 3 H), 1.91–2.11 (m, 2 H), 3.18 (dd, J = 4.3, 10.6 Hz, 1 H); ^{13}C NMR (50 MHz) δ 11.92 (q), 24.03 (t), 26.41 (t), 26.70 (t), 29.14 (q), 29.41 (t), 39.37 (s), 41.11 (t), 44.03 (d), 52.17 (t), 70.85 (s), 80.14 (d); MS *m*/*z* (relative intensity) 198 (M^+, 1.6), 183 (3), 180 (7), 147 (11), 124 (20), 107 (22), 81 (24), 67 (28), 55 (13), 43 (100); calcd for $C_{12}H_{20}O$ (M^+–18) *m*/*z* 180.1514, found *m*/*z* 180.1517. Anal. Calcd for $C_{12}H_{22}O_2$: C, 72.67; H, 11.18. Found: C, 72.45; 11.48.

(4'aα)-Tetrahydro-4'a,7',7'-trimethylspiro[1,3-dithiolane-2,2'(3'*H*)-naphthalen]-5'(6'*H*)-one (86). To a stirred solution of 20.0 g (97.1 mmol) of **85** and 9.20 g of *p*-TsOH in 50 mL of AcOH was added 10.5 mL (125 mmol) of 1,2-ethanedithiol. The mixture was stirred at rt for 18 h, poured into 100 mL of water, and then extracted with five 50-mL portions of CH_2Cl_2. The combined organic layers were washed with two 150-mL portions of 4 M aqueous NaOH and one 50-mL portion of water, and then dried. Evaporation and crystallization from diisopropyl ether/EtOAc yielded 25.00 g (91%) of **86**: mp 150–153 °C; ^{1}H NMR (200 MHz) δ 0.72 (s, 3 H), 1.03 (s, 3 H), 1.23 (s, 3 H), 1.63-2.30 (m, 6 H), 2.45-2.60 (m, 2 H), 3.11–3.40 (m, 4 H), 5.59 (br s, 1 H); ^{13}C NMR (50 MHz) δ 24.00 (q), 25.37 (q), 30.35 (t), 30.72 (q), 34.11 (s), 37.26 (t), 39.43 (t), 40.02 (t), 44.74 (t), 47.95 (s), 51.15 (t), 64.66 (s), 129.31 (d), 139.22 (s), 213.10 (s); MS *m*/*z* (relative intensity) 282 (M^+, 62), 267 (65), 264 (9), 254 (8), 239 (16), 221 (44), 189 (19), 118 (100), 105 (34), 91 (24), 83 (20), 41 (29); calcd for $C_{15}H_{22}OS_2$ (M^+) *m*/*z* 282.1112, found *m*/*z* 282.1112.

Dissolving Metal Reduction of 86. To dry, distilled NH_3 (250 mL) was added dropwise a solution of 25.6 g (90.0 mmol) of **86** in 100 mL of dry ether at –78 °C. To the vigorously stirred solution were added small pieces of sodium metal until the blue color persisted. The cooling bath was removed, and the blue solution was kept at reflux for 1 h. Saturated aqueous Na_2SO_4 (5 mL) was added cautiously to the reaction flask, and the ammonia was allowed to evaporate overnight. Water (300 mL) was added to the residue, and the aqueous phase was extracted with three 150-mL portions of EtOAc. The combined organic layers were dried and evaporated. The remaining residue was flash chromatographed (20:1 petroleum ether (bp 40–60 °C)/EtOAc) to yield 1.39 g (8%) of α-hydroxy olefin **87a** and 14.02 g (80%) of its β-isomer **87b**.

(1α,8aβ)-1,2,3,4,6,7,8,8a-Octahydro-3,3,8a-trimethyl-1-naphthalenol (87a): ^{1}H NMR (200 MHz) δ 0.91 (s, 3 H), 0.97 (s, 3 H), 1.05 (s, 3 H), 1.23–2.24 (m, 11 H), 3.52 (m, 1 H), 5.51 (m, 1 H); ^{13}C NMR

(50 MHz) δ 19.36 (t), 25.02 (q), 25.44 (t), 28.16 (q), 31.65 (s), 32.11 (t), 33.11 (q), 39.06 (s), 41.62 (t), 45.04 (t), 76.91 (d), 124.67 (d), 138.04 (s); MS *m/z* (relative intensity) 194 (M^+, 23), 179 (14), 176 (65), 161 (57), 147 (48), 133 (45), 119 (24), 109 (92), 91 (64), 85 (72), 67 (71), 55 (45), 41 (100); calcd for $C_{13}H_{22}O$ (M^+) *m/z* 194.1670, found *m/z* 194.1669.

(1α,8aα)-1,2,3,4,6,7,8,8a-Octahydro-3,3,8a-trimethyl-1-naphthalenol (87b): ^1H NMR (200 MHz) δ 0.73–2.15 (m, 11 H), 0.80 (s, 3 H), 0.90 (s, 3 H), 0.93 (s, 3 H), 3.46 (dd, *J* = 8.1, 8.5 Hz, 1 H), 5.43 (m, 1 H); ^{13}C NMR (50 MHz) δ 16.81 (q), 18.69 (t), 25.28 (q), 25.59 (t), 31.98 (q), 31.98 (s), 35.81 (t), 39.43 (s), 43.61 (t), 44.93 (t), 75.70 (d), 123.48 (d), 139.85 (s); MS *m/z* (relative intensity) 194 (M^+, 17), 179 (8), 176 (68), 161 (71), 147 (78), 133 (73), 120 (25), 109 (73), 91 (57), 85 (58), 67 (65), 41 (100); calcd for $C_{13}H_{22}O$ (M^+) *m/z* 194.1670, found *m/z* 194.1664.

(1α,8aα)-1-[(*tert*-Butyldimethylsilyl)oxy]-1,2,3,4,6,7,8,-8a-octahydro-3,3,8a-trimethylnaphthalene (88). To a solution of 5.72 g (29.5 mmol) of **87b** in 200 mL of DMF were added 6.60 g (95.0 mmol) of imidazole and 7.01 g (46.6 mmol) of TBDMSCl. The reaction mixture was stirred at rt for 48 h and then poured into 250 mL of water. The two-phase mixture was separated, and the aqueous layer was extracted with ten 25-mL portions of CH_2Cl_2. The combined organic layers were washed with 100 mL of brine, dried, and evaporated. The resulting product was flash chromatographed (petroleum ether (bp 40–60 °C)) to give 8.12 g (89%) of **88** as a clear oil: ^1H NMR (200 MHz) δ 0.02 (s, 6 H), 0.81 (s, 3 H), 0.90 (s, 9 H), 0.93 (s, 3 H), 0.96 (s, 3 H), 1.20–1.81 (m, 7 H), 1.90–2.03 (m, 2 H), 2.13 (m, 1 H), 3.44 (dd, *J* = 4.8, 11.5 Hz, 1 H), 5.34 (m, 1 H); ^{13}C NMR (50 MHz) δ –4.98 (q), –4.19 (q) 17.20 (q), 17.83 (s), 18.86 (t), 25.33 (q), 25.66 (3q), 25.66 (t), 31.69 (s), 32.12 (q), 36.46 (t), 39.94 (s), 44.41 (t), 45.04 (t), 75.90 (d), 123.08 (d), 140.45 (s); MS *m/z* (relative intensity) 308 (M^+, 1.6), 293 (4), 251 (92), 199 (100), 177 (42), 176 (54), 151 (8), 133 (10), 75 (51); calcd for $C_{19}H_{36}OSi$ (M^+) *m/z* 308.2535, found *m/z* 308.2535.

(4aα,5α,8aβ)-5-[(*tert*-Butyldimethylsilyl)oxy]octahydro-4a,7,7-trimethyl-1(2*H*)-naphthalenone (89). To a stirred solution of 7.41 g (24.1 mmol) of **88** in 150 mL of dry THF, cooled to 0 °C, was added dropwise 35 mL (35 mmol) of BH_3•THF (1.0 M in THF). The reaction mixture was stirred at rt for 6 h and then heated at reflux for 1 h. The reaction mixture was cooled to 0 °C and another 20 mL (20 mmol) of BH_3•THF (1.0 M in THF) was added dropwise. Stirring was continued at rt for an additional 30 min. The reaction mixture was cooled again to 0 °C and 10 mL of water was added dropwise, immediately followed by addition of 45 mL of 4 M NaOH and 50 mL of 35% H_2O_2. The mixture was stirred at rt for 16 h and concentrated under reduced pressure. The remaining aqueous phase was extracted with six 100-mL portions of petroleum ether (bp 40–60 °C). The combined organic layers were dried and evaporated. The resulting clear oil was treated with PDC (10.0 g, 25.1 mmol) as described above for the synthesis of **81**. After the usual workup the resulting residue was dissolved in 200 mL of dry MeOH. After addition of 30 mL of 1 M NaOMe in dry MeOH, the solution was stirred at rt for 1 h and then neutralized with 4 N HCl. MeOH was distilled off under reduced pressure, and the aqueous phase was extracted with seven 50-mL portions of EtOAc. The combined organic layers were dried and evaporated. Recrystallization from *n*-

hexane gave 6.5 g (83%) of **89**: mp 80–81 °C; ^{1}H NMR (200 MHz) δ 0.01 (s, 3 H), 0.02 (s, 3 H), 0.67 (s, 3 H), 0.84 (s, 9 H), 0.87 (s, 3 H), 0.93 (s, 3 H), 1.15–1.50 (m, 5 H), 1.70–2.07 (m, 3 H), 2.20–2.38 (m, 3 H), 3.58 (dd, *J* = 5.6, 10.4 Hz, 1 H); ^{13}C NMR (50 MHz) δ –5.01 (q), –4.22 (q), 10.48 (q), 17.77 (s), 22.39 (t), 25.57 (3q), 25.86 (q) 30.16 (s), 32.63 (t), 32.90 (q), 36.56 (t), 41.04 (t), 43.09 (t), 44.87 (s), 52.44 (d), 75.57 (d), 212.46 (s); MS *m/z* (relative intensity) 324 (M^+, 1.2), 267 (68), 225 (6), 175 (20), 133 (15), 119 (26), 105 (24), 75 (100), 41 (38); calcd for $C_{19}H_{36}O_2Si$ (M^+) *m/z* 324.2484, found *m/z* 324.2481. Anal. Calcd for $C_{19}H_{36}O_2Si$: C, 70.33; H, 11.18. Found: C, 70.54; H, 11.18.

(1α,4aα,5α,8aβ)-5-[(*tert*-Butyldimethylsilyl)oxy]decahydro-1,4a,7,7-tetramethyl-1-naphthal-enol (90). The ketone **89** (3.11 g, 9.60 mmol) was treated with 2.6 M MeMgI in ether for 2 h as described for the synthesis of **82**. After workup, the crude product was purified by flash chromatography (10:1 petroleum ether (bp 40–60 °C)/EtOAc) to yield 2.75 g (84%) of **90** as a clear oil: ^{1}H NMR (200 MHz) δ –0.01 (s, 6 H), 0.86 (s, 9 H), 0.91 (s, 3 H), 0.92 (s, 3 H), 0.94 (s, 3 H), 1.06–1.41 (m, 10 H), 1.11 (s, 3 H), 1.60–1.90 (m, 2 H), 3.25 (dd, *J* = 4.5, 11 Hz, 1 H); ^{13}C NMR (50 MHz) δ –4.96 (q), –4.27 (q), 10.97 (q), 17.57 (t), 17.82 (s), 25.65 (3q), 26.69 (q), 30.40 (q), 30.41 (s), 33.24 (q), 33.24 (t), 37.56 (t), 39.55 (s), 40.95 (t), 43.33 (t), 46.18 (d), 71.77 (s), 77.01 (d); MS *m/z* (relative intensity) 340 (M^+, 0.5), 283 (1), 265 (100), 247 (2), 189 (10), 169 (20), 107 (10), 95 (13), 75 (72), 55 (14), 43 (37); calcd for $C_{20}H_{40}O_2Si$ (M^+) *m/z* 340.2797, found *m/z* 340.2797.

(1α,4aβ,5β,8aα)-5-[(*tert*-Butyldimethylsilyl)oxy]octahydro-4a,7,7-trimethylspironaphthal-ene-1(2*H*),2'-oxirane] (92). The procedure described for the synthesis of **69** was employed by using 75 mL of 0.33 M (dimethylsulfinyl)sodium in dry DMSO, 10.8 g (30 mmol) of Ph_3PCH_3Br, and 2.50 g (7.71 mmol) of **89** in 50 mL of dry ether.[21] When the dropwise addition of the etheral solution was complete, ether was distilled off at 50 °C. After stirring at rt for an additional 1 h, the usual workup afforded 2.26 g of a clear oil [^{1}H NMR (200 MHz) δ 0.02 (s, 6 H), 0.62 (s, 3 H), 0.86 (s, 9 H), 0.93 (s, 3 H), 0.94 (s, 3 H), 1.01–1.98 (m, 10 H), 2.28 (m, 1 H), 3.47 (dd, *J* = 5.0, 11.1 Hz, 1 H), 4.42 (br s, 1 H), 4.70 (br s, 1 H)]. This crude product was treated with oxone[11] for 21 h as described for the synthesis of **84**. Workup and flash chromatography (25:1 petroleum ether (bp 40–60 °C)/EtOAc) afforded 2.276 g (87%) of **92** as a clear oil: ^{1}H NMR (200 MHz) δ 0.00 (s, 6 H), 0.75 (s, 3 H), 0.83–1.94 (m, 11 H), 0.84 (s, 9 H), 0.88 (s, 3 H), 0.90 (s, 3 H), 2.48 (d, *J* = 4.7 Hz, 1 H), 2.69 (br d, *J* = 4.7 Hz, 1 H), 3.41 (dd, *J* = 5.4, 10.5 Hz, 1 H); ^{13}C NMR (50 MHz) δ –4.96 (q), –4.24 (q), 10.16 (q), 17.82 (s), 20.72 (t), 25.63 (3q), 25.84 (q), 30.48 (s), 31.82 (t), 33.19 (q), 35.30 (t), 37.30 (t), 41.69 (s), 41.69 (d), 43.61 (t), 50.60 (t), 58.76 (s), 76.37 (d); MS *m/z* (relative intensity) 338 (M^+, 0.1), 323 (3), 281 (100), 263 (4), 251 (4), 199 (11), 189 (17), 132 (17), 76 (56); calcd for $C_{20}H_{38}O_2Si$ (M^+) *m/z* 338.2641, found *m/z* 338.2641.

(1α,4aα,5α,8aβ)-Decahydro-1,4a,7,7-tetramethyl-1,5-naphthalenediol (91). To a solution of 2.50 g (7.35 mmol) of **90** in 75 mL of acetonitrile were added five drops of 40% aqueous HF. The reaction mixture was stirred at rt for 2 h. Then two drops of 40% aqueous HF were added every 2 h over a period of

8 h. After this time, the reaction mixture was poured into 150 mL of saturated aqueous $NaHCO_3$. The aqueous layer was extracted with five 25-mL portions of CH_2Cl_2, after which the combined organic layers were dried and evaporated. The crude product was flash chromatographed (5:1 petroleum ether (bp 40-60 °C)/EtOAc) to yield 1.27 g (76%) of **91**: mp 133–135 °C (from petroleum ether (bp 40–60 °C)); ^{1}H NMR (200 MHz) δ 0.93 (s, 3 H), 0.95 (s, 3 H), 0.97 (s, 3 H), 0.98–1.92 (m, 13 H), 1.13 (s, 3 H), 3.29 (dd, J = 6.7, 9.7 Hz, 1 H); ^{13}C NMR (50 MHz) δ 10.65 (q), 17.40 (t), 26.70 (q), 30.65 (q), 30.65 (s), 33.13 (q), 33.30 (t), 36.94 (t), 39.15 (s), 40.88 (t), 42.76 (t), 45.96 (d), 71.62 (s), 76.77 (d); MS m/z (relative intensity) 226 (M^+, 1.3), 211 (8), 193 (6), 190 (12), 175 (10), 150 (30), 135 (20), 95 (21), 71 (28), 43 (100); calcd for $C_{14}H_{26}O_2$ (M^+) m/z 226.1933, found m/z 226.1935. Anal. Calcd for $C_{14}H_{26}O_2$: C, 74.28; H, 11.58. Found: C, 74.32; H, 11.72.

(1α,4aβ,5β,8aα)-Decahydro-1,4a,7,7-tetramethyl-1,5-naphthalenediol (93). The epoxide **92** (2.01 g, 5.95 mmol) was treated with $LiAlH_4$ for 2 h as described for the reduction of **70**. The excess $LiAlH_4$ was destroyed by careful addition of a small amount of saturated aqueous Na_2SO_4 to the cooled reaction mixture. After drying and evaporation, flash chromatography (15:1 petroleum ether (bp 40–60 °C)/EtOAc) gave 1.90 g of a clear oil. This oil was taken up in 150 mL of DMSO and 7.5 mL of TBAF (1.1 M in THF) was added. The reaction mixture was stirred at 100 °C for 90 min and then poured into 100 mL of water. The aqueous mixture was extracted with eight 25-mL portions of EtOAc. The combined organic layers were dried and evaporated. Flash chromatography (10:1 to 5:1 petroleum ether (bp 40–60 °C)/EtOAc) gave 1.09 (82%) of **93** as a white solid: mp 161–162 °C (from petroleum ether (bp 40–60 °C)/EtOAc); ^{1}H NMR (200 MHz) δ 0.78 (s, 3 H), 0.95 (s, 3 H), 0.96 (s, 3 H), 1.01-1.81 (m, 13 H), 1.11 (s, 3 H), 3.34 (m, 1 H); ^{13}C NMR (50 MHz) δ 10.56 (q), 19.59 (t), 22.89 (q), 26.38 (q), 30.62 (s), 33.20 (q), 33.21 (t), 36.65 (t), 40.06 (s), 42.86 (t), 42.94 (t), 48.76 (d), 71.63 (s), 77.17 (d); MS m/z (relative intensity) 226 (M^+, 3), 208 (8), 193 (22), 190 (17), 175 (14), 150 (100), 135 (35), 95 (28), 70 (50), 43 (47); calcd for $C_{14}H_{26}O_2$ (M^+) m/z 226.1933, found m/z 226.1933. Anal. Calcd for $C_{14}H_{26}O_2$: C, 74.28; H, 11.58. Found: C, 74.52; H, 11.97.

(4α,4aα)-4-[(*tert*-Butyldimethylsilyl)oxy]-3,4,4a,5-tetrahydro-4a,8-dimethylnaphthalene-1(2*H*),7(6*H*)-dione (95). The enedione acetate **94** (12.46 g, 19.82 mmol) was treated with NaOMe at 0 °C as described for the synthesis of **89**. After workup and flash chromatography (1:1 petroleum ether (bp 40–60 °C)/EtOAc) 8.02 g of a crude alcohol was obtained [^{1}H NMR (200 MHz) δ 1.05 (s, 3 H), 1.69 (s, 3 H), 1.85–2.16 (m, 4 H), 2.33–2.57 (m, 4 H), 2.88 (d, J = 5.0 Hz, 1 H), 3.85 (dd, J = 4.7, 8.9 Hz, 1 H)]. This alcohol was treated with TBDMSCl for 5 d at 40 °C as described for the silylation of **87b**. After workup, the crude product was purified by flash chromatography (10:1 petroleum ether (bp 40–60 °C)/EtOAc) to yield 10.20 g (63%) of **95** as a white solid: mp 63–65 °C (from petroleum ether (bp 40–60 °C)); ^{1}H NMR (200 MHz) δ 0.06 (s, 6 H), 0.88 (s, 9 H), 1.08 (s, 3 H), 1.75 (s, 3 H), 1.77–2.09 (m, 4 H), 2.33–2.55 (m, 4 H), 3.81 (dd, J = 5.8, 9.8 Hz, 1 H); ^{13}C NMR (50 MHz) δ –5.08 (q), –4.25 (q), 12.35 (q), 15.26 (q), 17.75 (s), 25.49 (3q), 29.13 (t), 33.17 (t), 33.74 (t), 39.87 (t), 43.94 (s), 76.26 (d), 133.13 (s), 153.38 (s), 199.28 (s), 204.13 (s); MS m/z (relative intensity) 322 (M^+, 1), 307 (3), 265 (81), 247 (18), 173 (17), 143 (29), 75 (100), 41 (23); calcd

for $C_{14}H_{21}O_3Si$ (M^+–57) *m/z* 265.1260, found *m/z* 265.1259. Anal. Calcd for $C_{18}H_{30}O_3Si$: C, 67.03; H, 9.38. Found: C, 67.11; H, 9.70.

Lithium-ammonia Reduction of 95. To vigorously stirred dry liquid NH_3 (30 mL) were added small pieces of lithium metal (0.20 g) at –78 °C. A solution of 0.50 g (1.55 mmol) of **95** in 15 mL of dry THF was added dropwise at –78 °C and the mixture was allowed to stir at reflux temperature for 30 min, after which time the ammonia was quickly evaporated under reduced pressure. The remaining THF solution was stirred at 0 °C for 30 min. Then 0.50 g of NH_4Cl was added at once to the vigorously stirred reaction mixture. After stirring for an additional 15 min, the mixture was poured into 50 mL of icewater, and extracted with three 75-mL portions of EtOAc. The combined organic layers were dried and evaporated. The remaining residue was flash chromatographed (15:1 petroleum ether (bp 40–60 °C)/EtOAc) to yield 0.088 g (17%) of **(4α,4aα,7α,8β,8aβ)-4-[(*tert*-butyldimethylsilyl)oxy]octahydro-7-hydroxy-4,8-dimethyl-1(2*H*)-naphthaleneone (96):** ^1H NMR (200 MHz) δ 0.04 (s, 6 H), 0.86 (s, 12 H), 0.91–1.89 (m, 6 H), 1.05 (d, *J* = 7.1 Hz, 3 H), 1.98–2.09 (m, 2 H), 2.20–2.47 (m, 3 H), 3.64–3.49 (m, 2 H); ^{13}C NMR (50 MHz) δ –4.98 (q), –4.25 (q), 9.44 (q), 14.77 (q), 17.77 (s), 25.06 (t), 25.55 (3q), 29.70 (t), 33.28 (d), 36.50 (t), 38.68 (t), 44.37 (s), 56.54 (d), 73.13 (d), 78.16 (d), 209.19 (s); MS *m/z* (relative intensity) 311 (M^+–15, 1), 269 (100), 252 (25), 177 (18), 159 (23), 135 (46), 75 (37); calcd for $C_{17}H_{31}O_3Si$ (M^+–15) *m/z* 311.2042, found *m/z* 311.2041, and 0.347 g (69%) of a 3:5 mixture of two isomeric diketones **97**. A larger scale reduction of **95** gave a lower yield and a different ratio of **96** (22%) and **97** (35%).

A sample of 0.90 g (2.78 mmol) of **97** was treated with NaOMe as described for the synthesis of **89**. After workup, the crude product was acetalized with MED as described for the preparation of **75**. Workup and flash chromatography (15:1 petroleum ether (bp 40–60 °C)/EtOAc) afforded, in order of elution, 0.663 g (65%) of pure **98a**, 0.091 g (9%) of a 4:1 mixture of **98a** and **98b**, respectively, and 0.200 g (19%) of pure **98b** . The spectroscopic data of **98a** and **98b** are shown below

(4'α,4'aα,8'β,8'aβ)-4'-[(*tert*-Butyldimethylsilyl)oxy]octahydro-4'a,8'-dimethylspiro[1,3-dioxolane-2,7'(6'*H*)-naphthalen]-1'(2'*H*)-one (98a). ^1H NMR (200 MHz) δ 0.03 (s, 6 H), 0.74 (s, 3 H), 0.79 (d, *J* = 7.7 Hz, 3 H), 0.82 (s, 9 H), 1.29–2.25 (m, 9 H), 2.32 (d, *J* = 11.6 Hz, 1 H), 3.72 (dd, *J* = 5.2, 10.8 Hz, 1 H), 3.87 (m, 4 H); ^{13}C NMR (50 MHz) δ –4.78 (q), –4.08 (q), 11.01 (q), 11.29 (q), 17.94 (q), 25.76 (3q), 30.29 (t), 31.90 (t), 34.31 (d), 35.01 (t), 40.27 (t), 43.85 (s), 58.28 (d), 64.97 (t), 65.12 (t), 77.57 (d), 110.55 (s), 209.97 (s); MS *m/z* (relative intensity) 368 (M^+, 0.9), 311 (24), 249 (4), 193 (11), 175 (8), 99 (100), 75 (30), 41 (11); calcd for $C_{20}H_{36}O_4Si$ (M^+) *m/z* 268.2383, found *m/z* 268.2383.

(4'α,4'aα,8'β,8'aα)-4'-[(*tert*-Butyldimethylsilyl)oxy]octahydro-4'a,8'-dimethylspiro[1,3-dioxolane-2,7'(6'*H*)-naphthalen]-1'(2'*H*)-one (98b). ^1H NMR (200 MHz) δ –0.01 (s, 1 H), 0.68 (d, *J* = 5.66 Hz, 3 H), 0.81 (s, 3 H), 0.84 (s, 9 H), 0.96–2.49 (m, 10 H), 3.93 (m, 4 H), 4.36 (dd, *J* = 5.4, 11.1 Hz, 1 H); ^{13}C NMR (50 MHz) δ –4.91 (q), –4.22 (q), 11.07 (q), 18.01 (s), 20.98 (q), 25.74 (3q), 30.51 (t), 30.68 (t), 32.35 (t), 36.30 (t), 37.85 (d), 41.23 (s), 63.39 (d), 65.08 (t), 65.38 (t), 66.66 (d), 109.09 (s), 212.17 (s); MS *m/z* (relative intensity) 368 (M^+, < 0.1), 311 (45), 249 (11), 223 (10), 183 (13), 99 (100), 75 (40), 41 (14); calcd for $C_{20}H_{36}O_4Si$ (M^+) *m/z* 268.2383, found *m/z* 268.2385.

(1α,4aβ,5β,8β,8aα)-5-[(*tert*-Butyldimethylsilyl)oxy]octahydro-8-hydroxy-1,4a,8-trimethyl-2(3*H*)-naphthalenone (99). Treatment of **98a** (0.60 g, 1.63 mmol) with MeMgI as described for the preparation of **82** gave, after workup, 0.62 g of a crude product. This was taken up in 25 mL of acetone and 1.5 mL of 4 M HCl was added. After stirring at rt for 3 h, the solution was neutralized with 4 M NaOH. After dilution with 100 mL of water, the reaction mixture was extracted with three 50-mL portions of EtOAc. The combined organic layers were washed with 50 mL of brine, dried and evaporated. Flash chromatography (10:1 petroleum ether (bp 40–60 °C)/EtOAc) gave 0.385 g (70%) of **99**: ^{1}H NMR (200 MHz) δ 0.01 (s, 3 H), 0.03 (s, 3 H), 0.86 (s, 9 H), 0.93 (s, 3 H), 1.21 (s, 3 H), 1.27 (d, J = 9.0 Hz, 3 H), 1.33–2.09 (m, 8 H), 2.32–2.59 (m, 3 H), 3.24 (dd, J = 3.8, 11.1 Hz, 1 H); ^{13}C NMR (50 MHz) δ –5.08 (q), –4.13 (q), 13.32 (q), 17.81 (s), 21.74 (q), 25.59 (3q), 26.96 (t), 30.24 (q), 33.22 (t), 34.58 (t), 39.57 (t), 39.90 (s), 42.70 (d), 56.31 (d), 71.43 (s), 78.47 (d), 216.98 (s); MS m/z (relative intensity) 319 (M^+–57, 47), 265 (15), 191 (100), 174 (21), 149 (79), 133 (78), 76 (89); calcd for $C_{15}H_{27}O_3Si$ (M^+–57) m/z 283.1729, found m/z 283.1732.

(1α,4α,4aα,7α,8β,8aβ)-4-[(*tert*-Butyldimethylsilyl)oxy]decahydro-1,4a,8-trimethyl-1,7-naphthalenediol (100). a. The ketone **99** (0.28 g, 0.81 mmol) was treated with $LiAlH_4$ for 10 min as described for the synthesis of **73**. After workup, the crude product was purified by recrystallization from 5:1 diisopropyl ether/EtOAc to give 0.255 g (92%) of **100**: mp 84–85 °C; ^{1}H NMR (200 MHz) δ –0.09 (s, 3 H), –0.08 (s, 3 H), 0.75 (s, 9 H), 0.83–1.62 (m, 8 H), 1.02 (s, 3 H), 1.11 (d, J = 6.8 Hz, 3 H), 1.25 (s, 3 H), 1.64–1.85 (m, 4 H), 3.00 (m, 2 H); ^{13}C NMR (50 MHz) δ –5.25 (q), –4.34 (q), 12.63 (q), 17.20 (q), 17.68 (s), 25.47 (3q), 26.72 (t), 30.37 (t), 34.14 (q), 36.67 (t), 37.00 (d), 40.32 (s), 41.96 (t), 54.22 (d), 72.38 (s), 76.20 (d), 79.48 (d); MS m/z (relative intensity) 285 (M^+–57, 2), 267 (20), 175 (100), 133 (26), 120 (23), 96 (20), 73 (30); calcd for $C_{15}H_{29}O_3Si$ (M^+–57) m/z 285.1886, found m/z 283.1888. Anal. Calcd for $C_{19}H_{38}O_3Si$: C, 66.61; H, 11.18. Found: C, 66.38; H, 11.37.

b. The same procedure as for the synthesis of **82** was employed by using 0.40 g (1.23 mmol) of **96**. After the usual workup and flash chromatography, **100** was isolated in 92% yield.

Reductive Alkylation of 95. The procedure described for the lithium-ammonia reduction of **95** was employed by using 0.90 g of lithium, 100 mL of freshly distilled NH_3, and 2.49 g (7.74 mmol) of the enedione TBDMS-ether **95** in 50 mL of dry THF. When the dropwise addition of the THF-solution was complete, NH_3 was quickly evaporated under reduced pressure. The solution was warmed to 0 °C and then 0.50 mL (8.02 mmol) of MeI in 10 mL of dry THF was added dropwise. The mixture was allowed to stir at 0 °C for 10 min, after which time the reaction mixture was poured into 500 mL of icewater, and extracted with six 200-mL portions of EtOAc. The combined organic layers were washed with 100 mL of brine, dried and evaporated. The remaining residue was flash chromatographed (15:1 petroleum ether (bp 40–60 °C)/EtOAc) yielding 0.649 g (25%) of **(4α,4aα,8aβ)-4-[(*tert*-butyldimethylsilyl)oxy]octahydro-4a,8,8-trimethyl-1(2*H*),7(6*H*)-naphthalenedione (101)**: mp 67–69 °C (from petroleum ether (bp 40–60 °C));. ^{1}H NMR (200 MHz) δ 0.04 (s, 3 H), 0.06 (s, 3 H), 0.85 (s, 9 H), 1.08 (s, 3 H), 1.12 (s, 3 H), 1.41–

1.55 (m, 1 H), 1.44 (s, 3 H), 1.75–2.35 (m, 7 H), 2.77 (m, 1 H), 3.64 (dd, J = 5.5, 10.3 Hz, 1 H); ^{13}C NMR (50 MHz) δ –5.04 (q), –4.241 (q), 13.53 (q), 17.74 (s), 21.61 (q), 23.73 (q), 25.52 (3q), 30.74 (t), 33.68 (t), 37.74 (t), 40.61 (t), 43.23 (s), 46.45 (s), 61.45 (d), 78.29 (d), 208.32 (s), 214.06 (s); MS m/z (relative intensity) 338 (M^+, 0.2), 323 (2), 281 (60), 183 (26), 171 (29), 147 (35), 75 (100), 41 (41); calcd for $C_{19}H_{34}O_3Si$ (M^+) m/z 338.2277, found m/z 338.2277. Anal. Calcd for $C_{19}H_{34}O_3Si$: C, 67.41; H, 10.12. Found: C, 67.88; H, 10.58. Further elution afforded 1.25 g (47%) of **(4α,4aα,7α,8aβ)-4-[(*tert*-butyldimethylsilyl)oxy]octahydro-7-hydroxy-4a,8,8-trimethyl-1(2*H*)-naphthalenone (102)**: mp 134–135 °C (from diisopropyl ether); ^{1}H NMR (200 MHz) δ 0.03 (s, 6 H), 0.85 (s, 12 H), 1.04 (s, 3 H), 1.15 (s, 3 H), 1.41–2.00 (m, 8 H), 2.10–2.39 (m, 2 H), 3.07 (dd, J = 5.1, 10.5 Hz, 1 H), 3.58 (dd, J = 5.2, 10.6 Hz, 1 H); ^{13}C NMR (50 MHz) δ –4.97 (q), –4.22 (q), 13.66 (q), 14.73 (q), 17.77 (s), 25.55 (3q), 26.47 (t), 27.23 (q), 30.96 (t), 36.62 (t), 37.12 (s), 40.78 (t), 43.54 (s), 61.27 (d), 78.57 (d), 78.88 (d), 109.20 (s); MS m/z (relative intensity) 325 (M^+–15, 2.8), 297 (17), 283 (100), 164 (11), 149 (20), 73 (41), 41 (29); calcd for $C_{18}H_{33}O_3Si$ (M^+–15) m/z 325.2199, found m/z 325.2200. Anal. Calcd for $C_{19}H_{36}O_3Si$: C, 67.01; H, 10.65. Found: C, 66.72; H, 10.82.

(4'α,4'aα,8'aβ)-4'-[(*tert*-Butyldimethylsilyl)oxy]octahydro-4'a,8',8'-trimethylspiro[1,3-dioxolane-2,7'(6'*H*)-naphthalen]-1'(2'*H*)-one (103). The dione **101** (0.65 g, 1.58 mmol) was treated with MED for 24 h as described above for the synthesis of **75**. After the usual workup and flash chromatography 0.475 g (79%) of **103** was obtained: mp 112–114 °C (from diisopropyl ether); ^{1}H NMR (200 MHz) δ –0.03 (s, 3 H), – 0.01 (s, 3 H), 0.80 (s, 9 H), 0.83 (s, 3 H), 0.85 (s, 3 H), 1.25 (s, 3 H), 1.31–1.49 (m, 2 H), 1.59–1.88 (m, 5 H), 2.03–2.37 (m, 2 H), 2.42 (br s, 1 H), 3.63 (dd, J = 5.6, 11.2 Hz, 1 H), 3.78–3.93 (m, 4 H); ^{13}C NMR (50 MHz) δ –4.96 (q), –4.29 (q), 13.58 (q), 17.71 (s), 19.42 (q), 21.41 (q), 25.52 (3q), 26.30 (t), 31.09 (t), 34.92 (t), 40.60 (s), 40.79 (t), 43.17 (s), 59.39 (d), 64.60 (t), 64.78 (t), 78.60 (d), 112.15 (s), 209.67 (s); MS m/z (relative intensity) 382 (M^+, 5.2), 325 (8), 239 (4), 147 (1), 99 (100), 75 (17); calcd for $C_{21}H_{38}O_4Si$ (M^+–15) m/z 382.2539, found m/z 382.2538. Anal. Calcd for $C_{21}H_{38}O_4Si$: C, 65.93; H, 10.01. Found: C, 65.75; H, 10.15.

(1α,4α,4aα,7α,8aβ)-4-[(*tert*-Butyldimethylsilyl)oxy]decahydro-1,4a,8,8-tetramethyl-1,7-napthalenediol (104). To a stirred solution of 10 mL (16 mmol) of MeLi (1.6 M in ether), cooled to –78 °C, was added dropwise over a period of 15 min a solution of 0.35 g (1.03 mmol) of **102** in 25 mL of dry THF. When the addition was complete, the reaction mixture was allowed to stir at –78 °C for an additional 1.5 h. The excess MeLi was then quenched by careful addition of saturated aqueous NH_4Cl. After addition of 50 mL of water, the two-phase mixture was separated, and the aqueous layer was extracted with three 25-mL portions of EtOAc. The combined organic layers were washed with 50 mL of brine, dried, and evaporated. The crude product was purified by recrystallization from diisopropyl ether to give 0.275 g (75%) of **104** as white crystals: mp 140–141 °C; ^{1}H NMR (200 MHz) δ 0.00 (s, 3 H), 0.02 (s, 3 H), 0.86 (s, 9 H), 1.19 (s, 3 H), 1.21 (s, 3 H), 1.23 (s, 3 H), 1.36–1.87 (m, 11 H), 1.41 (s, 3 H), 3.08 (m, 2 H); ^{13}C NMR (50 MHz) δ –5.01 (q), –4.11 (q), 15.29 (q), 16.61 (q), 17.83 (s), 25.65 (3q), 27.19 (t), 27.47 (t), 31.35 (q), 34.62 (q), 38.25 (t), 41.01 (s), 41.40 (s), 43.39 (t), 56.89 (d), 75.08 (s), 79.08 (d), 80.68 (d); MS m/z (relative

intensity) 299 (M^+–57, 2), 189 (100), 159 (12), 133 (50), 73 (32), 41 (27); calcd for $C_{16}H_{31}O_3Si$ (M^+–57) *m/z* 299.2037, found *m/z* 299.2037. Anal. Calcd for $C_{20}H_{40}O_3Si$: C, 67.36; H, 11.31. Found: C, 67.88; H, 11.36.

General Procedure for the Preparation of Mesylates 58–67.[22] Method A. To a solution (0.1–0.15 M) of the corresponding diols **75** and **76** in dry pyridine was added MsCl (ca. 1.5 equiv). The reaction was stirred at rt and followed by TLC.[23] At completion, the mixture was concentrated at reduced pressure. The remaining residue was submitted directly to flash chromatography (1:1 petroleum ether (bp 40–60 °C)/EtOAc). By using this procedure the mesylates **60** and **61** were prepared.

(4'aα,5'α,8'α,8'aα)-Octahydro-4'a,8'-dimethylspiro[1,3-dioxolane-2,2'(1'*H*)-naphthalene]-5',8'-diol 5'-(Methanesulfonate) (60): yield 96%; mp 155 °C (from diisopropyl ether) dec; ^{1}H NMR (200 MHz) δ 1.13 (s, 3 H), 1.14 (s, 3 H), 1.33–2.01 (m, 11 H), 2.17 (m, 1 H), 2.99 (s, 3 H), 3.85–4.00 (m, 4 H), 4.35 (dd, *J* = 4.3, 11.9 Hz, 1 H); ^{13}C NMR (50 MHz) δ 12.14 (q), 24.69 (t), 29.35 (q), 30.04 (t), 30.30 (t), 36.25 (t), 38.04 (s), 38.44 (q), 38.90 (t), 47.66 (d), 63.85 (t), 64.14 (t), 70.35 (s), 89.77 (d), 108.95 (s); MS *m/z* (relative intensity) 319 (M^+–15, 1.5), 316 (2), 238 (44), 221 (17), 209 (21), 181 (15), 167 (25), 99 (100), 86 (70), 71 (48); calcd for $C_{14}H_{23}O_6S$ (M^+–15) *m/z* 319.1215, found *m/z* 319.1218. Anal. Calcd for $C_{15}H_{26}O_6S$: C, 53.87; H, 7.84. Found: C, 53.96; H, 7.78.

(4'aα,5'α,8'β,8'aβ)-Octahydro-4'a,8'-dimethylspiro[1,3-dioxolane-2,2'(1'*H*)-naphthalene]-5',8'-diol 5'-(Methanesulfonate) (61): yield 77%; mp 144–145 °C (from diisopropyl ether); ^{1}H NMR (200 MHz) δ 0.97 (s, 3 H), 1.09 (s, 3 H), 1.38–2.10 (m, 12 H), 2.97 (s, 3 H), 3.83–4.08 (m, 4 H), 4.35 (dd, *J* = 4.7, 11.2 Hz, 1 H); ^{13}C NMR (50 MHz) δ 12.63 (q), 21.99 (q), 26.50 (t), 30.04 (t), 30.26 (t), 37.58 (t), 38.29 (s), 38.37 (q), 40.44 (t), 50.05 (d), 63.95 (t), 64.13 (t), 70.21 (s), 89.04 (d), 108.64 (s); MS *m/z* (relative intensity) 334 (M^+, < 0.1), 319 (2), 316 (1), 238 (44), 221 (20), 209 (25), 181 (11), 167 (23), 99 (100), 86 (40); calcd for $C_{15}H_{26}O_6S$ (M^+) *m/z* 334.1450, found *m/z* 334.1452. Anal. Calcd for $C_{15}H_{26}O_6S$: C, 53.87; H, 7.84. Found: C, 53.71; H, 7.87.

Method B. The diols **72, 73, 82, 84, 91, 93, 100,** and **104** were treated with MsCl as above, except that, after concentration, the residues were taken up in EtOAc and washed successively with two portions of 10% aqueous H_2SO_4, two portions of saturated aqueous $NaHCO_3$, and one portion of brine. After drying and evaporation, further purification was accomplished by flash chromatography or by recrystallization. By using this procedure the corresponding mesylates were prepared.

(1α,4β,4aβ,7α,8aα)-4-[(*tert*-Butyldimethylsilyl)oxy]decahydro-1,4a-dimethyl-1,7-naphthalenediol 7-(Methanesulfonate) (58): yield 94%; mp 140–143 °C (from diisopropyl ether); ^{1}H NMR (200 MHz) δ 0.00 (s, 6 H), 0.83 (s, 12 H), 1.05 (s, 3 H), 1.21–2.04 (m, 11 H), 2.21 (br d, *J* = 9.5 Hz, 1H), 3.01 (s, 3 H), 3.33 (dd, *J* = 6.1, 7.0 Hz, 1 H), 5.06 (m, $W_{1/2}$ = 9 Hz, 1 H); ^{13}C NMR (50 MHz) δ –5.05 (q), –4.18 (q), 12.32 (q), 17.79 (s), 21.99 (q), 25.59 (3q), 26.07 (t), 26.71 (t), 28.83 (t), 34.60 (t), 38.63 (q), 39.27 (s), 40.82 (t), 45.66 (d), 70.63 (s), 78.96 (d), 79.76 (d); MS, *m/z* (relative intensity) 310 (M^+–96, 1), 295 (1), 253 (83), 159 (36), 119 (32), 105 (61), 75 (100), 43 (44); calcd for $C_{18}H_{34}O_2Si$ (M^+–96) *m/z* 310.2328, found *m/z* 310.2328. Anal. Calcd for $C_{19}H_{38}O_5SSi$: C, 56.11; H, 9.42. Found: C, 55.97; H, 9.35.

(1α,4β,4aβ,7β,8aα)-4-[(*tert*-Butyldimethylsilyl)oxy]decahydro-1,4a-dimethyl-1,7-naphthalenediol 7-(Methanesulfonate) (59): yield 93%; mp 99–100 °C (from diisopropyl ether); ^{1}H NMR (200 MHz) δ –0.02 (s, 3 H), 0.00 (s, 3 H), 0.83 (s, 9 H), 0.86 (s, 3 H), 0.87–2.00 (m, 11 H), 1.08 (s, 3 H), 2.22 (m, 1 H), 2.98 (s, 3 H), 3.19 (dd, J = 5.5, 7.2 Hz, 1 H), 4.58 (m, $W_{1/2}$ = 25 Hz, 1 H); ^{13}C NMR (50 MHz) δ –5.12 (q), –4.20 (q), 13.01 (q), 17.76 (s), 22.44 (q), 25.56 (3q), 27.47 (t), 28.21 (t), 28.78 (t), 38.57 (q), 38.72 (s), 38.74 (t), 40.60 (t), 50.70 (d), 70.81 (s), 79.07 (d), 82.39 (d); MS, *m/z* (relative intensity) 310 (M^+–96, 1.5), 277 (5), 253 (100), 159 (33), 105 (54), 75 (89), 43 (39); calcd for $C_{18}H_{34}O_2Si$ (M^+–96) *m/z* 310.2328, found *m/z* 310.2328. Anal. Calcd for $C_{19}H_{38}O_5SSi$: C, 56.11; H, 9.42. Found: C, 56.07; H, 9.41.

(2α,4aβ,8α,8aα)-Decahydro-2,8a-dimethyl-2,8-naphthalenediol 8-(Methanesulfonate) (62): yield 97%; mp 105–107 °C (from diisopropyl ether); ^{1}H NMR (200 MHz) δ 0.98–2.00 (m, 14 H), 1.10 (s, 3 H), 1.19 (s, 3 H), 2.97 (s, 3 H), 4.27 (dd, J = 5.5, 10.6 Hz, 1 H); ^{13}C NMR (50 MHz) δ 11.81 (q), 23.80 (t), 24.15 (t), 26.53 (t), 27.58 (t), 33.27 (q), 38.71 (q), 39.32 (s), 39.32 (t), 44.38 (d), 48.72 (t), 70.21 (s), 90.74 (d); MS *m/z* (relative intensity) 261 (M^+–15, 13), 180 (52), 165 (100), 147 (35), 123 (87), 110 (57), 96 (33), 81 (30), 71 (24), 43 (52); calcd for $C_{12}H_{21}O_4S$ (M^+–15) *m/z* 261.1161, found *m/z* 261.1171. Anal. Calcd for $C_{13}H_{24}O_4S$: C, 56.49; H, 8.75. Found: C, 56.56; H, 8.91.

(2α,4aα,8β,8aβ)-Decahydro-2,8a-dimethyl-2,8-naphthalenediol 8-(Methanesulfonate) (63): yield 98%; mp 90–92 °C (from *n*-pentane/diisopropyl ether); ^{1}H NMR (200 MHz) δ 0.86 (s, 3 H), 0.93–1.50 (m, 9 H), 1.29 (s, 3 H), 1.65–1.98 (m, 5 H), 2.98 (s, 3 H), 4.29 (dd, J = 5.1, 11.0 Hz, 1 H); ^{13}C NMR (50 MHz) δ 12.61 (q), 23.73 (t), 26.19 (2t), 27.66 (t), 29.09 (q), 38.54 (q), 39.01 (s), 40.88 (t), 44.40 (d), 52.05 (t), 70.39 (s), 91.00 (d); MS *m/z* (relative intensity) 261 (M^+–15, 5), 180 (61), 165 (57), 147 (50), 123 (100), 110 (71), 96 (39), 81 (43), 43 (57); calcd for $C_{12}H_{21}O_4S$ (M^+–15) *m/z* 261.1161, found *m/z* 261.1163. Anal. Calcd for $C_{13}H_{24}O_4S$: C, 56.49; H, 8.75. Found: C, 56.42; H, 8.82.

(1α,4aα,5α,8aβ)-Decahydro-1,4a,7,7-tetramethyl-1,5-naphthalenediol 5-(Methanesulfonate) (64): yield 92%; mp 108–110 °C (from diisopropyl ether); ^{1}H NMR (200 MHz) δ 0.97 (s, 3 H), 1.00 (s, 3 H), 1.04 (s, 3 H), 1.08–1.90 (m, 12 H), 1.14 (s, 3 H), 2.96 (s, 3 H), 4.38 (dd, J = 6.2, 10.7 Hz, 1 H); ^{13}C NMR (50 MHz) δ 11.66 (q), 17.14 (t), 26.33 (q), 30.63 (q), 31.12 (s), 32.81 (q), 33.04 (t), 37.11 (t), 38.58 (q), 38.88 (s), 40.74 (2t), 46.05 (d), 71.45 (s), 88.46 (d); MS *m/z* (relative intensity) 289 (M^+–15, 7), 208 (14), 190 (21), 175 (27), 150 (100), 135 (33), 96 (39), 82 (27), 43 (45); calcd for $C_{14}H_{25}O_4S$ (M^+–15) *m/z* 289.1473; found *m/z* 289.1474. Anal. Calcd for $C_{15}H_{28}O_4S$: C, 59.17; H, 9.27. Found: C, 59.04; H, 9.31.

(1α,4aβ,5β,8aα)-Decahydro-1,4a,7,7-tetramethyl-1,5-naphthalenediol 5-(Methanesulfonate) (65): yield 94%; mp 102 °C (from *n*-pentane); ^{1}H NMR (200 MHz) δ 0.86 (s, 3 H), 1.00 (s, 6 H), 1.03–1.84 (m, 12 H), 1.12 (s, 3 H), 2.96 (s, 3 H), 4.42 (dd, J = 7.1, 9.7 Hz, 1 H); ^{13}C NMR (50 MHz) δ 11.55 (q), 19.30 (t), 22.85 (q), 25.92 (q), 31.23 (s), 32.86 (q), 32.86 (t), 36.75 (t), 38.61 (q), 39.67 (s), 40.96 (t), 42.61 (t), 48.73 (d), 71.35 (s), 88.66 (d); MS *m/z* (relative intensity) 289 (M^+–15, 7), 208 (18), 190 (38), 175 (34), 150 (100), 135 (38), 124 (40), 96 (50), 82 (34), 43 (22); calcd for $C_{14}H_{25}O_4S$ (M^+–15) *m/z* 289.1473; found *m/z* 289.1473. Anal. Calcd for $C_{15}H_{28}O_4S$: C, 59.17; H, 9.27. Found: C, 58.90; H, 9.28.

(1α,4α,4aα,7α,8β,8aβ)-4-[(*tert*-Butyldimethylsilyl)oxy]decahydro-1,4a,8-trimethyl-1,7-naphthalenediol 7-(Methanesulfonate) (66): yield 100%; mp 115–116 °C (from petroleum ether (bp 40–60

°C)); ^{1}H NMR (200 MHz) δ –0.01 (s, 3 H), 0.01 (s, 3 H), 0.85 (s, 9 H), 0.90–1.94 (m 8 H), 1.07 (s, 3 H), 1.22 (d *J* = 6.4 Hz, 3 H), 1.30 (s, 3 H), 2.08–2.24 (m, 3 H), 3.00 (s, 3 H), 3.09 (dd, *J* = 3.8, 11.1 Hz, 1 H), 4.29 (m, $W_{1/2}$ = 21 Hz, 1 H); ^{13}C NMR (50 MHz) δ –5.09 (q), –4.17 (q), 12.66 (q), 17.47 (q), 17.79 (s), 25.60 (3q), 26.63 (t), 28.60 (t), 34.47 (q), 34.90 (d), 36.34 (t), 38.77 (q), 40.30 (s), 42.60 (t), 54.27 (d), 72.43 (s), 79.14 (d), 87.89 (d); MS *m/z* (relative intensity) 307 (M^+–113, < 0.1), 292 (0.2), 268 (14), 250 (11), 200 (13), 176 (100), 159 (20), 135 (28), 120 (64), 96 (50), 75 (55); calcd for $C_{19}H_{35}OSi$ (M^+–113) *m/z* 307.2457; found *m/z* 307.2454. Anal. Calcd for $C_{20}H_{40}O_5SSi$: C, 57.10; H, 9.58. Found: C, 56.79; H, 9.70.

(1α,4aα,4aα,7α,8aβ)-4-[(*tert*-Butyldimethylsilyl)oxy]decahydro-1,4a,8,8-tetramethyl-1,7-naphthalenediol 7-(Methanesulfonate) (67): yield 82%; ^{1}H NMR (C_6D_6, 200 MHz) δ 0.11 (s, 6 H), 0.56–1.43 (m, 6 H), 1.02 (s, 9 H), 1.17 (s, 3 H), 1.26 (s, 3 H), 1.32 (s, 3 H), 1.38 (s, 3 H), 1.82–2.01 (m, 4 H), 2.39 (s, 3 H), 2.88 (dd, *J* = 3.6, 11.2 Hz, 1 H), 4.30 (dd, *J* = 5.1, 11.7 Hz, 1 H); ^{13}C NMR (50 MHz) δ –4.97 (q), –4.19 (q), 15.00 (q), 17.69 (q), 17.79 (s), 24.96 (t), 25.64 (3q), 27.53 (t), 30.78 (q), 34.62 (q), 37.50 (t), 38.25 (q), 40.50 (s), 41.14 (s), 43.48 (t), 56.31 (d), 74.16 (s), 80.44 (d), 89.20 (d); MS *m/z* (relative intensity) 362 (M^+–57, 3.3), 281 (6), 265 (7), 190 (77), 153 (57), 147 (30), 121 (23), 75 (100); calcd for $C_{17}H_{33}O_5SSi$ (M^+–57) *m/z* 362.1583; found *m/z* 362.1577.

2.6 References and Notes

(1) Kesselmans, R. P. W.; Wijnberg, J. B. P. A.; de Groot, A.; de Vries, N. K. *J. Org. Chem.* **1991**, *56*, 7232-7236.

(2) Kesselmans, R. P. W.; Wijnberg, J. B. P. A.; Minnaard, A.; Walinga, R.; de Groot, A. *J. Org. Chem.* **1991**, *56*, 7237-7244.

(3) Wijnberg, J. B. P. A.; Jenniskens, L. H. D.; Brunekreef, G. A.; de Groot, A. *J. Org. Chem.* **1990**, *55*, 941-948.

(4) Jenniskens, L. H. D.; Wijnberg, J. B. P. A.; de Groot, A. *J. Org. Chem.* **1991**, *56*, 6585-6591.

(5) Wijnberg, J. B. P. A.; Vader, J.; de Groot, A. *J. Org. Chem.* **1983**, *48*, 4380-4387.

(6) Wijnberg, J. B. P. A.; Jongedijk, G.; de Groot, A. *J. Org. Chem.* **1985**, *50*, 2650-2654.

(7) For the Experimental Sections of this thesis the Chemical Abstracts numbering system is used.

(8) Brown, E.; Lebreton, J. *Tetrahedron* **1987**, *43*, 5827-5840.

(9) Kim, M.; Gross, R. S.; Sevestre, H.; Dunlap, N. K.; Watt, D. S. *J. Org. Chem.* **1988**, *53*, 93-98.

(10) Grundke, G.; Keese, W.; Rimpler, M. *Chem. Ber.* **1985**, *118*, 4288-4291.

(11) (a) Murray, R. W.; Jeyaraman, R. *J. Org. Chem.* **1985**, *50*, 2847-2853.
(b) Oxone, a mixture of $KHSO_5$, $KHSO_4$, and K_2SO_4 in the ratio 2:1:1, respectively.

(12) Heathcock, C. H.; Gray, D. *Tetrahedron* **1971**, *27*, 1239-1246.
(13) Ralls, J. W.; Riegel, B. *J. Am. Chem. Soc.* **1954**, *76*, 4479-4480.
(14) Corey, E. J.; Venkateswarlu, A. *J. Am. Chem. Soc.* **1972**, *94*, 6190-6191.
(15) Upon treatment of this mixture with NaOMe in dry MeOH, the ratio of **98a** and **98b** did not change.
(16) Only the diones **97** with a *trans* or *cis*-steroid conformation can be transformed into a dioxolane. See also reference 5.
(17) Browne, L. M.; Klinck, R. E.; Stothers, J. B. *Org. Magn. Reson.* **1979**, *12*, 561-568.
(18) Stork, G.; Logusch, E. W. *J. Am. Chem. Soc.* **1980**, *102*, 1218-1219.
(19) Stork, G.; Logusch, E. W. *J. Am. Chem. Soc.* **1980**, *102*, 1219-1220.
(20) Buhler, J. D. *J. Org. Chem.* **1973**, *38*, 904-906.
(21) Compound **89** is insoluble in DMSO.
(22) The mesylates **39** and **40** were prepared as described previously.[4]
(23) If the reaction appears to be proceeding too slowly (>20 h), heating at 40 °C may be helpful.

Chapter 3

Intramolecular Alkoxide Induced Heterolysis of Perhydronaphthalene-1,4-diol Monosulfonate Esters through Orbital Interactions over Three C-C Single Bonds*

3.1 Introduction

The base-induced fragmentation of cyclic 1,3-diol monosulfonate esters, known as the Wharton reaction[1], is an typical example of the Grob fragmentation. It has been shown that stereochemical[2] and stereoelectronic[3] factors are important in this reaction (see also Chapter 1, Sections 1.2.2 and 1.2.8).

From recent work of Jenniskens *et al.* on the total synthesis of sesquiterpenes,[4,5] it is known that cyclic 1,4-diol monosulfonate esters react very smoothly upon treatment with sodium *tert*-amylate in refluxing benzene or toluene. These reactions have been rationalized by assuming that deprotonation of the (tertiary) hydroxyl group induces intramolecularly the heterolysis of the sulfonate ester bond, just as in the Wharton reaction. It should be emphasized that in these reactions the hydroxyl group and the mesylate group are separated by four σ-bonds, whereas in the Wharton reaction only three σ-bonds connect both functionalities.
In chapter 1 it was mentioned that the elimination reaction of the mesylates **39** and **40** follow the above reaction principle upon treatment with sodium *tert*-amylate. Both compounds probably react *via* a common dipolar intermediate (Scheme 3.1).[5] In the context of this chapter it is important to note that during the elimination reaction of **40** some side products were formed. In the primary experiments the interest was focussed on an optimum yield of the olefin **41** and little attention was paid to the presence of these side products. However, a more careful examination revealed the presence of a fragmentation product, whose identity was established as **105** (*vide infra*). This result stimulated us to examine the reactivity of this type of cyclic 1,4-diol monosulfonate ester under strongly basic conditions in more detail.

* This chapter has been published for the greater part: Orrū, R. V. A.; Wijnberg, J. B. P. A.; Jenniskens, L. H. D.; de Groot, A. *J. Org. Chem.* **1993**, *58*, 1199.

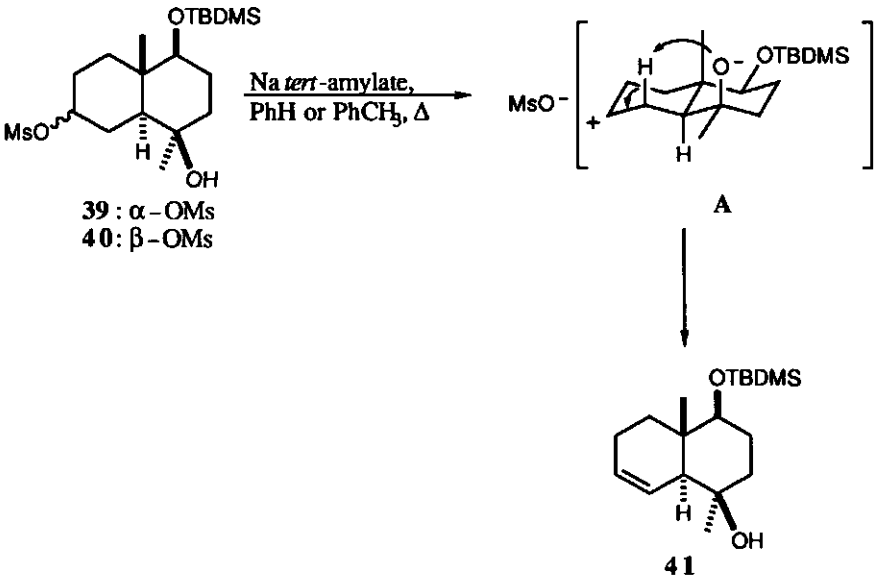

39 : α-OMs
40: β-OMs

41

Scheme 3.1

In addition to **39** and **40**, with an axial hydroxyl group at C_6, the mesylates **58** and **59**, with an equatorial hydroxyl group at this position, were investigated to obtain more information about the stereochemical factors governing these reactions. The O-silylated mesylates **106** and **107** were subjected to strongly basic conditions as well in order to gather more evidence for our assumption that deprotonation of the hydroxyl group induces ionization of the sulfonate ester bond. Finally, experiments were performed to affect the electron donating ability of the alkoxide group in order to determine the impact on reaction rate and product composition in these processes.

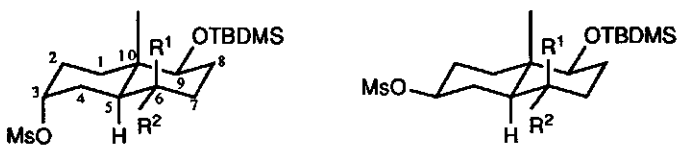

39 : $R^1 = OH$; $R^2 = CH_3$
58 : $R^1 = CH_3$; $R^2 = OH$
106 : $R^1 = CH_3$; $R^2 = OTMS$

40 : $R^1 = OH$; $R^2 = CH_3$
59 : $R^1 = CH_3$; $R^2 = OH$
107 : $R^1 = CH_3$; $R^2 = OTMS$

Chart 3.1

3.2 Results and Discussion

In order to obtain comparable data about the effects of strong bases on the reactivity of the mesylates depicted in Chart 3.1, all compounds were subjected to the same reaction conditions. The reactions were run in benzene at reflux temperature with *ca.* 5 equiv of sodium *tert*-amylate. Apart from sodium *tert*-amylate, also lithium *tert*-amylate and sodium *tert*-amylate in combination with 15-crown-5 were used. A reaction time of 10 min was maintained in all cases, unless otherwise noted. Except for the reactions in which 15-crown-5 was used, the reaction time of 10 min was too short to complete the reactions. By comparing the quantities of recovered starting material, a rough estimate of the relative reaction rates could be obtained. The results of these studies are collected in Table 3.1.

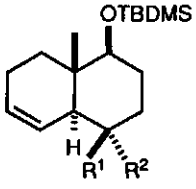

41 : $R^1 = OH$; $R^2 = CH_3$
109 : $R^1 = CH_3$; $R^2 = OH$

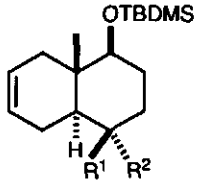

108 : $R^1 = OH$; $R^2 = CH_3$
110 : $R^1 = CH_3$; $R^2 = OH$
113 : $R^1 = CH_3$; $R^2 = OTMS$

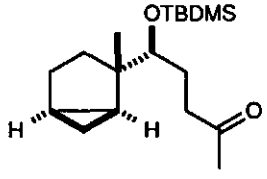

105

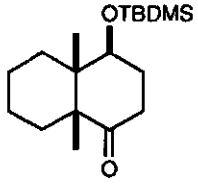

111

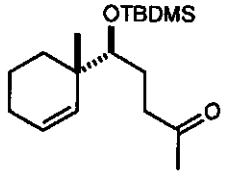

112

Chart 3.2

The initial reactions of the mesylates **39, 40, 58** and **59** with sodium *tert*-amylate in refluxing benzene (entries 1-4) were performed to investigate the influence of the stereochemistry of the hydroxyl and sulfonate ester group on the course of the reaction. The α-mesylate **39** gave a 12:1 mixture (78%) of the olefins **41** and **108**, respectively, together with 18% of recovered **39**. The olefins **41** and **108** were also obtained from the β-mesylate **40**, but now in a ratio of 6.5:1, respectively, and in a lower yield (53%).[6] In this reaction a smaller amount (8%) of starting material was

Table 3.1. Reactions of the mesylates 39, 40, 58, 59, 106, and 107 with alkali metal tert-amylate or TBAF.

			Products, % yield[a]					
entry	mesylate	conditions[b]	41+108[c]	105	109+110[c]	111	other	recov of mesylate, yield %[d]
1	**39**	A	78 (12 :1)					18
2	**40**	A	53 (6.5:1)	22				8
3	**58**	A		2	58 (2.8:1)	4	e	24
4	**59**	A		69	7.5 (2.2:1)	2		8
5	**106**	A (3 h)						96
6	**107**	A (3 h)						98
7	**40**	B	7 (1.2:1)	1				84
8	**40**	B (3 h)	72 (1.2:1)	5				-
9	**59**	B		5		3		91
10	**59**	B (7 h)		20	23 (1.2:1)	22		-
11	**39**	C	98 (60 :1)					-
12	**40**	C	20 (8.5:1)	54				-
13	**58**	C			100 (1:10)			-
14	**59**	C		83	2 (1: 2)	1.5		-
15	**106**	C (24 h)					f	53
16	**107**	C (24 h)						84
17	**106**	D			78 (1: 1)			-
18	**107**	D		77				-

[a] Based on GC analysis. [b] All reactions were performed in refluxing benzene with ca. 5 equiv of base (entries 1-16) or with 1 equiv of TBAF (entries 17 and 18). Reaction time was 10 min unless otherwise noted. A, Na *tert*-amylate; B, Li *tert*-amylate; C, Na *tert*-amylate + 0.5 equiv of 15-crown-5; D, TBAF. [c] Ratio in parentheses were determined by GC. [d] Isolated yields. [e] In this reaction 4% of **112** was formed. [f] In this reaction 46% of **113** was formed.

regained. Additionally, a 22% yield of a fragmentation product, the cyclopropane derivative **105**, was isolated. It should be noted that the yield of this product was somewhat diminished by aldol condensation reactions.[7] The presence of a cyclopropane ring in **105** was concluded from the proton coupled ^{13}C NMR spectrum. The signals of the tertiary cyclopropane carbon atoms appear at δ 17.59 (d, J_{CH} = 166 Hz) and 24.58 (d, J_{CH} = 167 Hz), while the signal due to the secondary cyclopropane carbon atom appears at δ 6.07 (t, J_{CH} = 158 Hz).

The α-mesylate **58** produced predominantly a 2.8:1 mixture (58%) of the olefins **109** and **110**, respectively. As minor products, **105** (2%), the *cis*-fused ketone **111** (4%), and another fragmentation product (4%) whose identity was established as **112**, were formed. The quantity of regained **58** amounted to 24%. The most valuable information for the identification of the olefins **109** and **110** was obtained from the signals of the olefinic protons in their ^1H NMR spectra. In the ^1H NMR spectrum of **109**, the olefinic signals appear as a broad singlet at δ 5.66. After addition of 0.5 equiv of Eu(fod)$_3$ to the ^1H NMR sample of **109**, the original olefinic two-proton signal (br s) at δ 5.66 splits up into two signals appearing at δ 5.89 (ddd, J = 3, 7, 10 Hz, 1 H) and 6.83 (dd, J = 2, 10 Hz, 1 H). The ^1H NMR spectrum of **110** shows the olefinic signals at δ 5.54 (ddd, J = 3.2, 5.0, 10.1 Hz, 1 H) and 5.61 (ddd, J = 2.4, 4.7, 10.1 Hz, 1 H). These multiplicities unequivocally establish the identity of **109** and **110**. In the NMR spectra of **111** recorded at room temperature, coalescence was observed for some signals which frustrated the interpretation of these spectra. However, increase of the temperature to 67 °C led to sharpening of these signals through which the structure of **111** could be established.

Treatment of the β-mesylate **59** with sodium *tert*-amylate afforded the cyclopropane derivative **105** as the major product (69%),[7] together with small amounts of a 2.2:1 mixture (7.5%) of the olefins **109** and **110**, respectively, the *cis*-fused ketone **111** (2%), and recovered **59** (8%).

The importance of the presence of a free hydroxyl group in the substrates was demonstrated with the O-silylated mesylates **106** and **107**.[8] After prolonged heating (3h) with sodium *tert*-amylate, these compounds showed no reaction at all (entries 5 and 6). The mesylates **106** and **107** were regained almost quantitatively.

Using lithium *tert*-amylate instead of sodium *tert*-amylate retarded the reaction rates considerably (entries 7-10). Also the product composition changed dramatically. Heating of the β-mesylate **40** until completion of the reaction (3h) led to a 1.2:1 mixture (72%) of **41** and **108**, respectively, together with a small amount of **105**. The cyclopropane derivative **105** (20%),[7] a 1.2:1 mixture (23%) of **109** and **110**, respectively, and a considerable amount (22%) of the *cis*-fused ketone **111** were formed after completion of the reaction of the β-mesylate **59** (7h).

Both the reaction rate and the selectivity increased when sodium *tert*-amylate in combination with 15-crown-5 was used (entries 11-14). The α-mesylates **39** and **58** both showed a fast reaction in which olefin formation was the only process observed. The α-mesylate **39** afforded a 60:1 mixture (98%) of **41** and **108**, respectively, while in case of **58** a 1:10 mixture of **109** and **110**, respectively, was produced in quantitative yield. On the other hand, with the β-mesylates **40** and **59** a fast fragmentation leading to the cyclopropane derivative **105** was the main process (54 and 83% yield,[7] respectively).
The O-silylated α-mesylate **106** reacted only very slowly under these conditions (entry 15). After a reaction time of 24 h, the O-silylated olefin **113** (46%) and unreacted **106** (53%) were isolated. Selective desilylation of **113** to the known olefin **110** confirmed its structure. The corresponding β-mesylate **107** did not give any detectable reaction product after a 24 h reflux period (entry 16). On the contrary, fast reactions were observed when **106** and **107** were treated with 1 equiv of TBAF (entries 17 and 18). Within 10 min both reactions were completed and either elimination or fragmentation was observed dependent on the orientation of the mesylate group.
These results clearly show that the structural features of the mesylates studied have profound effects on the course of the reactions of these compounds. It is also demonstrated that the product composition and reaction rate are dependent on the nature of the base. Finally, deprotonation of the tertiary hydroxyl group appears to be of great importance to the reactivity of these mesylates. The experiments with **106** and **107**, in which the hydroxyl proton is replaced by a TMS-group, show this nicely (entries 5, 6, and 15-18). The enormous differences in reaction rate found in the reactions of **106** and **107** with sodium *tert*-amylate, in the absence or presence of 15-crown-5, and with TBAF must be attributed to alkoxide formation. The very slow but selective formation of the olefin **113** in the reaction of **106** with sodium *tert*-amylate and 15-crown-5 is probably the result of an intermolecular *anti* E2 mechanism[9] in which the less sterically hindered β proton on C_2 is abstracted exclusively.[10]
Alkoxide formation must also be responsible for the reactivity of the mesylates **39, 40, 58** and **59**, a feature they have in common with the Wharton reaction. The above results suggest the existence of a long-range orbital interaction through the intervening C–C single bonds between the alkoxide and the mesylate group as a result of which the mesylate group splits off more easily. Nucleophilic participation by the solvent (benzene) or by the poorly nucleophilic base (alkali metal *tert*-amylate) in the ionization process can be excluded.
Because all reactions are performed in benzene, contact ion pairs are probably involved in the intramolecularly induced departure of the mesylate group.[11] This means that the α-mesylates (**39** and **58**) and the β-mesylates (**40** and **59**) will react *via* the stereoisomeric dipolar intermediates **A1** and **A2**, respectively (Chart 3.3). If the

mesylate group remains associated with the carbocationic center, long enough to affect seriously the behavior of that ion, this will lead to different products and/or differences in product ratios. The results collected in Table 3.1 show that this is the case.

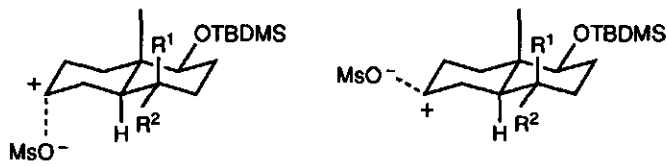

(39): $R^1 = O^-$; $R^2 = CH_3$ **(40)**: $R^1 = O^-$; $R^2 = CH_3$

(58): $R^1 = CH_3$; $R^2 = O^-$ **(59)**: $R^1 = CH_3$; $R^2 = O^-$

Chart 3.3

The α-mesylates **39** and **58**, which are supposed to react *via* the intermediate **A1**, can undergo facile intra- and/or intermolecular *anti* elimination. In the intermediate **A1(39)** the tertiary alkoxide group and the β H-4 are 1,3-diaxially positioned. This makes the intramolecular proton abstraction to **41** the most favorable process (entry 1). A similar intramolecular elimination is not possible in the intermediate **A1(58)** because the tertiary alkoxide group and the β H-4 are not properly aligned. An intramolecular elimination of the α H-4 is rejected because of stereoelectronic factors.[12] Therefore, intermolecular elimination becomes more important. The observed small elimination product ratio of 2.8:1 for the olefins **109** and **110**, respectively, suggests a more thermodynamically controlled elimination process (entry 3). The reaction of **106** with TBAF (entry 17) supports this supposition. Since no external base is present when TBAF is used and an intramolecular elimination is unlikely (*vide supra*), the elimination ratio of 1:1 found for **109** and **110** in this reaction must be the consequence of thermodynamic control. A further support is obtained from MM2 force field calculations[13] which also give the conclusion that **109** and **110** are equal in energy.

The presence of intermediate **A1(58)** can explain the formation of the other products **111** and **112** from **58** as well. A 1,2-H shift of the β H-4 to the carbocationic center at C_3 is not unlikely since this H atom and the associated mesylate group are oriented in an *anti* fashion.[14] The resulting secondary carbocationic intermediate can undergo a Grob fragmentation to give the olefinic fragmentation product **112**, but can also react further by way of a 1,2-H shift ($C_5 \rightarrow C_4$) and a 1,2-Me shift ($C_1 \rightarrow C_5$) to afford the

ketone **111**. The formation of a small amount (2%) of **105** in this reaction will be discussed later.

The two chief pathways by which the intermediate **A2** (derived from the β-mesylates **40** and **59**) reacts, are elimination and homofragmentation[15] (entries 2 and 4). The formation of the olefin **41** from **40** can be explained by an intramolecular *syn* elimination in which the intermediate **A2(40)** is involved. This mechanism is similar to that given in Scheme 3.1. The homofragmentation process leading to **105** can be rationalized by assuming a through-space interaction (1,3-bridging)[16] in the intermediates **A2**. The back lobe of the C_5–C_6–O^- orbital at C_5 overlaps with the incipient empty p orbital of the carbocationic center at C_3 and this will ultimately lead to C_3–C_5 bond formation with simultaneous breaking of the C_6–C_5 bond. If intramolecular elimination is not possible, as is the case with **59**, homofragmentation is the preferred pathway. The formation of a small amount of **111** in this reaction must proceed *via* a direct 1,3-H shift ($C_5 \rightarrow C_3$) and a successive (or simultaneous) 1,2-Me shift ($C_6 \rightarrow C_5$). This route to **111** differs from the one which starts from **58** owing to the stereospecificity of these shifts.

Another point of interest is the tendency of the equatorial β-mesylates **40** and **59** to react slightly faster then the axial α-mesylates **39** and **58** under the same conditions as can be concluded from the quantities of recovered starting material (entries 1-4). This means that the intermediates **A2** derived from **40** and **58** are formed more easily and thus are better stabilized, by 1,3-bridging, than the intermediates **A1** generated by the reactions of **39** and **58**. When the mesylate group is axially positioned (as in **A1**) 1,3-bridging is greatly reduced owing to repulsion of the electrons around C_5 by the mesylate anion of the incipient ion pair at C_3.[17]

Circumstantial evidence for the occurrence of the bridged intermediate **A2** comes from the following observations: (1) The formation of the cyclopropane derivative **105**, which must be the result of a bonding 1,3-interaction, is only observed when the intermediates **A2** are involved. (2) Careful analysis of the regained starting materials has revealed that during the reactions of the axial α-mesylates **39** and **58** small but distinct amounts of the β-mesylates **40** and **59**, respectively, are formed. These findings are confirmed by independent experiments in which **39** and **58** were treated with sodium *tert*-amylate in refluxing benzene for 3 min. In both cases the regained starting material contained about 10% of its equatorial C_3 isomer. This inversion process also explains the formation of the small amount (2%) of **105** in the reaction of **58** (entry 3). A direct formation of **105** from the intermediate **A1** is not very likely. Internal return with inversion of the stereochemistry of the mesylate group was not observed during the reactions of the β-mesylates **40** and **59**. These results suggest a reaction pathway in which both the axial and the equatorial mesylates react *via* a

stepwise mechanism with **A1** and the somewhat more stable bridged **A2**, respectively, as intermediates (Scheme 3.2).

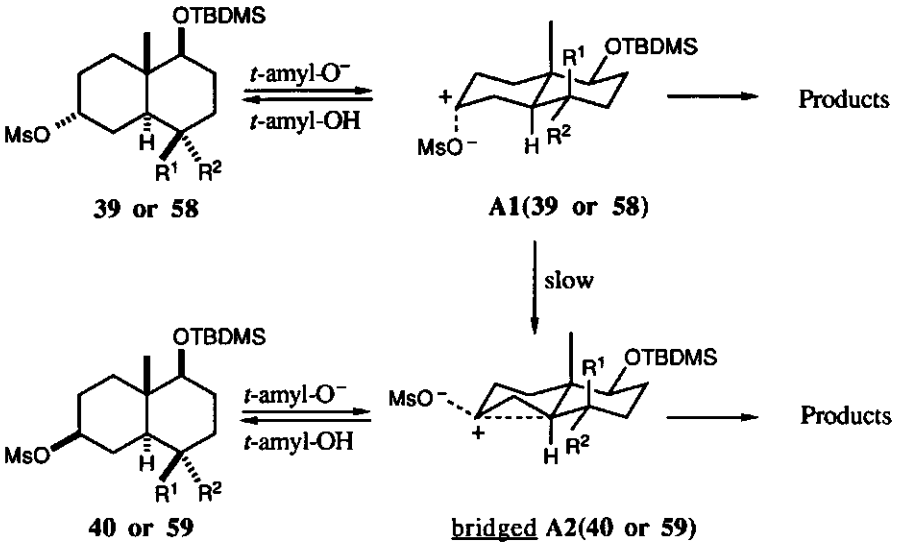

Scheme 3.2

The ionization of the axial mesylate group in the α-series must be ascribed to through-bond induction alone and results in the unbridged intermediates **A1**. In the β-series, with an equatorial mesylate group, through-space induction (1,3-bridging) accompanies through-bond induction resulting in the bridged intermediates **A2**.

The reactions of **40** and **59** with lithium *tert*-amylate and sodium *tert*-amylate in combination with 15-crown-5 underline the existence of 1,3-bridging in this type of compound. As expected, due to the relatively low basicity of lithium *tert*-amylate,[18] deprotonation of the tertiary hydroxyl group will be more difficult. Hence, the reaction rates slow down considerably (entries 7 and 9). Completion of the reactions (entries 8 and 10) shows that the formation of **105** is reduced compared with the reactions of **40** and **59** in which sodium *tert*-amylate is used. An explanation for this behavior is found in the decrease of the electron donating ability of the alkoxide group when Li^+ is the counterion.[19] This decrease of inductivity[21] gives rise to less overlap of the back lobe of the C_5–C_6–O^- orbital at C_5 with the incipient empty p orbital at C_3, which results in weakly bridged intermediates **A2**. Formation of the cyclopropane derivative **105** is therefore diminished. Elimination, and in case of **59** also formation of **111**, becomes now more important. It is evident that the β-mesylate **40** can not give any **111** because the methyl group at C_6 has the wrong stereochemistry.

It is also noteworthy that the elimination product ratios approach unity when lithium *tert*-amylate is used as the external base. In case of **59**, this levelling could be ascribed to an E1-like mechanism in which the weakly bridged intermediate **A2(59)** loses either its β H-2 or its β H-4 under thermodynamic control. This view is supported by MM2 force field calculations. For the olefins **41** and **108** the MM2 force field calculations predicted a thermodynamic 1:6 mixture, respectively.[22] The result of these calculations is in strong contrast with the 1.2:1 mixture found experimentally for these olefins (entries 7 and 8). This means that in the weakly bridged intermediate **A2(40)** intramolecular proton abstraction must still be the main elimination pathway. The use of sodium *tert*-amylate in combination with 15-crown-5 in the reactions of **40** and **59** (entries 12 and 14) show a considerable increase of both the reaction rate and the yield of the cyclopropane derivative **105** as compared with the reactions in which only sodium *tert*-amylate is used. It is known that addition of crown ethers to solutions of alkali metal alkoxides results in stronger bases.[23] Consequently, deprotonation of the tertiary hydroxyl group and hence the reaction will be faster. Because the Na^+ counterion will be captured by the crown ether, the resulting "naked" alcoholate function at C_6 will exhibit a more intense $+I$ effect. This leads to a strengthening of the 1,3-bridging as a result of which homofragmentation occurs more readily.

Another remarkable outcome of the use of 15-crown-5 is the almost exclusive formation of **41** from **39** (entry 11). This indicates that in this case the elimination process is highly intramolecularly directed. On the other hand, the preferential formation of **110** in the reaction of **58** (entry 13) must be the result of an intermolecular elimination process. Apparently, the specific features of the alkali metal alkoxide-crown ether mixture[10,11] control the elimination process here.

3.3 Concluding Remarks

It is evident that deprotonation of the alcohol function of the mesylates studied here is needed to split off the sulfonate ester group in apolar solvents such as benzene. The 1,4-diol monosulfonate esters react stepwise and involve initial ionization of the sulfonate ester group to form dipolar intermediates. The observed internal return with inversion of the axial mesylate group gives extra support for this idea. The reactivity of the α-mesylates is controlled by through-bond induction alone, whereas the reactivity of the corresponding β-mesylates is determined by the sum of a through-bond and a through-space interaction. In the latter compounds the additional through-space interaction (1,3-bridging) leads to the more stable bridged

intermediates. As a result, the β-mesylates react slightly faster than the corresponding α-mesylates. The extent of 1,3-bridging varies with the inductivity of the alkoxide function and is reflected in the degree of cyclopropane ring formation in the homofragmentation process. If 1,3-bridging is strongly inhibited, as is the case in the α-mesylates, elimination is the main pathway. Thus, not only the relative reaction rates of the α- and β-mesylates are determined by the degree of bridging but also are the product distributions. Finally, dependent on the stereochemistry a highly selective product formation can occur, especially when sodium *tert*-amylate in combination with 15-crown-5 is used.

3.4 Experimental Section

General.[24] A stock solution of sodium *tert*-amylate (2.2 M in toluene) was prepared by the procedure of Conia[25] and stored under an Ar atmosphere in a refrigerator. A stock solution of lithium *tert*-amylate was prepared by dropwise addition of 1 equiv of dry *tert*-amyl alcohol to a stirred solution of *t*-BuLi (1.7 M in pentane) in toluene at –78 °C under an Ar atmosphere. When the addition was complete, the reaction mixture was allowed to come to rt. Stirring was continued at rt for 2 h, after which time the pentane was removed by distillation. The so-obtained stock solution of lithium *tert*-amylate (1.7 M in toluene) was stored under an Ar atmosphere in a refrigerator.

(2α,4aβ,5β,8α,8aα)-5-[(*tert*-Butyldimethylsilyl)oxy]decahydro-4a,8-dimethyl-8-[(trimethylsilyl)oxy]-2-naphthalenol 2-(Methanesulfonate) (106). To a solution of 0.375 g (0.92 mmol) of mesylate **58** in 15 mL of dry pyridine were added 1 mL (4.7 mmol) of hexamethyldisilazane (HMDS) and 0.5 mL (3.5 mmol) of TMSCl. The reaction mixture was stirred at rt for 3 h and then concentrated under reduced pressure. The resulting residue was flash chromatographed on silica gel (2:1 petroleum ether (bp 40–60 °C)/EtOAc) to afford 0.422 g (96%) of **106** as a colorless oil: ^{1}H NMR (200 MHz) δ –0.04 (s, 9 H), –0.01 (s, 6 H), 0.83 (s, 12 H), 1.06 (s, 3 H), 1.07–1.96 (m, 10 H), 2.14 (m, 1 H), 2.97 (s, 3 H), 3.27 (dd, J = 7.0, 8.1 Hz, 1 H), 5.04 (m, $W_{1/2}$ = 8 Hz, 1 H); ^{13}C NMR (50 MHz) δ –5.07 (q), –4.24 (q), 2.53 (3q), 12.62 (q), 17.75 (s), 22.70 (q), 25.57 (3q), 25.84 (t), 26.90 (t) 28.82 (t), 34.98 (t), 38.96 (q), 39.22 (s), 40.54 (t), 46.15 (d), 74.35 (s), 78.93 (d), 80.14 (d); MS, *m/z* (relative intensity) 421 (M^+–57, 33), 335 (40), 331 (20), 324 (16), 251 (12), 239 (67), 235 (33), 165 (100), 56 (60), 54 (60); calcd for $C_{18}H_{37}O_5SSi_2$ (M^+–57) *m/z* 421.1900, found *m/z* 421.1888.

(2α,4aα,5α,8β,8aβ)-5-[(*tert*-Butyldimethylsilyl)oxy]decahydro-4a,8-dimethyl-8-[(trimethylsilyl)oxy]-2-naphthalenol 2-(Methanesulfonate) (107). The mesylate **59** (0.290 g, 0.71 mmol) was treated with HMDS and TMSCl for 3.5 h as described above for the silylation of the mesylate **58**. Workup and flash chromatography on silica gel (2:1 petroleum ether (bp 40–60 °C)/EtOAc) gave 0.328 g (97%) of **107**

as a colorless oil: ^{1}H NMR (200 MHz) δ –0.03 (s, 3 H), –0.01 (s, 3 H), 0.00 (s, 3 H), 0.05 (s, 6 H), 0.83 (s, 9 H), 0.85 (s, 3 H), 0.88–2.11 (m, 10 H), 1.09 (s, 3 H), 2.19 (m, 1 H), 3.00 (s, 3 H), 3.19 (dd, J = 6.9, 7.8 Hz, 1 H), 4.57 (m, $W_{1/2}$ = 24 Hz, 1 H); ^{13}C NMR (50 MHz) δ –5.04 (q), –4.21 (q), 2.53 (3q), 13.35 (q), 17.74 (s), 22.82 (q), 25.57 (3q), 27.47 (t), 28.30 (t), 28.89 (t), 38.62 (q), 38.68 (s), 39.09 (t), 40.66 (t), 51.44 (d), 74.30 (s), 79.16 (d), 82.88 (d); MS, m/z (relative intensity) 421 (M^+–57, 60), 335 (62), 331 (38), 324 (12), 251 (12), 239 (44), 235 (28), 165 (100), 56 (48), 54 (46); calcd for $C_{18}H_{37}O_5SSi_2$ (M^+–57) m/z 421.1900, found m/z 421.1894.

Base-Promoted Reactions of the Mesylates. General Procedure. All reactions were carried out on 0.25–0.50 mmol of substrate at a concentration of ca. 0.1 M in dry benzene. These solutions were degassed and refluxed under an Ar atmosphere. The stock solutions of sodium and lithium *tert*-amylate (2.2 and 1.7 M, respectively, in toluene) were used. *Ca.* 5 equiv of sodium or lithium *tert*-amylate were added at once, *via* syringe, to the refluxing solution of the mesylate in dry benzene. Unless otherwise indicated, the reaction mixture was heated at reflux temperature for 10 min, quenched with precooled saturated aqueous NH_4Cl, and then quickly cooled to 0 °C. The mixture was vigorously stirred for 20 min, followed by extraction with ten 15-mL portions of CH_2Cl_2. The combined organic layers were dried and evaporated to afford the crude reaction product. Product ratios, yields, and pure compounds were obtained by chromatographical techniques.

Reactions of the Mesylates 39, 40, 58, 59, 106, and 107 with Sodium *tert*-Amylate. a. The general procedure was employed by using 0.190 g (0.47 mmol) of **39** in 5 mL of dry benzene and 1.25 mL of 2.2 M sodium *tert*-amylate in toluene. Workup and flash chromatography on silica gel (5:1 petroleum ether (bp 40–60 °C)/EtOAc) afforded 0.114 g (78%) of a 12:1 mixture of **41** and **108**, respectively, and 0.035 g (18%) of unreacted **39**. The spectroscopic data for **41** and **108** were identical with those reported previously.[5]

b. The general procedure was employed by using 0.194 g (0.48 mmol) of **40** in 5 mL of dry benzene and 1.25 mL of 2.2 M sodium *tert*-amylate in toluene. Workup and flash chromatography on silica gel (10:1 petroleum ether (bp 40-60 °C)/ EtOAc) gave 0.134 g of a mixture of at least three compounds and 0.016 g (8%) of unreacted **40**. Column chromatography of the mixture (0.134 g) on silica gel (50:1 petroleum ether (bp 40–60 °C)/EtOAc) afforded 0.018 g of a "dimeric" oil[26] [MS, m/z (relative intensity) 602 (M^+, < 0.1), 587 (0.3), 545 (10), 507 (23), 413 (10), 375 (5), 305 (26), 253 (32), 239 (100), 219 (40), 215 (18), 75 (35); calcd for $C_{35}H_{63}O_3Si_2$ (M^+–15) m/z 587.4312, found m/z 587.4316], 0.078 g (53%) of a 6.5:1 mixture of **41** and **108**, respectively, and 0.033 g (22%) of **(5*R*)-5-[(*tert*-butyldimethylsilyl)oxy]-5-[(1′α,2′α,5′α)-2′-methylbicyclo[3.1.0]hexan-2′-yl]pentan-2-one (105)**: ^{1}H NMR (200 MHz) δ 0.02 (s, 3 H), 0.03 (s, 3 H), 0.05 (m, 1 H), 0.28 (m, 1 H), 0.62–1.25 (m, 3 H), 0.88 (s, 9 H), 0.93 (s, 3 H), 1.47–2.03 (m, 5 H), 2.12 (s, 3 H), 2.37-2.73 (m, 2 H), 3.37 (dd, J = 3.6, 6.7 Hz, 1 H); ^{13}C NMR (50 MHz) δ –4.13 (q), –3.31 (q), 6.07 (t, J = 158 Hz), 17.59 (d, J =166 Hz), 18.43 (s), 20.99 (q), 24.58 (d, J = 167 Hz), 26.18 (3q), 26.98 (t), 27.19 (t), 30.05 (q), 31.10 (t), 41.25 (t), 48.32 (s), 77.00 (d), 209.19 (s); MS, m/z (relative intensity) 295 (M^+–15, 0.5), 253 (19), 239 (2), 215 (100), 199 (3), 173 (5), 145 (12), 115 (5), 95 (12), 73 (36); calcd for $C_{14}H_{25}O_2Si$ (M^+–57) m/z 253.1624, found m/z 253.1623.

c. The general procedure was employed by using 0.200 g (0.49 mmol) of **58** in 5 mL of dry benzene and 1.25 mL of 2.2 M sodium *tert*-amylate in toluene. Workup and flash chromatography on silica gel (10:1 petroleum ether (bp 40–60 °C)/EtOAc) gave 0.105 g of a mixture of at least five compounds and 0.048 g (24%) of unreacted **58**. The mixture (0.105 g) was column chromatographed on silica gel (50:1 petroleum ether (bp 40–60 °C)/EtOAc) to afford, in order of elution, 0.015 g (10%) of a 1:2:2 mixture of **105**, **111**, and **112**, respectively, 0.040 g (26%) of pure **109**, and 0.048 g (32%) of a 1.1:1 mixture of **109** and **110**, respectively. The spectroscopic data of **110** and **111** are given in the following experiments, those of **109** and **112**[27] are shown below.

(1α,4β,4aβ,8aα)-4-[(*tert*-Butyldimethylsilyl)oxy]-1,2,3,4,4a,5,6,8a-octahydro-1,4a-dimethyl-1-naphthalenol (109): ^{1}H NMR (200 MHz) δ 0.01 (s, 6 H), 0.81 (s, 3 H), 0.87 (s, 9 H), 1.11 (s, 3 H), 1.14-1.83 (m, 7 H), 1.99-2.05 (m, 3 H), 3.30 (dd, *J* = 5.9, 9.0 Hz, 1 H), 5.66 (br s, 2 H); ^{13}C NMR (50 MHz) δ –5.09 (q), –4.22 (q), 12.45 (q), 17.83 (s), 22.29 (q), 22.57 (t), 25.62 (3q), 29.09 (t), 35.88 (t), 38.23 (s), 40.56 (t), 52.30 (d), 71.39 (s), 78.06 (d), 124.71 (d), 127.01 (d); MS, *m/z* (relative intensity) 295 (M^+–15, 1), 253 (80), 177 (16), 159 (27), 145 (20), 119 (35), 105 (55), 91 (32), 75 (100), 43 (51); calcd for $C_{18}H_{34}O_2Si$ (M^+) *m/z* 310.2328, found *m/z* 310.2330. In the ^{1}H NMR (200 MHz) of a 2:1 mixture of **109** and Eu(fod)$_3$, respectively, the following main signals are observed: δ 3.27 (br s, 1 H), 3.65 (dd, *J* = 5, 9 Hz, 1 H), 5.89 (ddd, *J* = 3, 7, 10 Hz, 1 H), 6.83 (dd, *J* = 2, 10 Hz, 1 H).

(5*R*)-5-[(*tert*-Butyldimethylsilyl)oxy]-5-[(3′α)-3′-methylcyclohex-1′-en-3′-yl]pentan-2-one (112): ^{1}H NMR (200 MHz) (main peaks) δ 0.01 (s 6 H), 0.88 (s, 9 H), 1.22 (s, 3 H), 2.10 (s, 3 H), 2.31–2.76 (m, 2 H), 3.37 (dd, *J* = 3.4, 6.9 Hz, 1 H), 5.38 (br d, *J* = 10.2 Hz, 1 H), 5.60 (dt, *J* = 3.6, 3.6, 10.2 Hz, 1 H); ^{13}C NMR (50 MHz) (main peaks) δ 126.65 (d), 134.49 (d), 208.83 (s); MS, *m/z* (relative intensity) 295 (M^+–15, 0.6), 253 (22), 215 (77), 159 (8), 145 (29), 115 (14), 95 (12), 73 (100), 43 (20).

d. The general procedure was employed by using 0.200 g (0.49 mmol) of **59** in 5 mL of dry benzene and 1.25 mL of 2.2 M sodium *tert*-amylate in toluene. Workup and column chromatography on silica gel (50:1 to 15:1 petroleum ether (bp 40–60 °C)/EtOAc) gave, in order of elution, 0.010 g of the "dimeric" oil, 0.127 g (78.5%) of a 33:2.5:1.1:1 mixture of **105**, **109**, **110**, and **111**, respectively, and 0.016 g (8%) of unreacted **59**.

e. When the mesylates **106** and **107** were treated with sodium *tert*-amylate for 3 h according to the general procedure, these compounds were recovered in 96 and 98%, respectively.

Reactions of the Mesylates 40 and 59 with Lithium *tert*-Amylate. a. The general procedure was employed by using 0.050 g (0.12 mmol) of **40** in 1.5 mL of dry benzene and 0.4 mL of 1.7 M lithium *tert*-amylate in toluene. Workup and flash chromatography on silica gel (10:1 petroleum ether (bp 40–60 °C)/EtOAc) gave 0.003 g (8%) of a 4:3:1 mixture of **41**, **108**, and **105**, respectively, and 0.042 g (84%) of unreacted **40**.

b. The same as above, except that the reaction mixture was heated at reflux temperature until completion (3 h). Workup and column chromatography on silica gel (50:1 petroleum ether (bp 40–60

°C)/EtOAc) gave 0.005 g of the "dimeric" oil and 0.030 g (77%) of a 8:6.5:1 mixture of **41**, **108**, and **105**, respectively.

c. The general procedure was employed by using 0.100 g (0.25 mmol) of **59** in 2.5 mL of dry benzene and 0.75 mL of 1.7 M lithium *tert*-amylate in toluene. Workup and flash chromatography on silica gel (15:1 petroleum ether (bp 40–60 °C)/EtOAc) gave 0.006 g (8%) of a 1.7:1 mixture of **105** and **111**, respectively, and 0.091 g (91%) of unreacted **59**. Trace amounts of **109** and **110** were also detected.

d. The same as above, except that the reaction mixture was heated at reflux temperature until completion (7 h). Starting from 0.200 g (0.49 mmol) of **59**, workup and column chromatography on silica gel (50:1 petroleum ether (bp 40–60 °C)/EtOAc) gave, in order of elution, 0.040 g of the "dimeric" oil, 0.065 g (42%) of a 1:1.1 mixture of **105** and **111**, respectively, and 0.035 g (23%) of a 1.2:1 mixture of **109** and **110**, respectively. Preparative GC of the mixture of **105** and **111** afforded a pure sample of **(4α,4aα,8aα)-4-[(*tert*-butyldimethylsilyl)oxy]-octahydro-4a,8a-dimethyl-1(2*H*)-naphthalenone (111)**: ^{1}H NMR (C_6D_6, 200 MHz, 67 °C) δ 0.03 (s, 3 H), 0.06 (s, 3 H), 0.87 (s, 3 H), 0.96 (s, 9 H), 1.02–2.12 (m, 10 H), 1.20 (s, 3 H), 2.27 (m, 1 H), 2.49 (m, 1 H), 3.85 (m, $W_{1/2}$ = 15.0 Hz, 1 H); ^{13}C NMR (C_6D_6, 50 MHz, 67 °C) δ –5.33 (q), –4.68 (q), 17.40 (q), 17.65 (s), 20.40 (q), 20.89 (t), 21.43 (t), 25.44 (3q), 29.44 (t), 32.14 (t), 32.66 (t), 33.74 (t), 43.12 (s), 51.68 (s), 71.75 (d), 211.81 (s); MS, *m/z* (relative intensity) 295 (M^+–15, 6), 253 (95), 161 (91), 143 (60), 119 (60), 105 (38), 91 (17), 75 (100), 41 (47); calcd for $C_{14}H_{25}O_2Si$ (M^+–57) *m/z* 253.1624, found *m/z* 253.1627.

Reactions of the Mesylates 39, 40, 58, 59, 106, and 107 with Sodium *tert*-Amylate in the Presence of 15-Crown-5. a. The general procedure was employed by using a mixture of 0.086 g (0.21 mmol) of **39** and 0.027 g (0.12 mmol) of 15-crown-5 in 2.5 mL of dry benzene, and 0.6 mL of 2.2 M sodium *tert*-amylate in toluene. Workup and flash chromatography on silica gel (10:1 petroleum ether (bp 40–60 °C)/EtOAc) gave 0.065 g (98%) of a 60:1 mixture of **41** and **108**, respectively.

b. The general procedure was employed by using a mixture of 0.195 g (0.48 mmol) of **40** and 0.055 g (0.25 mmol) of 15-crown-5 in 5 mL of dry benzene, and 1.25 mL of 2.2 M sodium *tert*-amylate in toluene. Workup and column chromatography on silica gel (50:1 petroleum ether (bp 40–60 °C)/EtOAc) gave, in order of elution, 0.027 g of the "dimeric" oil, 0.081 g (54%) of **105**, and 0.030 g (20%) of an 8.5:1 mixture of **41** and **108**, respectively.

c. The general procedure was employed by using a mixture of 0.200 g (0.49 mmol) of **58** and 0.055 g (0.25 mmol) of 15-crown-5 in 5 mL of dry benzene, and 1.25 mL of 2.2 M sodium *tert*-amylate in toluene. Workup gave 0.150 g (100%) of a 1:10 mixture of **109** and **110**, respectively. Careful column chromatography on silica gel (100:1 to 25:1 petroleum ether (bp 40–60 °C)/EtOAc) afforded a pure sample of **(1α,4β,4aβ,8aα)-4-[(*tert*-butyldimethylsilyl)oxy]-1,2,3,4,4a,5,8,8a-octahydro-1,4a-dimethyl-1-naphthalenol (110)**: ^{1}H NMR (200 MHz) δ 0.01 (s, 6 H), 0.80 (s, 3 H), 0.85 (s, 9 H), 1.16 (s, 3 H), 1.31-2.22 (m, 10 H), 3.30 (dd, *J* = 6.0, 9.7 Hz, 1 H), 5.54 (ddd, *J* = 3.2, 5.0, 10.1 Hz, 1 H), 5.61 (ddd, *J* = 2.4, 4.7, 10.1 Hz, 1H); ^{13}C NMR (50 MHz) δ –5.08 (q), –4.15 (q), 12.12 (q), 17.81 (s), 22.40 (t), 22.73 (q), 25.60 (3q), 29.01 (t), 38.33 (s), 40.66 (t), 42.02 (t), 48.75 (d), 71.62 (s), 79.87 (d), 124.73 (d), 125.25 (d); MS, *m/z* (relative

intensity) 310 (M^+, 1), 295 (1), 253 (54), 159 (32), 119 (30), 105 (55), 91 (27), 75 (100), 43 (50); calcd for $C_{18}H_{34}O_2Si$ (M^+) *m/z* 310.2328, found *m/z* 310.2326.

d. The general procedure was employed by using a mixture of 0.100 g (0.25 mmol) of **59** and 0.027 g (0.12 mmol) of 15-crown-5 in 2.5 mL of dry benzene, and 0.6 mL of 2.2 M sodium *tert*-amylate in toluene. Workup and column chromatography on silica gel (50:1 petroleum ether (bp 40-60 °C)/EtOAc) gave, in order of elution, 0.010 g of the "dimeric" oil and 0.067 g (86.5%) of a 67:0.5:1:1 mixture of **105**, **109**, **110**, and **111**, respectively.

e. The general procedure was employed by using a mixture of 0.239 g (0.50 mmol) of **106** and 0.055 g (0.25 mmol) of 15-crown-5 in 5 mL of dry benzene, and 1.25 mL of 2.2 M sodium *tert*-amylate in toluene. After heating at reflux temperature for 24 h, the mixture was quenched. Workup and flash chromatography on silica gel (50:1 petroleum ether (bp 40-60 °C)/EtOAc) gave 0.124g (53%) of unreacted **106** and 0.087 g (46%) of **(1α,4β,4aβ,8aα)-4-[(*tert*-butyldimethylsilyl)oxy]-1,2,3,4,4a,5,8,8a-octahydro-1-[(trimethylsilyl)oxy]-1,4a-dimethylnaphthalene (113)**: ^{1}H NMR (200 MHz) δ 0.03 (s, 6 H), 0.07 (s, 9 H), 0.81 (s, 3 H), 0.87 (s, 9 H), 1.19 (s, 3 H), 1.41–2.32 (m, 9 H), 3.30 (dd, *J* = 5.8, 8.7 Hz, 1 H), 5.49-5.62 (m, 2 H); ^{13}C NMR (50 MHz) δ –5.07 (q), –4.14 (q), 2.59 (3q), 12.38 (q), 17.84 (s), 22.65 (t), 23.34 (q), 25.63 (3q), 29.12 (t), 38.37 (s), 40.77 (t), 42.45 (t), 49.23 (d), 75.04 (s), 79.95 (d), 124.45 (d), 125.99 (d); MS, *m/z* (relative intensity) 382 (M^+, 0.6), 367 (5), 325 (80), 248 (40), 239 (100), 235 (90), 160 (60), 56 (70), 54 (50); calcd for $C_{21}H_{42}O_2Si_2$ (M^+) *m/z* 382.2723, found *m/z* 382.2728.

f. When the mesylate **107** was treated with sodium *tert*-amylate in the presence of 15-crown-5 for 24 h according to the general procedure, no reaction products could be isolated. The starting material was recovered in 84%.

Treatment of the Mesylates 106 and 107 with TBAF. a. A solution of 0.050 g (0.11 mmol) of **106** in 1.5 mL of dry benzene was treated according to the general procedure, using 0.1 mL of 1.1 M TBAF in THF in place of alkali metal *tert*-amylate. Workup and flash chromatography on silica gel (10:1 petroleum ether (bp 40–60 °C) /EtOAc) gave 0.028 g (78%) of a 1:1 mixture of **109** and **110**.

b. A solution of 0.060 g (0.13 mmol) of **107** in 1.8 mL of dry benzene was treated with 0.13 mL of 1.1 M TBAF in THF as described above. Workup and flash chromatography on silica gel (10:1 petroleum ether (bp 40-60 °C)/EtOAc) yielded 0.030 g (77%) of **105** as the sole product.

3.5 References and Notes

(1) For an extensive review of the Wharton reaction, see: Caine, D. *Org. Prep. Proced. Int.* **1988**, *20*, 1-51.

(2) Wharton, P. S.; Hiegel, G. A. *J. Org. Chem.* **1965**, *30*, 3254-3257.

(3) Deslongchamps, P. *Stereoelectronic Effects in Organic Chemistry*; Pergamon Press: Oxford, 1983, pp 259-261.

(4) Wijnberg, J. B. P. A.; Jenniskens, L. H. D.; Brunekreef, G. A.; de Groot, A. *J. Org. Chem.*, **1990**, *55*, 941-948.

(5) Jenniskens, L. H. D.; Wijnberg, J. B. P. A; de Groot, A. *J. Org. Chem.* **1991**, *56*, 6585-6591.

(6) These reactions performed in toluene gave similar product ratios of **41** and **108**. See also reference 5.

(7) During this reaction, a "dimeric" product with a molecular weight of 602 was formed. Although the structure of this product could not be elucidated, its formation is probably the result of an aldol condensation reaction of **105** under the influence of the strong base used in this reaction. See reference 1 and references cited therein.

(8) Reaction of **58** and **59** with TMSCl in combination with hexamethyldisilazane (HMDS) produced the O-silylated mesylates **106** and **107**, respectively. The axial hydroxyl group of **39** and **40** could not be silylated under these conditions, probably as a result of steric hindrance of the angular methyl group at C_{10}.

(9) Bartsch, R. A.; Allaway, J. R.; Lee, J. G. *Tetrahedron Lett.* **1977**, 779-780.

(10) Saunders, W. H.; Cockerill, A. F. *Mechanisms of Elimination Reactions*; Wiley-Interscience: New York, 1973, p 217-235.

(11) Collins, C. J. *Chem. Soc. Rev.* **1975**, *4*, 251-262.

(12) See reference 3, pp 190-191.

(13) Allinger, N. L. *J. Am. Chem. Soc.* **1977**, *99*, 8127-8134.

(14) Sorensen, T. S.; Whitworth, S. M. *J. Am. Chem. Soc.* **1990**, *112*, 6647-6651.

(15) Flury, P.; Grob, C. A. *Helv. Chim. Acta* **1983**, *66*, 1971-1980.

(16) Fischer, W.; Grob, C. A.; Hanreich, R.; von Sprecher, G.; Waldner, A. *Helv. Chim. Acta* **1981**, *64*, 2298-2311.

(17) Grob, C. A. *Acc. Chem. Res.* **1983**, *16*, 426-431.

(18) Bank, S. *J. Org. Chem.* **1972**, *37*, 114-118.

(19) The Li^+–O^- bond has a more covalent character than the Na^+–O^- bond[20]. As a result, the electron donating ability of the alkoxide function with Li^+ as the counterion will be diminished.

(20) Paquette, L. A.; Gilday, J. P. *J. Org. Chem.*, **1988**, *53*, 4972-4978.

(21) This term was introduced by Grob[17] to designate the intensity with which the *I* effect is transmitted to the reaction center.

(22) Since the mesylates **39** and **40** could not be silylated, it was not possible to verify these MM2 force field calculations experimentally.

(23) Bartsch, R. A. *Acc. Chem. Res.* **1975**, *8*, 239-245.

(24) For a general description of the experimental procedures employed in this research, see: chapter 2.

(25) Conia, M. J.-M. *Bull. Soc. Chim.* **1950**, *17*, 537.

(26) Although the structure of this oil could not be established with certainty, the NMR data reveal the presence of cyclopropane rings.

(27) This compound could not be isolated in pure form with column chromatography.

Chapter 4

Rearrangement *vs.* Homofragmentation; Chemical Consequences of Different σ-Relays on the TBI Induced Heterolysis of Sulfonate Esters*

4.1 Introduction

From the studies on 1,4-diol monosulfonate esters in which the ring carbon atoms adjacent to the carbon atom bearing the sulfonate ester are unsubstituted (see also Chapter 3), it was concluded that the formation of an alcoholate function intramolecularly induces heterolysis of the sulfonate ester group, probably *via* orbital interactions through the three intervening C–C bonds.[1] The resulting dipolar intermediates subsequently undergo homofragmentation[2], β-elimination, or rearrangement dependent on the location and orientation (axial or equatorial) of the sulfonate ester.

Whereas through-bond interaction (TBI) alone controls the reactivity of compounds with an axial sulfonate ester group, the reactivity of the corresponding compounds in which the sulfonate ester group is equatorially oriented is determined by the sum of TBI and a 1,3-bridged through-space interaction. Comparison of the reaction rates suggests that TBI largely controls the *reactivity* of these compounds, and that 1,3-bridging (if present) contributes little to the overall reaction rate. However, if 1,3-bridging occurs it can determine the product composition to a high degree.
Experimental and theoretical studies[3,4] have demonstrated that the extent of TBI between an electron rich function and an electron poor bond also depends on the σ-relay (the geometry of the intervening σ-framework). Although the 1,4-diol monosulfonate esters studied so far have been subjected to detailed mechanistic studies,[3,5] no attempts have yet been made to relate the TBI to the geometry of the four-carbon chain between the electron-donating alcoholate function and the nucleofugal sulfonate ester in these compounds. Therefore, we decided to examine the mesylates **60–65** under strongly basic conditions, *i.e.*, sodium *tert*-amylate in refluxing benzene.

* This chapter has been published for the greater part: Orrū, R. V. A.; Wijnberg, J. B. P. A.; Bouwman, C. T.; de Groot, A. *J. Org. Chem.* **1994**, *59*, 374-382.

These compounds all have the same structural features around the mesylate group. Because we assume that the orientation of the alcohol function will probably have little influence on the reaction rate,[7] the actual geometry in the compounds **60–65** can be represented by the three partial structures **I**, **II**, and **III** (Chart 4.1).

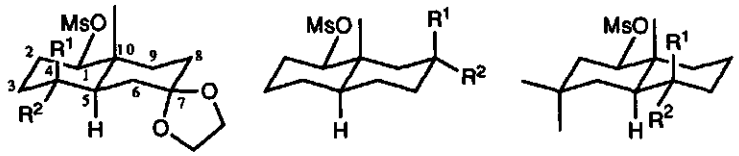

60 : R^1 = OH; R^2 = CH_3 **62** : R^1 = OH; R^2 = CH_3 **64** : R^1 = OH; R^2 = CH_3
61 : R^1 = CH_3; R^2 = OH **63** : R^1 = CH_3; R^2 = OH **65** : R^1 = CH_3; R^2 = OH

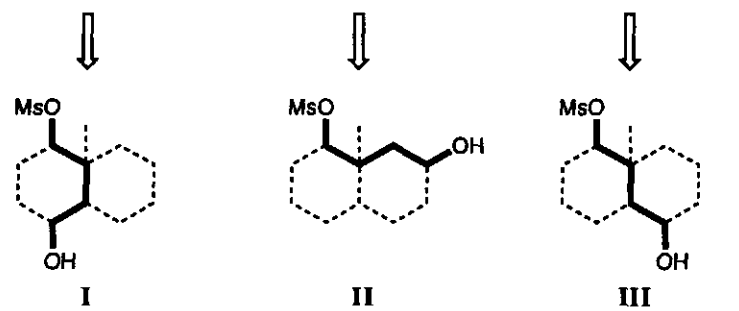

I **II** **III**

Chart 4.1

From the reactions of **60–65** with sodium *tert*-amylate in refluxing benzene we expect to gather more information about (*i*) to what extent transmission of TBI depends on the σ-relay, in particular in the situations **I**, **II**, and **III** depicted in Chart 4.1, and (*ii*) the influence of the σ-relay on the product composition or, in other words: what are the chemical consequences if a certain σ-relay is operating?

4.2 Results and Discussion

In order to obtain comparable data about the reactivity of the mesylates **60-65**, all these compounds were subjected to the same reaction conditions. The reactions were run in benzene at reflux temperature with *ca.* 5 equiv of sodium *tert*-amylate during 10 min. By comparing the quantities of recovered starting material a rough estimate of the relative reaction rates could be obtained. The results of these studies are collected in Table 4.1.

Table 4.1. Reactions of the mesylates 60-65 with sodium tert-amylate [a].

entry	mesylate	products (%)[b]	recovery[c]
1	**60**	**114** (76)[d]	21
2	**61**	**117** (34)	66
3	**62**	**118** (33)[e] + **119** (<10)	50
4	**63**	**118** (32)[e] + **120** (8)	50
5	**64**	**121** (76)[e]	--
6	**65**	**121** (72)[e]	--

[a] All reactions were performed in refluxing benzene with *ca.* 5 equiv of sodium *tert*-amylate for 10 min. [b] Isolated yield in parentheses. [c] Percentage of recovered starting material. [d] The compounds **115** and **116** were also isolated in a combined yield of 2%. [e] Yield is somewhat diminished due to aldol condensations under the influence of sodium *tert*-amylate.

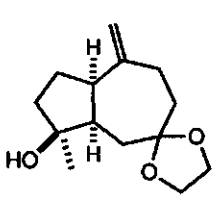

114

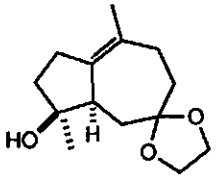

115

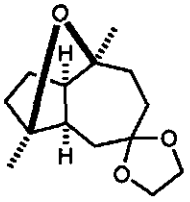

116

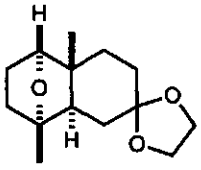

117

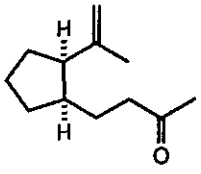

118

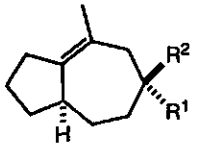

119 : $R^1 = CH_3$; $R^2 = OH$
120 : $R^1 = OH$; $R^2 = CH_3$

121

122

Chart 4.2

The mesylate **60** gave predominantly the rearranged product **114** (76%), together with small amounts of **115** and **116** (entry 1).[5] The quantity of regained **60** in this reaction amounted to 21%.

After reaction of the mesylate **61**, in which C_4 has the opposite stereochemistry compared with **60**, a larger amount (66%) of starting material was regained (entry 2). The sole product in this reaction was the cyclic ether **117** which was isolated in 34% yield. The presence of an ether bridge in **117** was concluded from its ^1H and ^{13}C NMR spectrum. In the ^1H NMR spectrum of **117** a one-proton signal appears at δ 4.09. The ^{13}C NMR spectrum of **117** shows a doublet and a singlet at δ 82.45 and 86.07, respectively.

Both the mesylates **62** and **63** gave the same quantity (50%) of recovered starting material (entries 3 and 4). Also the major product from these reactions was the same, *i.e.*, the rearranged fragmentation product **118**. In both reactions the yield of **118** (33 and 32%, respectively) was somewhat diminished by aldol condensations.[7] An inseparable mixture (10%) of several minor products, with the rearranged olefin **119** as the main component, was formed during the reaction of **62**. As a minor product from the reaction of **63**, the rearranged olefin **120** was isolated in 8% yield.

After the standard basic treatment of the mesylates **64** and **65**, no starting material could be detected (entries 5 and 6). In both cases, only fragmentation was observed leading to the same product. The yield of this product, the cyclopropane derivative **121**, was 76% from **64** and 72% from **65**. Also in these reactions the product yields were diminished by aldol condensations. When the reaction time was shortened to 1 min, **121** was isolated in almost quantitative yield from both **64** and **65**. The proton-coupled ^{13}C NMR spectrum of **121** shows a two-carbon signal (doublet) with J = 165 Hz, which is consistent with the presence of a cyclopropane ring. Together with other NMR data, this confirms our structural assignment of **121**. In an additional experiment **64** was treated with lithium *tert*-amylate instead of sodium *tert*-amylate. After completion of this reaction (2 h), a considerable amount of the rearranged cyclic ether **122** was isolated next to **121**.

The results of these studies on **60–65** clearly show that a different location of the hydroxyl group strongly affects the course of the reactions of these compounds. The two chief pathways by which these compounds react are rearrangement (entries 1, 3, and 4) and homofragmentation (entries 5 and 6). Homofragmentation occurs in a very fast reaction, within 1 min the reactions with **64** and **65** are complete. The rearrangement reactions and the reaction in which the cyclic ether **117** is formed (entry 2) take much more time. Considerable amounts (21–66%) of starting material are recovered after a reaction time of 10 min.

It is also demonstrated that two epimeric hydroxy mesylates (*e.g.* **62** and **63**, or **64** and **65**) react at the same rate. These results confirm our assumption that the orientation of the hydroxyl group is not very important for the reactivity of these compounds. This is not so surprising if stereoelectronic effects, as is probably the case here, play a dominant role. An electron pair of an oxygen anion can always adopt the most favorable orientation required for reaction.[8] On the other hand, the difference in reaction rate between **62** and **64**, or between **63** and **65**, is spectacular. This proves that the reactivity of these compounds is closely connected with the location of the hydroxyl group.

The relatively large difference in reaction rates found for the epimers **60** and **61** (entries 1 and 2) must be attributed, in the first instance, to steric hindrance and not to stereoelectronic factors. This steric hindrance is also responsible for the completely different product outcome (rearrangement *versus* cyclic ether formation) upon reaction of **60** and **61**. From examination of molecular models, it appears that the diaxial steric interaction between the angular methyl group and the methyl group at C_4 in **61** forces the equatorial hydroxyl group at C_4 and C_1 toward each other. Another consequence of this steric hindrance is that the C_5–C_{10} bond is no longer exactly antiperiplanar to the mesylate group and hence the tendency to rearrange will be diminished. As an overall result, ether formation is favored over rearrangement. Semi-empirical MNDO calculations provide some support for the disruption of the antiperiplanarity as illustrated in the Newman projections along the C_1–C_{10} bond of **60** and **61** (Figure 4.1).[9] The C_5–C_{10} bond in **60** deviates only 5° from the antiperiplanar orientation to the sulfonate ester bond. The C_5–C_{10} bond in **61**, on the other hand, diverges much more (16°).

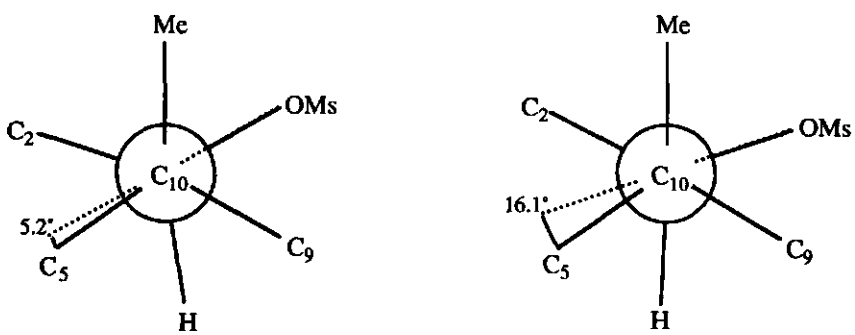

60 **61**

*Figure 4.1: Newman projections along the C_1–C_{10} bond of **60** and **61**.*

This difference in antiperiplanarity also explains the diminished reactivity of **61** as compared with that of **60**. It has been shown that in processes which involve initial ionization of a leaving group, the cationic center (or the developing cation) is stabilized by delocalization of a neighboring C–C bond.[10,11] The extent of this electronic delocalization depends on the alignment of the participating σ-bond with the leaving group.[12] The C_5–C_{10} bond in **61** is less favorably oriented for effective σ-participation in the ionization process than the one in **60**, and therefore **61** will react more slowly.

Rearrangement is the only reaction pathway observed for the mesylates **62** and **63** (entries 3 and 4). Just as the mesylate **60**[5] and probably also **61**, these compounds are supposed to react stepwise *via* dipolar intermediates. The initial formed dipolar intermediates **A(62)** and **A(63)** rapidly rearrange to the thermodynamically more stable intermediates **B(62)** and **B(63)** (Scheme 4.1). Both **B(62)** and **B(63)** give the cyclopentane derivative **118** as the major product *via* a fast Grob fragmentation. The formation of the minor products **119** and **120** from the intermediates **B** must be the result of a thermodynamically controlled proton loss. Olefin **120** can also be formed by an intramolecularly assisted proton abstraction.

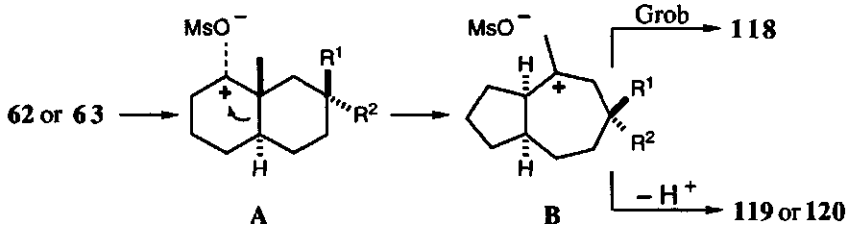

(62): $R^1 = O^-$; $R^2 = CH_3$

(63): $R^1 = CH_3$; $R^2 = O^-$

Scheme 4.1

As pointed out above, the (developing) cationic center generated at C_1 can be stabilized by delocalization of the C_5–C_{10} bond in these systems. It is suggested that electron-releasing substituents donate electrons to the participating σ-bond *via* TBI, thus enlarging the electron density of this bond and its ability to participate in the ionization process.[13] The slightly diminished reactivity of **62** and **63**, as compared with that of **60**, is easily understood on this basis. In the mesylate **60** the hydroxyl group is separated by one C–C bond from the C_5–C_{10} bond, in the mesylates **62** and **63** this number is two. The strongly electron-donating alkoxide group in **60** affects

therefore the electron density of the C_5–C_{10} bond, and consequently the reactivity, to a higher degree than it does in **62** and **63**.

A very fast homofragmentation is the only process observed for **64** and **65** upon treatment with sodium *tert*-amylate (entries 5 and 6). No rearrangement or other products are formed. Both **64** and **65** react at the same rate which proves again that the orientation of the hydroxyl group is not very important for the reactivity of these compounds. The selective formation of the cyclopropane derivative **121** can be explained if the assumption is made that through-space induction, which accompanies TBI,[14] involves bridging of the cationic center at C_1 by the back lobe of the C_5–C_6–O^- orbital. This homohyperconjugation effect,[15,16] as denoted by partial structure **C** in Chart 4.3, will ultimately lead to C_5–C_1 bond formation with simultaneous breaking of the C_5–C_6 bond.

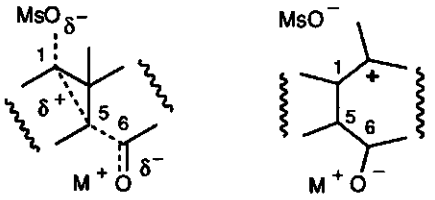

C (M = Na) **D** (M = Li)

Chart 4.3

The initially formed secondary carbocations in these processes can be expected to undergo rearrangement to more stable tertiary ions, with bridged ions being likely intermediates on the rearrangement path. The reactions of **64** with sodium and lithium *tert*-amylate support the existence of these bridged cationic intermediates. Being a bonding interaction, bridging is strengthened by electron donors and weakened by electron acceptors.[17] The strongly electron-donating alkoxide group with Na^+ as counterion pushes the back lobe of the C_5–C_6–O^- orbital toward the cationic center at C_1 to such an extent that **C** will be more stable than the rearranged tertiary cationic intermediate **D** (Chart 4.3). As a result, homofragmentation (formation of **121**) will be favored. On the other hand, replacement of Na^+ by Li^+ results in a decrease of the electron-donating ability of the alkoxide group.[18] This decrease of inductivity[19] leads to less bridging and rearrangement (formation of **122**) can now compete favorably with homofragmentation. Cyclopropanoid bridged structures being comparable to **C** have been proposed as intermediates in cationic processes before.[20] It is also noteworthy that processes similar to homofragmentation are thought to occur in the biosynthesis of certain compounds possessing a fused cyclopropane ring.[21-23]

The extremely fast rate by which **64** and **65** react might be explained as the result of the sum of σ-participation, 1,3-bridging, and TBI. The contribution of σ-participation in **64** and **65**, however, will be of the same magnitude as that in, for example, **62** and **63** because in all these compounds the C_5–C_{10} bond is antiperiplanar to the mesylate group. As a consequence, the large rate increase observed for **64** and **65** may not be ascribed to σ-participation. By comparing the reactivities of related mesylates relatively small rate enhancements are observed for reactions in which 1,3-bridging is operating.[1] These observations have led to the assumption that the contribution of 1,3-bridging on the reactivity of **64** and **65** is only modest. This should mean that TBI largely accounts for the large rate increase observed for **64** and **65**.

Since the extent of TBI depends on the geometry of the relaying σ-bonds, the observed differences in reaction rate of the compounds **60–65** can be principally attributed to the differently operating σ-relays **I**, **II**, and **III**. Transmission of TBI is highly favored in **III** (W-like configuration), which finds expression in a very fast reaction of **64** and **65**. The deviation of the "W" arrangement in **I** and **II** makes the transmission of TBI more difficult, thereby reducing the reactivity of **60–65**. These results are consistent with the "*trans* rule", which predicts that the extent of orbital interactions through σ-bonds is maximized for an "all *trans*" arrangement of σ-bonds.[3]

Also the product composition is strongly dependent on the geometry of the relaying σ-bonds. Rearrangement is found to occur preferentially with **I** and **II** as the operating σ-relays, whereas **III** shows homofragmentation as the main reaction path. Only if the back lobe of the polarized C–C–O^- bond is in a proper position for dorsal C-participation in the ionization process (as is the case in the "all *trans*" arrangement of σ-bonds), then homofragmentation can occur. Any other σ-relay in these compounds will lead to rearranged products. Steric effects are responsible for the exceptional behavior of **61**.

4.3 Experimental Section

General.[24] Compounds **114**, **115**, and **116** have been fully characterized before.[5]

Reactions of Mesylates 60-65 with Sodium *tert*-Amylate. General Procedure. All reactions were carried out on 0.50–1.00 mmol of mesylate at a concentration of *ca.* 0.1 M in dry benzene. These solutions were degassed and refluxed under an Ar atmosphere. *Ca.* 5 equiv of sodium *tert*-amylate (3.2 M in toluene) was added at once, *via* syringe, to the refluxing solution of the mesylate. Unless otherwise indicated, the reaction mixture was heated at reflux temperature for 10 min, quenched with precooled saturated aqueous NH_4Cl, and then quickly cooled to 0 °C. The mixture was vigorously stirred for 20 min, followed by

extraction with ten 15-mL portions of CH_2Cl_2. The combined organic layers were dried and evaporated to afford the crude reaction product. Product ratios, yields, and pure compounds were obtained by chromatographical techniques.

a. The general procedure was employed by using 0.167 g (0.50 mmol) of **60**. Workup and flash chromatography (15:1 petroleum ether (bp 40–60 °C)/EtOAc) afforded 0.091 g (76%) of **114** and 0.036 g (21%) of unreacted **60**. Small amounts (combined yield 2%) of **115** and **116** were also obtained.

b. The general procedure was employed by using 0.167 g (0.50 mmol) of **61**. Workup and flash chromatography (10:1 petroleum ether (bp 40–60 °C)/EtOAc) gave 0.041 g (34%) of **(4'aα,5'β,8'β,8'aβ)-octahydro-4'a,8'-dimethylspiro[1,3-dioxolane-2,2'(1'*H*)-[5',8']epoxynaphthalene] (117)**: ^{1}H NMR (200 MHz) δ 0.88 (m, 1 H) 0.92 (s, 3 H), 1.11–1.77 (m, 8 H), 1.30 (s, 3 H), 1.78–2.04 (m, 2 H), 3.90 (br s, 4 H), 4.09 (d, J = 4.0 Hz, 1 H); ^{13}C NMR (50 MHz) δ 16.84 (q), 19.90 (q), 28.89 (t), 30.44 (t), 31.06 (t), 33.54 (t), 35.19 (t), 40.99 (s), 56.14 (d), 63.58 (t), 64.26 (t), 82.45 (d), 86.07 (s), 110.22 (s); MS *m/z* (relative intensity) 238 (M^+, 8), 195 (4), 176 (4), 99 (100), 86 (62); calcd for $C_{14}H_{22}O_3$ (M^+) *m/z* 238.1569, found *m/z* 238.1571. Anal. Calcd for $C_{14}H_{22}O_3$: C, 70.55; H, 9.31. Found: C, 70.26; H, 9.28. Further elution afforded 0.110 g (66%) of unreacted **61**.

c. The general procedure was employed by using 0.138 g (0.50 mmol) of **62**. Workup and flash chromatography (10:1 petroleum ether (bp 40–60 °C)/EtOAc) gave 0.045 g of a mixture of at least three compounds and 0.069 g (50%) of unreacted **62**. Careful column chromatography of the mixture (0.045 g) on silica gel (70–230 mesh) (1:0 to 50:1 petroleum ether (bp 40–60 °C)/EtOAc) afforded, in order of elution, 0.008 g of a "dimeric" oil[25] [MS calcd for $C_{24}H_{38}O$ (M^+) *m/z* 342.3035, found *m/z* 342.3061], 0.030 g (33%) of **118** as a clear oil, and 0.009 g (10%) of an inseparable mixture of several compounds with probably **119** as the main component. The spectroscopic data of **118** and **119** are shown below.

4-[(1'α,2'α)-2'-(1-Methylethenyl)cyclopent-1'-yl]butan-2-one (118): ^{1}H NMR (200 MHz) δ 1.01–1.91 (m, 9 H), 1.71 (br s, 3 H), 2.09 (s, 3 H), 2.31–2.46 (m, 3 H), 4.65 (br s, 1 H), 4.78 (br s, 1 H); ^{13}C NMR (50 MHz) δ 22.32 (t), 23.17 (q), 23.48 (t), 27.15 (t), 29.64 (q), 29.86 (t), 40.39 (d), 42.40 (t), 50.40 (d), 110.34 (t), 145.84 (s), 209.18 (s); MS *m/z* (relative intensity) 180 (M^+, 8), 165 (2), 162 (3), 148 (10), 137 (17), 122 (100), 108 (25), 96 (24), 83 (24), 69 (29); calcd for $C_{12}H_{20}O$ (M^+) *m/z* 180.1514, found *m/z* 180.1514.

(6α,8aβ)-1,2,3,5,6,7,8,8a-Octahydro-4,6-dimethyl-6-azulenol (119): ^{1}H NMR (main peaks, 200 MHz) δ 1.21 (s, 3 H) 1.54 (br s, 3 H); MS *m/z* (relative intensity) 180 (M^+, 16), 162 (6), 122 (100).

d. The general procedure was employed by using 0.276 g (1.00 mmol) of **63**. Workup and flash chromatography (5:1 petroleum ether (bp 40–60 °C)/EtOAc) gave, in order of elution, 0.014 g of the above-mentioned "dimeric" oil[25], 0.057 g (32%) of **118**, and 0.014 g (8%) of **(6α,8aα)-1,2,3,5,6,7,8,8a-octahydro-4,6-dimethyl-6-azulenol (120)**: mp 126-127 °C (from diisopropyl ether); ^{1}H NMR (200 MHz) δ 1.16 (s, 3 H), 1.16–2.47 (m, 13 H), 1.62 (br s, 3 H), 2.57 (br d, J = 13.4 Hz, 1 H); ^{13}C NMR (50 MHz) δ 23.25 (q), 24.64 (q), 25.05 (t), 30.91 (t), 31.78 (t), 35.61 (t), 42.72 (d), 45.76 (t), 49.28 (t), 70.71 (s), 123.14 (s), 142.79 (s); MS *m/z* (relative intensity) 180 (M^+, 11), 162 (71), 147 (64), 135 (79), 123 (100), 110 (70), 94 (15), 80 (17), 68 (14); calcd for $C_{12}H_{20}O$ (M^+) *m/z* 180.1514, found *m/z* 180.1512. Anal. Calcd for $C_{12}H_{20}O$: C, 79.94; H, 11.18. Found: C, 79.92; H, 11.20. Further elution provided 0.138 g (50%) of unreacted **63**.

e. The general procedure was employed by using 0.152 g (0.50 mmol) of **64**. Workup and flash chromatography (50:1 petroleum ether (bp 40–60 °C)/EtOAc) gave 0.020 g of a "dimeric" oil"[26] [MS calcd for $C_{28}H_{46}O$ (M^+) *m/z* 398.3396, found *m/z* 398.3486] and 0.080 g (76%) of **5-[(1'α,2'α,6'α)-1',4',4'-trimethylbicyclo[3.1.0]hexan-1'-yl]pentan-2-one (121)**: ^{1}H NMR (200 MHz) δ 0.86 (s, 3 H), 0.89 (s, 3 H), 0.97 (s, 3 H), 0.98–1.70 (m, 10 H), 2.09 (s, 3 H), 2.34 (t, *J* = 7.4 Hz, 2 H); ^{13}C NMR (50 MHz) δ 11.22 (q), 20.80 (t), 26.31 (q), 26.65 (s), 29.52 (q), 30.36 (2d, *J* = 165 Hz), 30.62 (q), 39.00 (2t), 40.73 (t), 43.56 (t), 50.14 (s), 208.75 (s); MS *m/z* (relative intensity) 208 (M^+, 0.6), 193 (5), 190 (6), 175 (12), 150 (49), 135 (60), 107 (19), 95 (37), 81 (45), 43 (100); calcd for $C_{14}H_{24}O$ (M^+) *m/z* 208.1827, found *m/z* 208.1829.

f. The same as above, except that the reaction mixture was heated at reflux for 1 min. After workup and flash chromatography, **121** was isolated in 94% yield.

g. The general procedure was employed by using 0.152 g (0.50 mmol) of **65**. Workup and flash chromatography (100:1 petroleum ether (bp 40–60 °C)/EtOAc) gave 0.027 g of the above-mentioned "dimeric" oil and 0.075 g (72%) of **121**.

h. The same as above, except that the reaction mixture was heated at reflux for 1 min. After workup and flash chromatography, **121** was obtained in 96% yield.

Reaction of Mesylate 64 with Lithium *tert*-Amylate. The general procedure was employed by using 0.152 g (0.50 mmol) of **64**, except that 1.4 mL of lithium *tert*-amylate (1.8 M in toluene) was used instead of sodium *tert*-amylate, and that the reaction was run until completion (2 h). Workup and flash chromatography (100:1 petroleum ether (bp 40–60 °C)/EtOAc) gave, in order of elution, 0.032 g of the above-mentioned "dimeric" oil, 0.030 g (28%) of **122**, and 0.035 g (34%) of **121**. The spectroscopic data of **114** are shown below.

(3aα,4β,8β,8aα)-Decahydro-2,2,4,8-tetramethyl[4,8]epoxyazulene (122): ^{1}H NMR (200 MHz) δ 0.89 (s, 3 H), 1.04 (s, 3 H), 1.11 (s, 6 H), 1.14–1.81 (m, 10 H), 2.39-2.56 (m, 2 H); ^{13}C NMR (50 MHz) δ 17.50 (t), 22.77 (2q), 25.43 (q), 28.33 (q), 36.90 (2t), 40.56 (s), 42.22 (2t), 50.95 (2d), 79.83 (2s); MS *m/z* (relative intensity) 208 (M^+, 25), 190 (42), 175 (40), 147 (31), 123 (54), 109 (78), 91 (52), 85 (78), 41 (100); calcd for $C_{14}H_{24}O$ (M^+) *m/z* 208.1827, found *m/z* 208.1826.

4.4 References and Notes

(1) See chapter 3

(2) Fragmentation which generates a cyclopropane ring is termed homofragmentation. See: Flury, P.; Grob, C. A. *Helv. Chim. Acta* **1983**, *66*, 1971-1980.

(3) Paddon-Row, M. N. *Acc. Chem. Res.* **1982**, *15*, 245-251.

(4) Jordan, K. D.; Paddon-Row, M. N. *Chem. Rev.* **1992**, *92*, 395-410 and references cited therein.

(5) Wijnberg, J. B. P. A.; Jenniskens, L. H. D.; Brunekreef, G. A.; de Groot, A. *J. Org. Chem.* **1990**, *55*, 941-948.

(6) This assumption is based on the observation that 1,4-diol monosulfonate esters in which only the orientation of the alcohol function is different react with almost the same rate.[1]

(7) See reference 1 and references cited therein.

(8) Deslongchamps, P. *Stereoelectronic Effects in Organic Chemistry*; Pergamon Press: Oxford, 1983.

(9) The Newman projections were drawn based on full geometry optimizations by means of the MNDO (modified neglect of diatomic overlap) method. See: Dewar, M. J. S.; Thiel, W. *J. Am. Chem. Soc.* **1977**, *99*, 4899-4907.

(10) Jensen, F. R.; Smart, B. E. *J. Am. Chem. Soc.* **1969**, *91*, 5686-5689.

(11) (a) Traylor, T. G.; Hanstein, W.; Berwin, H. J.; Clinton, N. A.; Brown, R. S. *J. Am. Chem. Soc.* **1971**, *93*, 5715-5725.
(b) Hartmann, G. D.; Traylor, T. G. *J. Am. Chem. Soc.* **1975**, *97*, 6147-6151.

(12) Fischer, W.; Grob, C. A.; von Sprecher, G.; Waldner, A. *Tetrahedron Lett.* **1979**, *21*, 1905-1908.

(13) Lenoir, D.; Apeloig, Y.; Arad, D.; Schleyer, P. v. R. *J. Org. Chem.* **1988**, *53*, 661-675.

(14) Hoffmann, R. *Acc. Chem. Res.* **1971**, *4*, 1-9.

(15) Adcock, W.; Kok, G. B. *J. Org. Chem.* **1987**, *52*, 356-364.

(16) Grob, C. A.; Gründel, M.; Sawlewicz, P. *Helv. Chim. Acta* **1988**, *71*, 1502-1507.

(17) Grob, C. A. *Acc. Chem. Res.* **1983**, *16*, 426-431.

(18) The Li^+–O^- bond has a more covalent character than the Na^+–O^- bond. See: Paquette, L. A.; Gilday, J. P. *J. Org. Chem.* **1988**, *53*, 4972-4978. As a result, the electron-donating ability of the alkoxide function with Li^+ as the counterion will be diminished.

(19) This term was introduced by Grob[17] to designate the intensity with which the *I* effect is transmitted to the reaction center.

(20) Shiner, V. J., Jr.; Ensinger, M. W.; Kriz, G. S.; Halley, K. A. *J. Org. Chem.* **1990**, *55*, 653-661.

(21) Jakupovic, J.; Schuster, A.; Bohlmann, F.; King, R. M.; Haegi, L. *Phytochemistry*, **1989**, *28*, 1943-1948.

(22) Ahmed, A. A.; Jakupovic, J.; Bohlmann, F. *Phytochemistry*, **1990**, *29*, 3355-3358.

(23) Sakui, N.; Kuroyanagi, M.; Ishitobi, Y.; Sato, M.; Ueno, A. *Phytochemistry*, **1992**, *31*, 143-147.

(24) For general experimental details, see: chapter 2. Lithium and sodium *tert*-amylate were prepared by the procedures described in reference 1.

(25) Although the structure of this compound could not be elucidated, its formation is probably the result of an aldol condensation reaction of **118** under the influence of the strong base used in this reaction. Also see reference 1 and references cited therein.

(26) This "dimeric" oil is probably formed from **121**. See note 25 for further remarks.

Chapter 5

A MNDO Study of the Chemical Consequences of Different σ-Relays on the TBI Induced Reactions of 1,4-Diol Monosulfonate Esters*

5.1 Introduction

In the previous chapters it has been inferred that in rigid 1,4-diol monosulfonate esters deprotonation of the hydroxyl group results in (strong) TBI between the electron donor, the alcoholate anion, and the electron acceptor, the sulfonate ester bond.[1,2] It was demonstrated that, in these cases, the extent of TBI depends mainly on the geometry of the σ-bonds connecting the electron donor and acceptor substituents.[2] These observations are in line with predictions from theoretical models regarding TBI.[3,4]

The compounds in which an "all *trans*" or W-like arrangement of the σ-relay (I) is operating the transmission of TBI is highly favored. These compounds react very fast upon treatment with a strong non-nucleophilic base (sodium *tert*-amylate) in a refluxing apolar solvent (benzene). Homofragmentation[5] is the main reaction path observed. Deviation from this optimal "W" arrangement (for example the sickle-like arrangement in II and III) makes the delocalization of σ-electrons *via* TBI less efficient.[6] As a result, the reactivity of such compounds is reduced and rearrangement is found to occur preferentially.

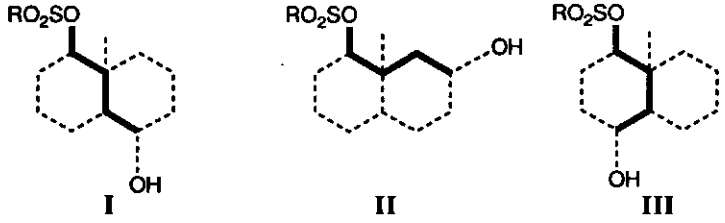

The product outcome, product ratio, and relative rate of the base-induced reactions of perhydronaphthalene-1,4-diol monosulfonate esters described in chapter 4 can be satisfactorily explained with the concept of TBI.

* This chapter will be published in a revised form: Orrū, R. V. A.; van der Kerk, S. M.; Wijnberg, J. B. P. A. *in preparation*.

However, the conclusions are all based on empirical results. In order to gather more information about the basic (stereo)electronic features underlying these reactions, a theoretical investigation was undertaken.
In this chapter the results of semi-empirical calculations, using the MNDO method, performed on model systems will be presented. The main purpose of these investigations is a more detailed understanding of the homofragmentation and rearrangement reaction.

5.2 Computational Details

Molecular Mechanics (MM) methods are very poorly equipped to deal with the formation and breaking of bonds and thus not suited for the study of reaction profiles. Furthermore, the size of the systems studied prevents the use of *ab initio* quantum mechanical methods. Therefore, we have employed the semi-empirical method MNDO.[7] All calculations were carried out on a Convex C120 minisuper computer, using VAMP, the Erlangen Vectorized Molecular Orbital Package (version 4.3).
For each model reaction the calculations were carried out in two series, for an axial and for an equatorial O^-.
Manipulation of the data obtained in "grid calculations" was performed with the software package Mathematica™ (Wolfram Research Inc., versions. 2.1, and 2.2) on an Apple MacIntosh SE-30 and an Apple MacIntosh IIci. Three-dimensional modelling was also carried out on these computers, with the aid of the program Chem3D Plus (Cambridge Scientific Computing Inc., version 3.0).

5.3 Model Compounds

The reactions of the 1,4-diol mesylates **60–65** with sodium *tert*-amylate in refluxing benzene can be described in a generalized way as shown in eq. 5.1.
In going from reactant to products, first the hydroxyl proton is abstracted, and next the mesylate leaving group is expelled. After this, either homofragmentation or rearrangement can take place to form the products. In the homofragmentation process the C_α–C_β bond is broken and the C_β–C_δ bond is formed. In the rearrangement process the C_β–C_γ bond is broken and the C_β–C_δ bond is formed. Consequently, it would appear as if these reactions have to be described in terms of four reaction coordinates at the very least.

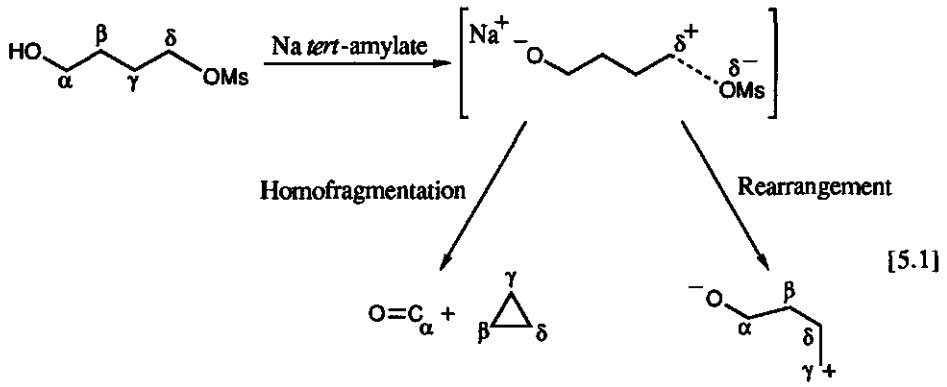

[5.1]

In the computational investigation of a reaction characterized by two reaction coordinates, *e.g.*, the breaking of one bond and the formation of another, the following approach is both useful and reliable. The ranges over which the two bond lengths are expected to vary are divided in *i.e,* four intervals each. For every different combination of points (25 in this case) a single-point calculation is carried out. This is a geometry optimization in which all bond lengths, bond angles, and torsion angles are left free to vary, except for the two fixed values for the bond lengths representing the reaction coordinates. In this way a grid of data points is obtained, defining a two-dimensional surface in a three-dimensional space. Each point represents the minimized energy (heat of formation) at two specific values of the reaction coordinates. The overall reaction coordinate is identical with the path of least energy over this two-dimensional surface. With the aid of data-processing software and interpolation procedures the transition state can be pinpointed fairly accurately. The values of the reaction coordinates at which this so-called saddle-point is found, can be used in a final single-point calculation to yield the bond lengths and angles in the transition state.

However, when the procedure sketched here would be applied to systems that have to be described by more than two reaction coordinates, it is clear that the number of single-point calculations that have to be carried out forms a barrier that is, to all practical purposes, unsurmountable. Simplifications, assumptions, and approximations have to be introduced in order to limit the number of reaction coordinates.

In the present case the following approach was chosen. First, substituents not essential to the line of reasoning are omitted in all of the calculations. Next, as the experimental results have shown the abstraction of the hydroxyl proton to be the initial step in all of the reactions described,[1] it was decided to use starting geometries for the calculations in which the hydroxyl proton has already been removed. The number of reaction variables was further reduced by removing the mesylate group,

leaving atom C_δ three-coordinated and with a positive charge. The choice of a carbocationic C_δ center as the potential electron acceptor may seem premature at this stage, but it should be realized that under the prevailing reaction conditions (sodium *tert*-amylate in refluxing benzene) contact ion pairs are probably involved in the intramolecularly induced departure of the mesylate group. Therefore, it seems reasonable to assume that at least a partial positive charge is present on the carbon atom to which the mesylate group is attached. Further, it is to be expected that under the actual reaction conditions the oxygen anion has a counter ion somewhere in its vicinity. In semi-empirical calculations this can be mimicked by the use of so-called "sparkles".[8] Within the framework of MNDO, sparkles are defined as pure ionic charges, "+" denoting a 100% ionic alkali metal atom and "–" denoting a 100% ionic halogen-like atom. In the software, sparkles have been given an ionic radius of 0.7 Å, a zero heat of atomization, no orbitals, and no ionization potential. All in all, a sparkle can be regarded as an unpolarizable ion of diameter 1.4 Å, with its charge delocalized over its surface. A sparkle does not contribute to the orbital count and can not donate or accept electrons. A negative sparkle was positioned at 1.411 Å (the C–OMs bond length) from C_δ and, a positive sparkle was positioned next to the anionic oxygen atom at the O–H bond length of 0.946 Å. In this way, the number of reaction coordinates could be limited to two, while still retaining a fair approximation of the actual reaction conditions. The geometry of the systems thus simplified (Chart 5.1) proved to be optimizable without large and unexpected changes in geometry taking place.

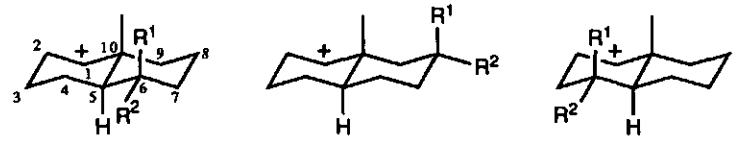

A1 : $R^1 = O^-$; $R^2 = CH_3$ **B1** : $R^1 = O^-$; $R^2 = CH_3$ **C1** : $R^1 = O^-$; $R^2 = CH_3$
A2 : $R^1 = CH_3$; $R^2 = O^-$ **B2** : $R^1 = CH_3$; $R^2 = O^-$ **C2** : $R^1 = CH_3$; $R^2 = O^-$

Chart 5.1

5.4 Results and Discussion

5.4.1 Calculations on the W-like Geometry A

Treatment of the compounds **64** and **65**, having a "W" geometry of the σ-relay, with sodium *tert*-amylate in refluxing benzene gave the cyclopropane derivative **121** (Scheme 5.1).[2]

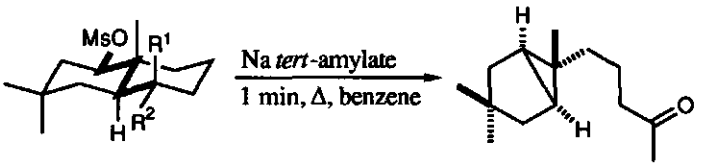

64 : R^1 = OH; R^2 = CH_3
65 : R^1 = CH_3; R^2 = OH

121 (94 – 96 %)

Scheme 5.1

All the simulations regarding this reaction are carried out on model structures **A** as defined in Chart 5.1. Starting from a model compound in which both a positive and a negative sparkle are present, in the first exploratory calculations the negative sparkle next to atom C_1 was removed in small steps to "infinity" (up to a distance of 6 Å). In the next series of calculations, on the other hand, the positive sparkle next to the oxygen atom was removed in the same way. At each of the C_1–sparkle or O^-–sparkle distances a single-point calculation was carried out. In both cases a cyclopropane derivative corresponding to **121** was formed. However, in both cases the calculated heats of formation plotted against the reaction coordinate yielded a discontinous curve, so it was not possible to determine an activation energy, and no useful quantitative data could be obtained. However, useful qualitative information was obtained from these calculations. Deprotonation of the hydroxyl group localizes on the oxygen atom a lot of negative charge, of which a certain amount flows into the σ-framework. This happens in a way typical for σ-delocalization (TBI).[9] The C_6 carbon atom acquires a small positive charge and C_5 (and also C_7) a small negative charge. Further, placing a negative charge on the oxygen atom has the effect of bond activation (*i.e.* weakening of a bond), but not of the $^-O–C_6$ bond, but of the bonds adjacent to this bond. This can be qualitatively explained as follows. When *more* electron density is put into a σ-bond this extra electron density enters *anti*-bonding orbitals (the bonding MO's being fully occupied in a saturated system) which leads to weakening of this bond. In short, upon placing a negative charge on the oxygen atom, charge density develops on C_5 (and C_7) while the bonds C_6–C_5 and C_6–C_7 get weaker (and longer). Further, it was seen that part of the electron density accumulating on C_5 flows in the direction of C_1, apparently leading to the formation of an intermediate three-membered ring.

At this point it should be mentioned that semi-empirical methods are not very well suited for the description of the breaking and formation of chemical bonds. Actually, on removing bonded atoms from each other in MNDO a bond does not *gradually*

diminish in strength, but suddenly "snaps". In the formation of a single bond a similar phenomenon occurs. This artefact in the calculations makes it clear why two atoms between which a bond is to be formed and two atoms between which a bond is to be broken can not be allowed to "freely choose" their interatomic distance. This interatomic distance has to be introduced in the input geometry as a fixed parameter which is varied stepwise throughout the calculations within a series. Only in this way it is possible to obtain a continuous reaction coordinate from which the position of the transition state can be derived. In the two introductory series of calculations the distance between the atoms C_5 and C_1 was not introduced into the input stream as a fixed variable, but was left to the program to be optimized. As a consequence, stepwise removal of either the positive or the negative sparkle results in the sudden formation of the C_5–C_1 bond and a plot of the calculated heats of formation shows, as mentioned above, a discontinuous curve.
However, when *at the same time* one bond is broken and another formed, MNDO can be applied successfully to obtain quantitative data, provided the interatomic distances of these bonds are taken to be fixed variables. This procedure was consistently followed in all calculations described hereafter.

Realizing that the intermediate formation of a three-membered ring might play a crucial role in the reactions of compounds **64** and **65**, it was decided to simulate these reactions with the model structures **A** wherein as the two reaction coordinates (fixed variables) the interatomic distances C_5,C_1 and C_6,C_5 (the bonds which are formed and broken, respectively) were defined. Single-point calculations were carried out for all combinations of the following interatomic distances: C_5,C_1 1.295, 1.536, 1.777, 2.018, 2.259, 2.500 Å, and C_6,C_5 1.620, 2.215, 2.810, 3.405, 4.000 Å.
Each of the resulting data points is a function of three parameters, *viz.* two interatomic distances and the heat of formation calculated for the optimized geometry corresponding to these distances. Making a plot of these data requires the representation of a three-dimensional surface in two dimensions. For this purpose a contour plot representation is best suited. With the aid of interpolation procedures a graph is obtained in which points having the same heat of formation are connected by lines: a "topographic map" of the three-dimensional potential surface. As an illustration, in Figure 5.1 the contour plot is shown for the potential surface as calculated for O^- axial (**A1**). The precise location of the transition state (TS), *i.e.*, the distances C_5,C_1 and C_6,C_5, was found by gradually "zooming in" on the saddle point; the reaction path (the path of lowest energy: dashed line) was obtained by making cross sections through the potential surface in appropriate directions and next determining (in each cross section) the location of the point with the lowest heat of

formation. At the begin and at the end of the reaction path in Figure 5.1 are given the points {C_5,C_1;C_6,C_5} as calculated for the starting model compound **A1** (IS, initial state) and the (homofragmentation) product (FS, final state), respectively.
A precise value for the heat of formation of the transition state as well as its geometrical parameters were obtained by carrying out a single-point calculation with the transition state values for C_5,C_1 and C_6,C_5.

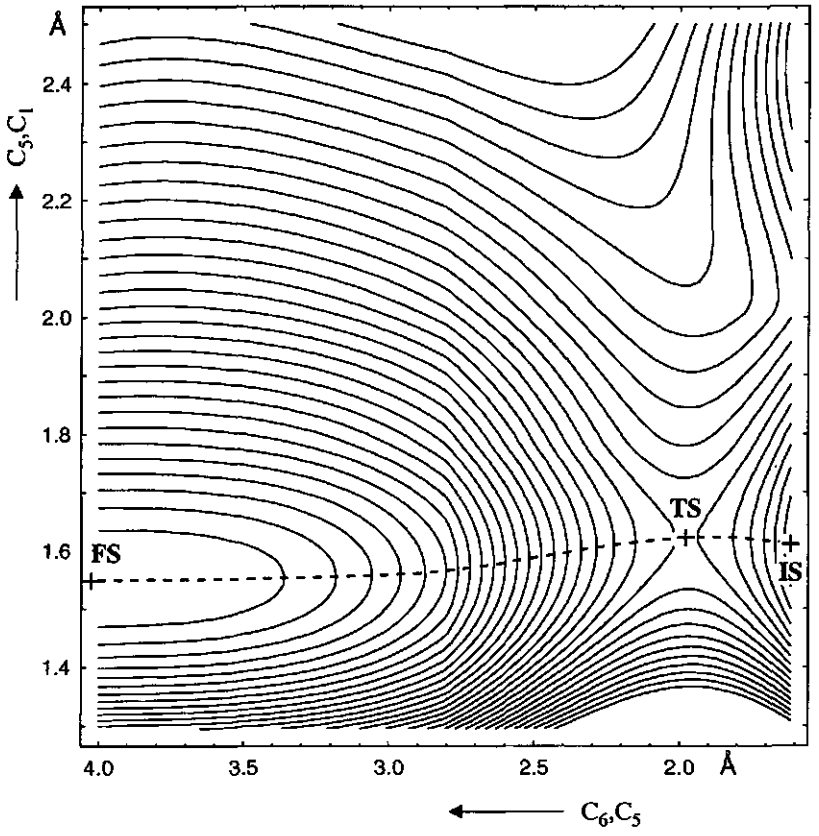

Figure 5.1: Contour plot as calculated for A1.

The initial state and the final state were optimized independently. Finally, by subtracting the heat of formation of the initial state from the transition state heat of formation, an activation energy $\Delta H^{\ddagger}$ was calculated. The values obtained are shown in Table 5.1, together with a number of relevant interatomic distances and atomic charges for initial states, transition states, and final states.

Table 5.1. Activation energies ($\Delta H^{\ddagger}$, in kCal/mole), interatomic distances (in Å), and atomic charges (q) for initial state (IS), transition state (TS), and final state (FS) of the fragmentation reactions of the model compounds A1 and A2.

	A1			A2		
	IS	TS	FS	IS	TS	FS
C_5,C_6*	1.616	1.989	–	1.622	1.993	–
C_5,C_1*	2.497	1.604	1.536	2.500	1.612	1.536
C_5–C_{10}	1.597	1.629	1.558	1.600	1.624	1.553
C10–C1	1.500	1.496	1.550	1.497	1.495	1.555
C_6–C_7	1.589	1.566	1.535	1.588	1.565	1.535
q(C_6)	+0.2633	+0.4483	+0.4686	+0.2667	+0.4568	+0.4682
q(C_5)	–0.0260	–0.3061	–0.1182	–0.0314	–0.3106	–0.1097
q(C_{10})	–0.1548	–0.0072	–0.1276	–0.1639	–0.0104	–0.1277
q(C_1)	+0.4428	+0.0241	–0.0496	+0.4454	+0.0257	–0.0572
$\Delta H^{\ddagger}$		10.86			10.18	

* reaction coordinate

Due to the presence of the negative charge on the oxygen atom a negative charge develops on C_5. Further, in the initial states the bonds C_5–C_6 and C_6–C_7 are seen to become activated and grow longer by the presence of the negative charge on the oxygen atom.[10] However, the negative charge pushed into the bond C_5–C_6 can flow away in the direction of C_1, thus making a start with the formation of the C_5–C_1 bond. In other words, the back lobe at C_5 grows and can overlap effectively with the (developing) p orbital at C_1. Through-space induction, which accompanies TBI,[3] involves bridging of the cationic center at C_1 by the back lobe of the C_5–C_6–O^- orbital. This homohyperconjugation effect[11] will ultimately lead to the simultaneous breaking of the C_5–C_6 bond and formation of the C_5–C_1 bond. A similar "outlet", *via* a combined action of TBI and TSI, for the charge accumulated in the bond C_6–C_7 is not possible.

In the process described above a secondary carbocation is formed initially, this can be expected to undergo rearrangement to a more stable tertiary ion. When compound **64** was treated with lithium *tert*-amylate instead of sodium *tert*-amylate, a considerable amount of the rearranged cyclic ether **122** was isolated next to **121** (Scheme 5.2).[2] Also the rate of this reaction is much slower and it has been suggested that bridged ions are intermediates on the rearrangement pathway.[12]

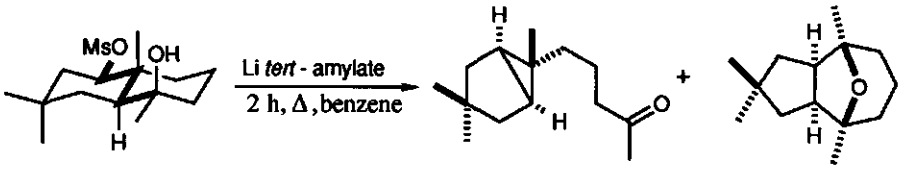

64 **121** (34%) **122** (28%)

Scheme 5.2

In order to investigate this process more closely, we decided to simulate the rearrangement process as well, *viz.* the formation of a zwitterionic [5,7] bicyclic system (Scheme 5.3).

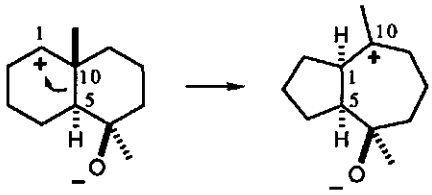

Scheme 5.3

To this purpose grid calculations were carried out, using the same model systems as for the homofragmentation reaction. This time the interatomic distances C_5,C_{10} and C_5,C_1 were used as reaction coordinates. The results of these calculations are summarized in Table 5.2.

*Table 5.2. Activation energies ($\Delta H^{\ddagger}$, in kCal/mole), interatomic distances (in Å), and atomic charges (q) for initial state (IS), transition state (TS), and final state (FS) of the rearrangement reaction of the model compound **A1**.*

	IS	TS	FS
C_5,C_{10}*	1.597	2.140	2.600
C_5,C_1*	2.497	2.348	1.596
C_{10}–C_1	1.500	1.405	1.495
C_5–C_6	1.616	1.588	1.608
C_6–C_7	1.589	1.586	1.594
q(C_6)	+0.2633	+0.2379	+0.2274
q(C_5)	–0.0260	+0.1580	–0.0240
q(C_{10})	–0.1548	–0.1321	+0.4016
q(C_1)	+0.4428	+0.1223	–0.1292
$\Delta H^{\ddagger}$		13.45	

* reaction coordinate

From the data in Table 5.2 it can be concluded that the rearrangement process is not as attractive as the homofragmentation reaction (see Table 5.1). In the transition states the distances C_5,C_{10} and C_5,C_1 are rather long, and in the final products the C_5–C_1 bond is too long while the C_{10}–C_1 bond is rather short. These phenomena are reflected in the activation energy for the formation of the [5,7] membered ringsystem (13.45 kcal/mole) as compared with that obtained in the calculations yielding the cyclopropane derivative (10.80 kcal/mole). Thus, formation of the bicyclic [3,5] system is more favorable by 2.65 kcal/mole. This difference is large enough to account for the exclusive formation of the cyclopropane derivative **121** in the reactions with sodium *tert*-amylate.

However, the experimental results show that in the reactions with lithium *tert*-amylate rearrangement can compete favorably with homofragmentation (see Scheme 5.2). The use of lithium instead of sodium as the counterion results in a decrease of the electron-donating ability of the alkoxide group.[13] This leads to a decrease of inductivity and to less effective bridging.[14] The extent to which bridging occurs depends on the particular system. With sodium as counterion, inductivity is high and bridging occurs to such an extent that homofragmentation is highly favored. With lithium as counterion, inductivity is much lower and as a result, the degree in which the C_5–C_6 bond is weakened (activated) is reduced and rearrangement can compete with homofragmentation (Chart 5.2).

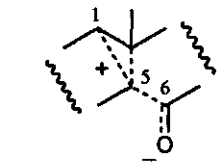

Homofragmentation product

Homohyperconjugatively stabilized transition state

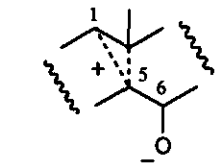

Rearrangement product

Transition state stabilized by σ-participation

Chart 5.2

From the calculations it follows that in the rearrangement process the electron density needed for the formation of the C_5–C_1 bond is taken from the C_5–C_{10} bond. It

is this bond that is broken, thereby localizing the positive charge on the tertiary C_{10} carbon atom. Here it should be noted that in the transition state for the homofragmentation process the C_5–C_{10} bond is weakened as well (see Table 5.1). The electron-donating oxygen anion enlarges, *via* TBI, the electron density of the C_5–C_{10} bond. Numerous studies have established that a cation is stabilized most effectively by β-CC bonding electrons when they are antiperiplanar to the developing p orbital.[15-17] The C_5–C_{10} bond is favorably oriented for effective σ-participation in the rearrangement process but also in the homofragmentation process. Both processes seem strongly related and proceed *via* similar cyclopropanoid bridged transition states (Chart 5.2).

5.4.2 *Calculations on the Sickle-like Geometry* **B**

Rearrangement is the only observed reaction pathway for the reactions of the mesylates **62** and **63** (Scheme 5.4) with sodium *tert*-amylate in refluxing benzene. The cyclopentane derivative **118** is formed almost quantitatively.[2] The initially formed secondary cations rearrange to the thermodynamically more stable tertiary ions. This rearrangement is followed by a fast Grob-fragmentation yielding **118**.

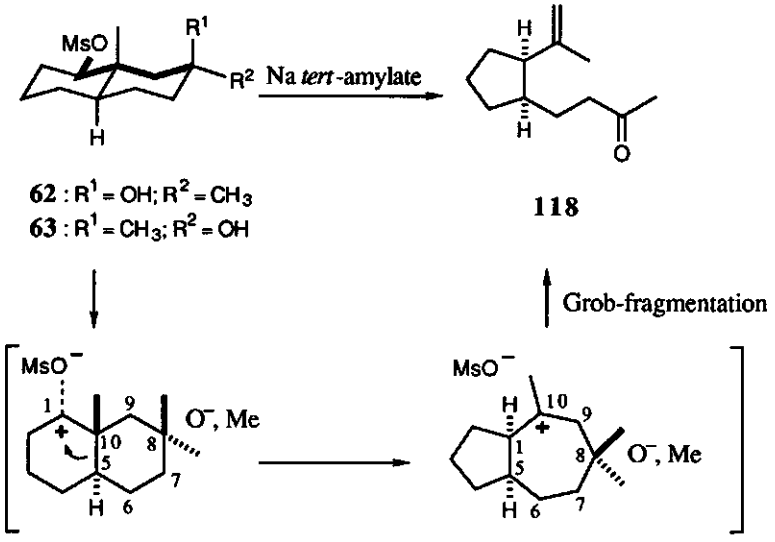

Scheme 5.4

The strategy that was followed to simulate these reactions on the model systems **B** was essentially the same as for the calculations carried out above for the "W"

geometry. In model system **B** a four carbon chain with a "sickle" geometry connects the electron donor substituent with the electron acceptor.

Exploratory calculations revealed that the perhydronaphthalene skeleton was transformed into a perhydroazulene skeleton, thus reproducing nicely the experimental observations. However, again a discontinuous curve for the reaction coordinates was obtained and it was not possible to determine the activation enthalpy or other quantitative data.

From the data obtained, the qualitative picture emerged that charge density develops on C_5, while the C_8–C_7 and C_8–C_9 bonds get weaker and longer, but also the central C_5–C_{10} bond becomes somewhat weaker and longer. Realizing that the electron density needed for the formation of the C_5–C_1 bond might be taken from the central bond, just as calculated above for the rearrangement reaction of **A**, it was decided to carry out grid calculations in which the interatomic distances C_5,C_{10} and C_5,C_1 were taken to be the reaction parameters. The same procedure as described for the calculations on **A** was employed using the following interatomic distances: C_5,C_{10} 1.600, 1.875, 2.150, 2.425, 2.700 Å, and C_5,C_1 1.580, 1.805, 2.030, 2.255, 2.480 Å. In this way the values for the activation enthalpy, together with interatomic distances and atomic charges were obtained (Table 5.3).

*Table 5.3. Activation energies ($\Delta H^{\ddagger}$, in kCal/mole), interatomic distances (in Å), and atomic charges (q) for initial state (IS), transition state (TS), and final state (FS) of rearrangement reactions of the model compounds **B1** and **B2**.*

	B1			**B2**		
	IS	TS	FS	IS	TS	FS
C_5,C_{10}*	1.577	1.890	2.573	1.576	1.891	2.571
C_5,C_1*	2.496	1.976	1.580	2.495	1.974	1.579
C_{10}–C_1	1.498	1.431	1.512	1.500	1.431	1.511
C_8–C_9	1.600	1.597	1.668	1.602	1.600	1.676
C_8–C_7	1.585	1.582	1.582	1.585	1.583	1.583
q(C_8)	+0.2484	+0.2502	+0.2979	+0.2537	+0.2568	+0.3142
q(C_7)	–0.0385	–0.0500	–0.0538	–0.0411	–0.0527	–0.0565
q(C_6)	+0.0084	+0.0140	–0.0172	+0.0032	+0.0074	–0.0236
q(C_5)	–0.0240	–0.0531	–0.0265	–0.0234	–0.0512	–0.0257
q(C_9)	–0.0051	–0.0357	–0.1520	–0.0072	–0.0390	–0.1632
q(C_{10})	–0.1531	+0.0093	+0.3484	–0.1560	+0.0048	+0.3443
q(C_1)	+0.4413	+0.1702	–0.1104	+0.4416	+0.1710	–0.1091
$\Delta H^{\ddagger}$		14.02			14.19	

* reaction coordinate

The interatomic distances collected for the initial states clearly show that when the hydroxylic proton is substituted by a positive sparkle the C_8–C_7 and C_8–C_9 bonds get "activated". Due to σ-conjugation the negative charge pushed into the C_8–C_7 bond can flow away *via* the C_7–C_6 and C_6–C_5 bonds, ultimately in the direction of C_1. This center is eminently suited for taking up charge density. A similar "outlet", *via* σ-conjugation, for the surplus charge density accumulated in the C_8–C_9 bond is not possible.

The atomic charges (for the initial states) collected in Table 5.3 show the "alternating effect", which is typical for TBI.[9] It is seen that, due to deprotonation, C_8 obtains a small positive charge, C_7 a small negative charge, C_6 in its turn a small positive charge, and lastly C_5 a small negative charge. This consequence of through-bond interaction ultimately results in formation of the C_5–C_1 bond. It is also clear that both the C_8–C_7 and C_8–C_9 bond get activated. The charge pushed into the C_8–C_7 bond can flow in the direction of C_5. Delocalization of the charge accumulated in the C_8–C_9 bond is not possible and it is this bond that is destabilized most. This is reflected in the final states representing the rearranged intermediates, the C_8–C_9 bond has grown longer. Further, it is seen that the largest amount of positive charge present on any C-atom in the initial states resides on C_1, a secondary carbon atom, but that in the final states it has moved to the tertiary carbon atom C_{10} and that its absolute magnitude has grown smaller. In the transition state the C_5–C_{10} bond is weakened, just as in the rearrangement and homofragmentation process described in the previous section. σ-Participation of this bond seems to play an important role here as well. The remote electron-donating substituent donates, *via* TBI, electrons to the central C_5–C_{10} bond, thus attenuating the electron density of this bond and its ability to stabilize the (developing) carbocationic center at C_1.[18] In this way the initial positive charge on C_1 is delocalized over C_1, C_{10}, and C_5.

Considering the characteristics collected for the final states , *i.e.*, the "vulnerability" of the C_8–C_9 bond and the positive charge concentrated on C_{10}, it is obvious that after the rearrangement process has occurred the positive charge on C_{10} can be annihilated by breaking of the C_8–C_9 bond (Grob-fragmentation),[19] yielding the fragmented cyclopentane product **118**.

The data obtained from these calculations are in good agreement with the results obtained experimentally for the compounds **62** and **63**. A remarkable outcome of the calculations is that they suggest that TBI is not operating *via* the four carbon chain C_8–C_9–C_{10}–C_1 but over the six carbon chain C_8–C_7–C_6–C_5–C_{10}–C_1 instead. This could be an explanation for the much slower reaction rates of the mesylates **62** and **63** as compared to the rates of **64** and **65**.[2]

5.4.3 Calculations on the Sickle-like Geometry C

The mesylate **60**, with an axial hydroxyl group, gave upon treatment with sodium *tert*-amylate in refluxing benzene predominantly the rearranged product **114** with an exocyclic double bond (Scheme 5.5).[20]

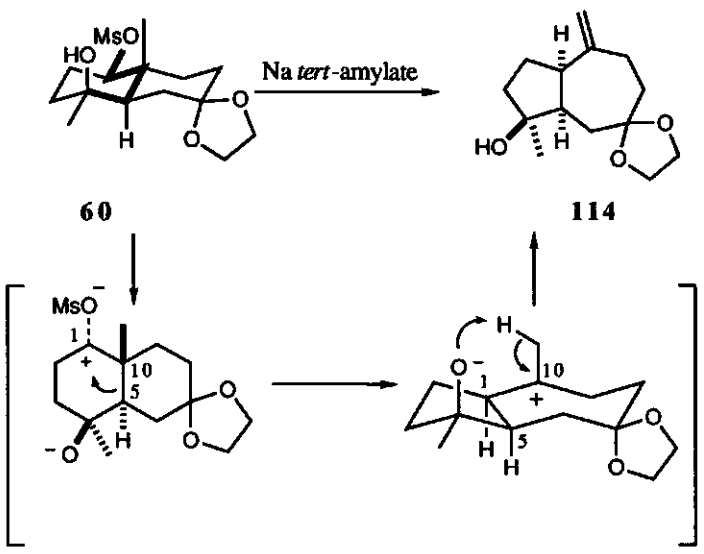

Scheme 5.5

From the calculations in the previous sections it should be clear that, after deprotonation of the hydroxyl group, part of the negative charge delocalizes to C_5, giving this atom the means to stabilize the positive charge on C_1 *via* TBI. σ-Participation of the central β-CC bond is expected to play an important role in this rearrangement process, just as was found before.

The reaction leading to the 5,7-membered ring system was investigated in the usual way starting from the model compound **C1**. In Table 5.4 the results are summarized.

From the results it is clear that the negative charge accumulates on C_5, and that the C_5–C_{10} bond is weakened due to the through-bond inductive effect of the axial O^- that enlarges the electron density of this bond. In the end it is this C_5–C_{10} bond that breaks and the C_5–C_1 bond is formed, just as is the case in the previous calculations. After the rearrangement has occurred, a fair amount of positive charge is located on C_{10}. In the follow-up reaction the relative close proximity of the anionic oxygen may

facilitate the abstraction of a proton of the C_{10} methyl group, thus producing the observed reaction product with an exocyclic double bond.[20]

Table 5.4. Activation energies ($\Delta H^{\ddagger}$, in kCal/mole), interatomic distances (in Å), and atomic charges (q) for initial state (IS), transition state (TS), and final state (FS) of the rearrangement reaction of C1.

	IS	TS	FS
C_5,C_{10}*	1.590	1.954	2.598
C_5,C_1*	2.531	2.037	1.593
C_1–C_{10}	1.493	1.413	1.492
C_4–C_5	1.612	1.621	1.617
q(C_4)	+0.2481	+0.2422	+0.2468
q(C_5)	–0.0395	–0.0153	–0.0283
q(C_{10})	–0.1615	–0.0411	+0.3882
q(C_1)	+0.4509	+0.1697	–0.1261
$\Delta H^{\ddagger}$		12.24	

* reaction coordinate

The sole product of the sodium *tert*-amylate reaction of the mesylate **61**, with an equatorial hydroxyl group, is the cyclic ether **117** (Scheme 5.6).[2] In this reaction a direct attack of the deprotonated hydroxyl group on the developing positive charge on C_1 prevails over the expected rearrangement reaction.

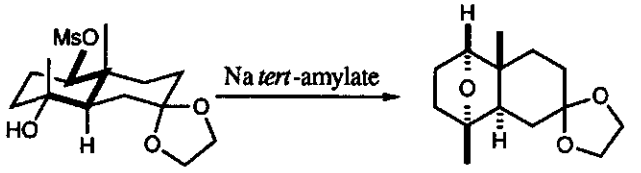

61 **117**

Scheme 5.6

In the exploratory calculations carried out on the model compound **C2** the distance between the carbocationic C_1 and the negative sparkle was increased in small steps to "infinity". However no reaction was found to take place in these calculations, and the perhydronaphthalene skeleton was unaffected. On the other hand, when the distance between C_1 and the oxygen anion was shortened in steps of 0.20 Å, over the range

3.60–1.40 Å, it proved to be possible to optimize the initial and final states of this reaction, and a continuous curve for the reaction coordinate was found. However, thus modelled the reaction has an activation energy zero. Of course this should not be too surprising because two atoms on which fair amounts of opposite charges are localized are brought to within bonding distance.

When the amount of regained starting products upon quenching the reaction mixture after 10 min is taken as a rough measure for the rate of the reactions (see Chapter 4), the rate at which the cyclic ether **117** is formed appears to be *lower* than the rate at which the rearranged product **114** is formed. From this it is to be expected that the formation of **117** does have an activation barrier and that this activation barrier is higher than for the formation of compound **114**. At this point the calculations are in contrast with the observations, which is not surprising considering the fact that in the model systems the leaving group has already been removed. In an additional series of calculations the effect of the leaving group was taken into account by attaching a mesylate group to C_1. Modelled in this way the formation of a cyclic ether proves to have an activation barrier. However, it is not permissible to compare the activation energie for the formation of the cyclic ether with that obtained for the formation of the rearranged product, due to the fact that both reactions were modelled in a different way. Within the possibilities of the modelling and calculational methods employed, it is impossible to calculate the differences in activation energy between the cyclic ether formation and the formation of the rearranged product.

5.5 Concluding Remarks

The trends in the results of the semi-empirical MNDO calculations on the model compounds **A**, **B**, and **C** are the same as those found in the reactions of the mesylates **60–65** with excess sodium *tert*-amylate in refluxing benzene (Chapter 4). Although care should be taken with conclusions drawn from the calculations on **C**, the results from the calculations on **A** and **B** correspond well with the experimental results. It is seen that MNDO calculations on carefully chosen model systems are a useful tool in the study of TBI effects in closely related donor-acceptor systems.

The calculations on the model systems **A**, with a "W" geometry of the σ-relay between the oxygen anion and the carbocationic center, showed that the accumulation of negative charge on the C_5 carbon atom leads to a bonding interaction between C_5 and the carbocationic C_1. The calculations also demonstrated that the C_5–C_6 bond becomes activated and grows longer. This accumulation of charge on a carbon atom next to the carbon atom that is directly attached to the electron donor substituent,

together with the "activation" of the vicinal σ-bonds are in line with the predictions from theoretical models concerning TBI.[3,21]

The same consequences of TBI are responsible for the behavior of the model compounds **B**. The calculations reproduced nicely the experimental results found for the mesylates **62** and **63**. However, it appeared that the donor-acceptor interaction is realized *via* a six carbon chain rather than *via* a four carbon chain.

Lastly, the simulations of the homofragmentation path (on **A**) and of the rearrangement path (on **A1**, **B**, and **C1**) showed that in all cases C_5 accumulates part of the negative charge pushed into the perhydronaphthalene skeleton by the oxygen anion. Furthermore the central C_5–C_{10} bond gets weaker in the rearrangement process but also in the homofragmentation process. Interaction of this bond with the incipient carbocationic center plays an important role in all of these reactions. Whether rearrangement or homofragmentation takes place depends on the geometry of the σ-relay, since homohyperconjugation is only possible when a "W" arrangement of connecting σ-bonds is operating. Additionally, the chosen reaction path is dependent on the inductivity of the system. The extent of 1,3-bridging, which is essential for the homohyperconjugative effect, is determined by the electron-donating ability of the alkoxide group. When inductivity is low, rearrangement is favored in these systems. Cyclopropanoid bridged structures seem to be involved in the rearrangement process as well as in the homofragmentation process.

5.6 References and Notes

(1) See Chapter 3.

(2) See Chapter 4.

(3) Hoffmann, R. *Acc. Chem. Res.* **1971**, *4*, 1-9.

(4) Paddon-Row, M. N.; Jordan, K. D. In *Modern Models of Bonding and Delocalization*; J. F. Liebman and A. Greenberg, Eds.; VCH publishers: New York, **1988**; chapter 3.

(5) Fragmentation which generates a cyclopropane ring is termed homofragmentation. See: Flury, P.; Grob, C. A. *Helv. Chim. Acta* **1983**, *66*, 1971-1980.

(6) Paddon-Row, M. N. *Acc. Chem. Res.* **1982**, *15*, 245-251.

(7) Dewar, M. J. S.; Thiel, W. *J. Am. Chem. Soc.* **1977**, *99*, 4899-4907.

(8) Stewart, J. J. P. *J. Comput. Chem.* **1989**, *10*, 209-220.

(9) Verhoeven, J. W. *Recl. Trav. Chim. Pays-Bas* **1980**, *99*, 369-379.

(10) The bond length for the C–C bond in cyclohexane is 1.540Å ± 0.015Å.

(11) (a) Adcock, W.; Kok, G. B. *J. Org. Chem.* **1987**, *52*, 356-364.

(b) Grob, C. A.; Gründel, M.; Sawlewicz, P. *Helv. Chim. Acta* **1988**, *71*, 1502-1507.
(c) Lambert, J. B.; Salvador, L. A.; So, J.-H. *Organometallics* **1993**, *12*, 697-703.

(12) Deslongchamps, P. *Stereoelectronic Effects in Organic Chemistry;* Pergamon Press: Oxford, **1983**.

(13) The Li^+–O^- bond has a more covalent character than the Na^+–O^- bond. See: Paquette, L. A.; Gilday, J. P. *J. Org. Chem.* **1988**, *53*, 4972-4978. As a result, the electron-donating ability of the alkoxide function with Li^+ as the counterion will be diminished.

(14) Grob, C. A. *Acc. Chem. Res.* **1983**, *16*, 426-431.

(15) Jensen, F. R.; Smart, B. E. *J. Am. Chem. Soc.* **1969**, *91*, 5686-5689.

(16) (a) Traylor, T. G.; Hanstein, W.; Berwin, H. J.; Clinton, N. A.; Brown, R. S. *J. Am. Chem. Soc.* **1971**, *93*, 5715-5725.
(b) Hartmann, G. D.; Traylor, T. G. *J. Am. Chem. Soc.* **1975**, *97*, 6147-6151.

(17) (a) Apeloig, Y.; Schleyer, P. v. R.; Pople, J. A. *J. Am. Chem. Soc.* **1977**, *99*, 5901-5909.
(b) Schleyer, P. v. R.; Lenoir, D.; Mison, P.; Liang, G.; Prakash, G. K. S.; Olah, G. A. *J. Am. Chem. Soc.* **1980**, *102*, 683-691.

(18) Lenoir, D.; Apeloig, Y.; Arad, D.; Schleyer, P. v. R. *J. Org. Chem.* **1988**, *53*, 661-675.

(19) Grob, C. A. *Angew. Chem., Int. Ed. Engl.* **1969**, *8*, 535-622. It has been demonstrated that TBI plays an important role in the Grob fragmentation. See: Gleiter, R.; Stohrer, W.; Hoffmann, R. *Helv. Chim. Acta* **1972**, *55*, 893-906.

(20) Wijnberg, J. B. P. A.; Jenniskens, L. H. D.; Brunekreef, G. A.; de Groot, A. *J. Org. Chem.* **1990**, *55*, 941-948. See also reference 2

(21) Jordan, K. D.; Paddon-Row, M. N. *Chem. Rev.* **1992**, *92*, 395-410 and references cited therein.

Chapter 6

Substituent Effects on the TBI Induced Heterolysis of Some Perhydronaphthalene-1,4-diol Monosulfonate Esters*

6.1 Introduction

Through-bond orbital interactions mediated *via* four σ-bonds are most likely responsible for the heterolysis of the sulfonate ester bond in the base-induced reactions of cyclic 1,4-diol monosulfonate esters.[1,2] As described in chapters 3 and 4 these compounds react smoothly upon treatment with strong non-nucleophilic base in apolar solvents. The initially formed dipolar intermediates undergo typical cationic processes like (homo)fragmentation, β-elimination, and/or rearrangement. Combination of the special stereoelectronic features connected with TBI (and TSI) provides a very useful concept to account for the formation of all the products found in these reactions and the overall reactivity of these compounds.

The extent of TBI, but also the occurrence of TSI, critically depends on the geometry of the σ-relay that is operating between the electron donor (alcoholate anion) and the electron acceptor (sulfonate ester bond).[3] It has been demonstrated that a W-like arrangement of the intervening carbon chain is a prerequisite for homofragmentation to occur. At the same time the "W" arrangement is the most favorable geometry for mediating through-bond orbital interactions, as a result of which the reactions will proceed very fast. For example, the mesylate **64** (Chart 6.1), having a W-like arrangement of the relaying σ-bonds gives the cyclopropane derivative **121**, exclusively, and reacts very fast.[2] On the other hand, the mesylates **60** and **62** in which the geometry of the σ-relay is sickle-like react much slower than **64** and no homofragmentation was observed at all. These findings are in good agreement with theoretical models concerning TBI.[4,5]

However, not only the geometry of the σ-relay of these compounds seems to be important for the selectivity and rate of these reactions. Comparison of the selectivity of the reactions of the mesylates **40** and **64** (Scheme 6.1), both possessing a W-like arrangement of the σ-relay, shows that **40** reacts much less selective and much slower

* This chapter will be published for the greater part: Orrū, R. V. A.; Wijnberg, J. B. P. A.; de Groot, A. *J. Org. Chem.* submitted.

than **64**. In the former compound the ring carbon atoms adjacent to the carbon atom bearing the sulfonate ester group are unsubstituted, whereas in **64** one of these ring carbon atoms is quaternary. In addition, in mesylate **64** the central carbon bond of the perhydronaphthalene skeleton is part of the relaying carbon chain, whereas in **40** this is not the case. As a consequence, in the latter compound the "W" arrangement of σ-bonds is not as rigidly anchored as in **64**.

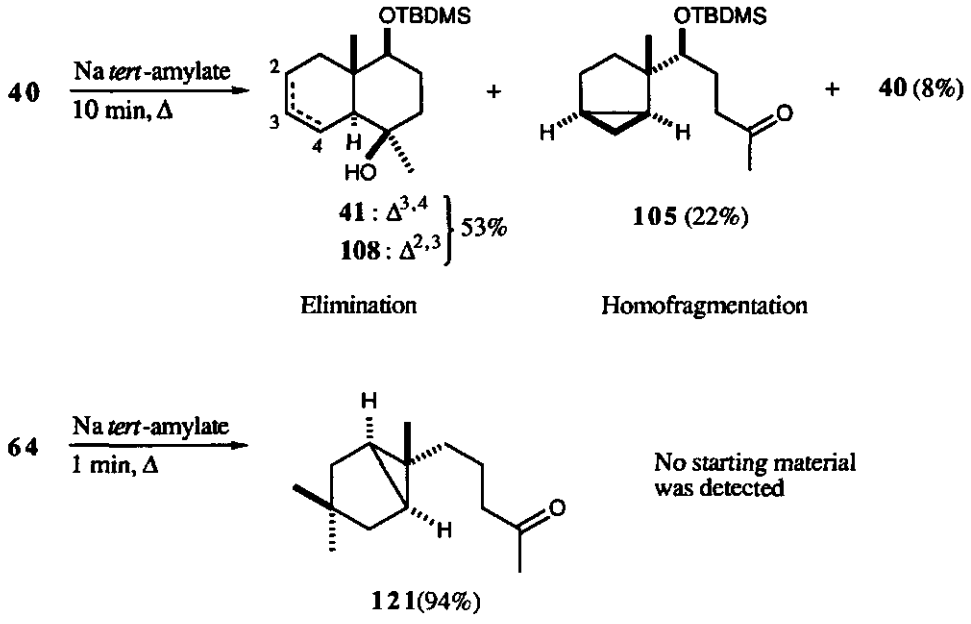

Scheme 6.1

This raises two questions: (*i*) to what extent do (small) distortions in the optimal "W" arrangement of the σ-relay determine the selectivity of the homofragmentation process, and (*ii*) does the reactivity of these compounds also depend on the order of substitution at ring carbon atoms next to the carbon atom bearing the leaving group. In order to answer these two related questions we decided to study the behavior of the mesylates **40**, **66**, and **67** (Chart 6.1) under the strongly basic standard conditions, *i.e.*, sodium *tert*-amylate in refluxing benzene.

The unsubstituted compound **40** and the monosubstituted compound **66** are supposed to have a more or less similar W-like arrangement of the carbon chain connecting the hydroxyl group and the mesylate group. On the other hand, we anticipated that steric factors will distort the W-like arrangement to some degree in case of the disubstituted compound **67**.

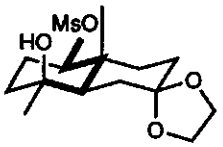

60

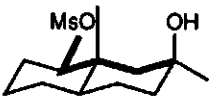

62

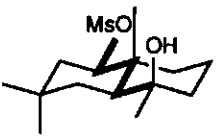

64

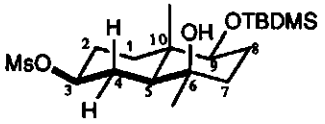

40

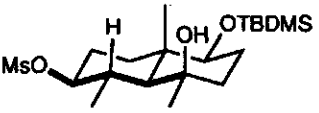

66

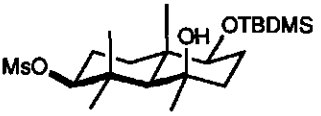

67

Chart 6.1

From comparison of the reaction outcome of **67** with that of **40** and **66** we expect to gather more information about to what degree the homofragmentation process is affected by distortions from the ideal "W" arrangement of the σ-relay. Further, we expect to gather some pertinent information about the electronic effects of alkyl substituents on the reactivity of this type of compounds. Because we know from earlier experiments (see Chapter 4) that the orientation of the alcohol group has little or no influence on the reaction rate, this study is limited to the 1,4-diol monosulfonate esters with an axial hydroxyl group at C_6 for practical reasons.

6.2 Results and Discussion

When the mesylates **40**, **66**, and **67** were treated with *ca.* 5 equiv of sodium *tert*-amylate in refluxing benzene for 10 min, the reactions of **66** and **67** were complete. As a result, the reactivity of these compounds could not be mutually compared. Therefore, the reaction time was reduced to 2 min. By comparing the quantities of recovered starting material from these 2 min reactions a rough estimate of the relative reaction rates was obtained. The results of these studies are collected in Table 6.1.

Treatment of the mesylate **40** with sodium *tert*-amylate in refluxing benzene for 2 min gave a 7:1 mixture (16%) of the olefins **41** and **108**, respectively, and the cyclopropane derivative **105** (4%).[6] The quantity of recovered **40** amounted to 80% (entry 1).

After a 2 min treatment of the C_4 monomethylated mesylate **66** with sodium *tert*-amylate, the reaction was almost complete. Only 6% of the starting material was regained (entry 2). A 3:1 mixture (46%) of the olefins **123** and **124**, respectively, and a considerable amount (32%) of the epoxide **125** were isolated.[7] The structure of the epoxide **125** follows from the ^1H and ^{13}C NMR data. In the ^1H NMR spectrum of **125** only the H-9 signal appears as a double doublet at low-field (δ 3.23). In the ^{13}C NMR spectrum of **125** two singlets appear at δ 63.07 and 65.56. These chemical shift values are typical for quaternary epoxide carbon atoms.[8] Together with the other NMR data, these observations established the identity of **125**.

Table 6.1. Reactions of the mesylates 40, 66, and 67 with sodium tert-amylate.[a]

entry	mesylate	products (%)[b]	recovery[c]
1	**40**	**41** + **108** + **105** (20)[d]	80
2	**66**	**123** (34) + **124** (12) + **125** (32)[e]	6
3	**67**	**126** (87)	11

[a] All reactions were performed in refluxing benzene with *ca.* 5 equiv of sodium *tert*-amylate for 2 min. [b] Isolated yields in parentheses. [c] Percentage of recovered starting material. [d] These products were isolated as a mixture in a ratio of 7:1:2, respectively. [e] GC analysis of the crude reaction mixture revealed the presence (15 % in total) of at least four other products.

After the standard basic treatment of the C_4 dimethylated mesylate **67**, the alcohol **126** with an exocyclic double bond was formed exclusively (87%). In this reaction 11% of starting material was regained (entry 3). The presence of an exocyclic double bond in **126** was concluded from its ^{13}C NMR spectrum, in which a secondary and a quaternary olefinic carbon atom appear at δ 149.46 and 110.24, respectively. That the position of the exocyclic double bond must be located at C_4 follows from a combination of NMR techniques. A homonuclear decoupling experiment shows that the allylic proton signal at δ 2.50 couples with a methyl signal which appears as a doublet at δ 1.05. In the ^1H NMR spectrum of **126** an one proton singlet is observed at δ 2.05. This singlet must arise from the proton at C_5, since irradiation of H-9 at δ 3.33 showed a strong NOE at δ 2.05. These observations also prove that a methyl group is attached to C_3. The axial orientation of this methyl group follows from a fairly large

NOE observed upon irradiation of the H-5 proton (δ 2.05) together with a rather small $W_{1/2}$ value (12 Hz) for the allylic H-3 signal at δ 2.50. These NMR data are in complete conformity with our structural assignments to compound **126**.

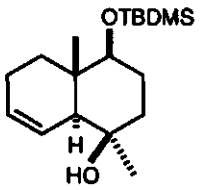

35

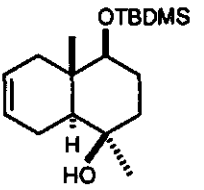

100

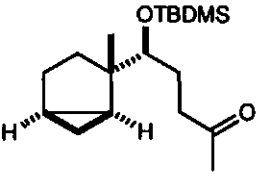

97

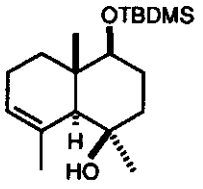

115

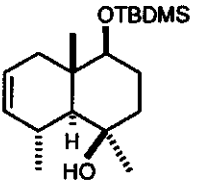

116

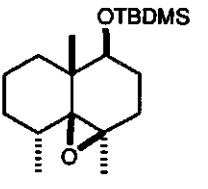

117

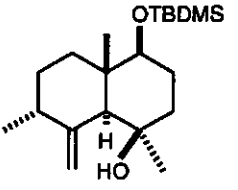

118

Chart 6.2

The results of these studies on the mesylates **40**, **66**, and **67** clearly show that substitution at C_4 seriously affects the course of the reactions of these compounds. Elimination and homofragmentation are the only processes found with the C_4 unsubstituted mesylate **40**, whereas the corresponding monomethylated compound **66** shows elimination and epoxide formation as the main reaction pathways. A 1,2-Me shift ($C_4 \rightarrow C_3$) is the exclusive process observed for the dimethylated mesylate **67**.

As we have already demonstrated, the product composition is strongly dependent on the geometry of the relaying σ-bonds. Only in an optimal W-like arrangement a combined action (= homohyperconjugation)[9] of 1,3-bridging (TSI) and TBI is possible and can result in homofragmentation.[2] The formation of the homofragmentation

product **105** from the reaction with the mesylate **40** proves that in this compound such a W-like σ-relay is operating (Scheme 6.2).

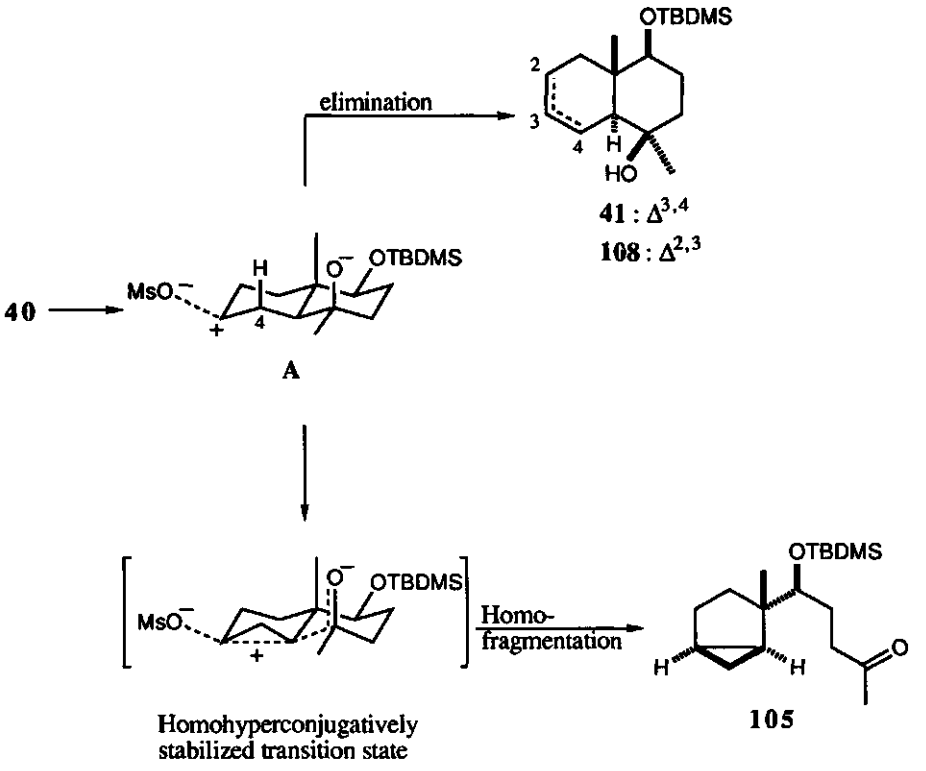

Scheme 6.2

Because no homofragmentation products are found after the reactions of the C_4 substituted mesylates **66** and **67**, we conclude that in these systems no 1,3-bridging can occur. Because all reactions are performed in benzene, contact ion pairs are probably involved in the intramolecularly induced departure of the mesylate group.[13] Therefore, we assume that conformational distortions are not only present in the ground state but also in the initially formed dipolar intermediates (or transition states). Semi-empirical MNDO calculations[10] support this conclusion. From these calculations, it appears that in the intermediates derived from mesylates **66** and **67** (**B** in Scheme 6.3, and **D** in Scheme 6.4, respectively) the ideal W-like arrangement is more distorted than in the intermediate **A** derived from **40**. The Newman projections (Figure 6.1) along the C_5–C_4 bond of the initially formed dipolar intermediates **A**, **B**, and **D**, respectively, illustrate these situations the best.

In **A** the deviation from the ideal W-like arrangement is very small (torsion angle between the H^{ax}–C_5–C_4 and the C_5–C_4–H^{ax} planes is ~ 180°) and therefore does not prevent homofragmentation. The corresponding torsion angles (φ) in **B** and **D** are −170° and +140°, respectively. Although in **B** the deviation from the ideal W-like arrangement is only *ca.* 10°, this value is apparently large enough to prevent effective homohyperconjugation. It will be clear that the deviation of *ca.* 40° calculated for **D** has the same effect.

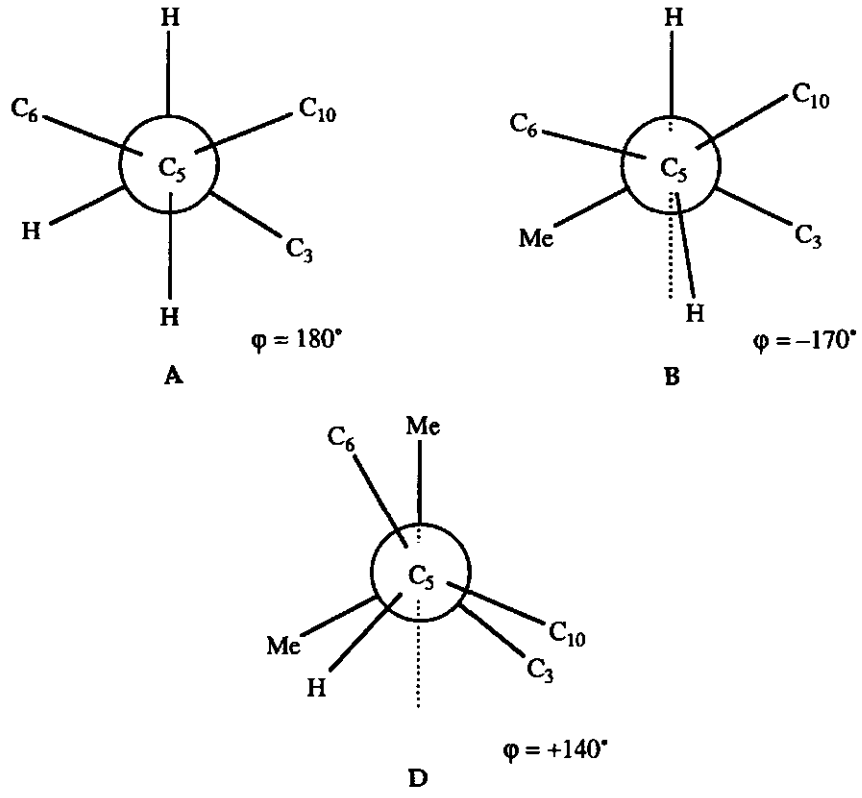

*Figure 4.1: Torsion angles φ between the axial substituent at C_4 (H or Me) and the proton at C_5 from Newman projections along the C_4–C_5 bond for the initially formed intermediates **A**, **B**, and **D**.*

Another very important outcome of these calculations is the opposite sign found for φ in **B** and **D**. This means that in **B**, derived from **66**, the chair conformation of the ring bearing the hydroxyl group (ring B) is somewhat flattened, whereas in **D**, derived from **67**, the chair conformation of the other ring (A) must be distorted. The flattening of the B-ring in **B** must be the result of the so-called 1,3-*peri*-effect.[11] This steric 1,3-

repulsion between the equatorial methyl groups at C_4 and C_6 forces the C_6 methyl group into a more downwards position. The combination of a repulsive 1,3-interaction between the axial methyl groups at C_4 and C_{10} and the *peri*-effect in **D** leads to a twist-boat conformation of ring A in which both the mesylate group at C_3 and the α-methyl at C_4 have a more axial orientation.[12]

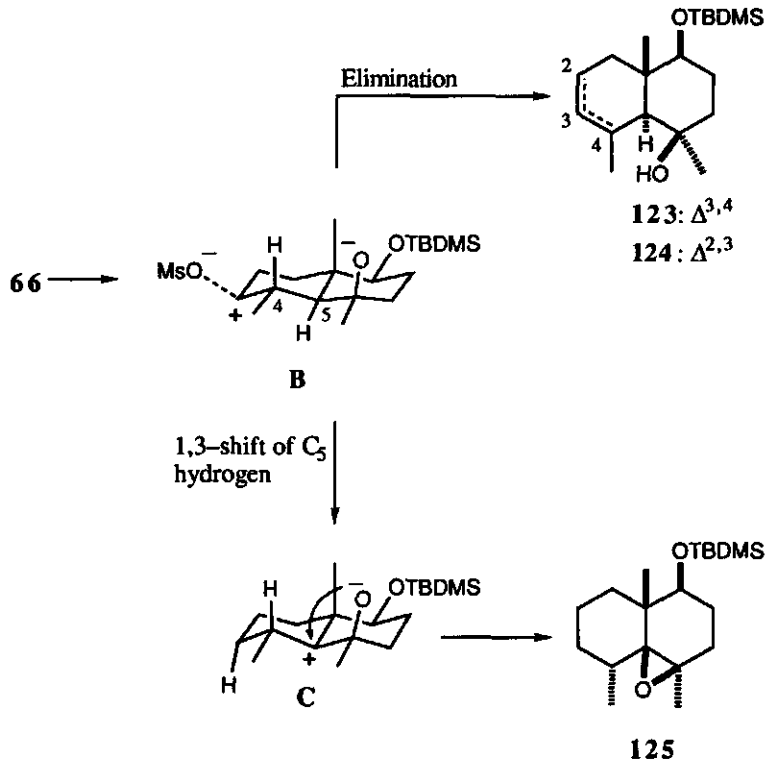

Scheme 6.3

These considerations make the product outcome of the reactions with the mesylates **66** and **67** more easily to understand.

Flattening of the B-ring in the initially formed dipolar intermediate **B** (from **66**) forces the bridgehead H-5 somewhat toward C_3. As a result, a 1,3-H shift[14] ($C_5 \rightarrow C_3$) can occur more easily (Scheme 6.3). The resulting tertiary carbocationic intermediate **C** undergoes ring closure to give the epoxide **125**. The formation of the elimination products **123** and **124** in this reaction with **66** can be explained by a similar mechanism as described in chapter 3 for the formation of **41** and **108** from **40** (see also Scheme 6.2). Only the product ratio of 3:1 in which **123** and **124** are formed deserves some comment. As we have demonstrated for the mesylate **40**, the formation of the

elimination products **41** and **108** (in a ratio of 7:1, respectively) proceeds *via* the dipolar intermediate **A**. In this intermediate the carbocationic center will facilitate elimination with the intramolecular process as the most favorable one because the alkoxide group at C_6 and the β H-4 are properly aligned (both axial).[15] In the intermediate **B** derived from **66** this alignment is less favorable for intramolecular elimination because the alkoxide group diverges somewhat from the axial orientation as a result of the 1,3-*peri*-effect. The intermolecular elimination process becomes now more important and this finds expression in the small ratio 3:1 found for **123** and **124**, respectively.

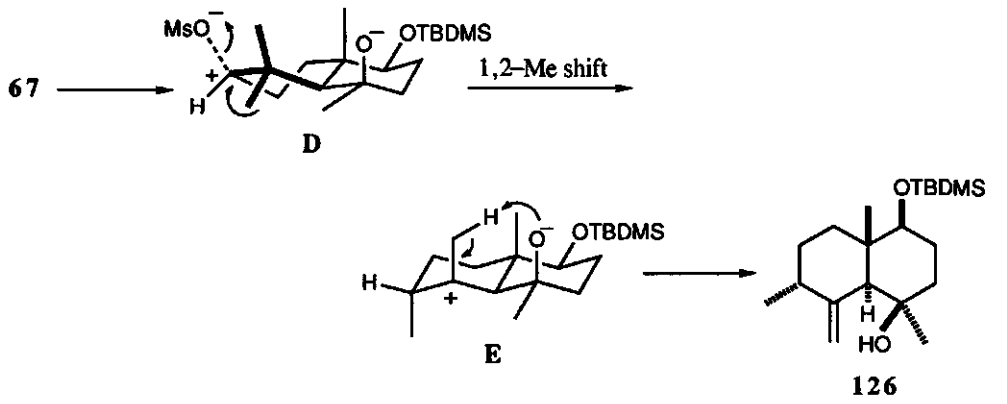

Scheme 6.4

Steric interactions must also play a dominant role in the exclusive formation of compound **126** upon treatment of **67** with sodium *tert*-amylate. As concluded from the MNDO calculations (*vide supra*), these steric interactions force both the mesylate and the β methyl group at C_4 into a more axial orientation (Scheme 6.4). This tendency toward an antiperiplanar relationship between the leaving group and the β methyl group at C_4 makes the 1,2-Me shift (**D** → **E**) a more facile process. An intramolecular proton abstraction in the tertiary carbocationic intermediate **E** must be responsible for the exclusive formation of **126** in this reaction.

The results of the studies on the mesylates **40**, **66**, and **67** clearly show that substitution at C_4 seriously affects the reactivities of these compounds as well. If C_4 is mono- or disubstituted the reactions are relatively fast (entries 2 and 3). The reaction of the C_4 unsubstituted mesylate **40** takes much more time (entry 1). Thus, methyl substituents at C_4 indeed accelerate these reactions. This means that the intermediates **B** and **D** derived from **66** and **67**, respectively, are formed more easily and thus are better

stabilized than the intermediate **A** generated by the reaction of **40**. It has been shown that in processes which involve initial ionization of a leaving group, the cationic center (or the developing cation) is stabilized by delocalization of a neighboring C–C bond.[16,17] The extent of this electronic delocalization depends on the alignment of the participating σ-bond with the leaving group.[18] From the MNDO calculations it follows that the C_4–C_5 bond in both **A** and **B** is almost exactly antiperiplanar to the mesylate group. This means that the (developing) cationic center at C_3 in the initially formed intermediates **A** and **B** is stabilized by delocalization of the C_4–C_5 bond to a similar degree. Apart from any other electronic effect, one should expect that **66** will react somewhat slower than **40** because in **A** (from **66**) the W-like arrangement of the relaying σ-bonds slightly diverges from the ideal situation as a result of the 1,3-*peri*-effect (*vide supra*). The increased reactivity observed for **66**, as compared with that of **40**, must therefore be the consequence of an extra stabilization by its C_4 methyl group. This result is consistent with a theory for stabilization of cations by delocalization of neighboring σ-bonds described by Traylor *et al.*[17a] A (slightly) polarized σ-bond stabilizes neighboring cationic centers without altering the length or angles around such bond as the transition state is approached (*vertical stabilization*, *σ-participation*, or C–C *hyperconjugation*). From this model it was predicted that inductively donating groups, like CH_3, at a position next to the leaving group have an accelerating effect on the formation of a carbocationic center.

In the mesylate **67** the <u>two</u> inductively donating methyl groups at C_4 can stabilize the incipient carbocationic center at C_3 in a similar way as described above for **66**. On the other hand, the Newman projections (Figure 6.1) show clearly that in **D** (from **67**) the C_4–C_5 bond is no longer antiperiplanar to the mesylate group. As a consequence, the tendency of this bond to participate effectively in the ionization process will be reduced. Furthermore, due to the combination of the 1,3-*peri*-effect and the 1,3-*diaxial*-effect, the geometry of the σ-relay in **D** is distorted to a greater extent than in **B** (*vide supra*). The combination of these related effects is responsible for the reactivity of **67**. Due to the higher order of substitution at C_4 compound **67** should react faster than **66**. The steric effects operating in **67**, however, prevent the most favorable orbital overlap and therefore transmission of TBI is not optimal. Consequently, the reactivity of **67** is somewhat reduced as compared with that of compound **66**.

Finally, our experimental results confirm the view that 1,3-bridging (TSI) contributes very little to the stabilization of the transition state in the formation of a cationic intermediate. It has been shown that prevention of such bridging does not alter the overall stabilization.[17a] 1,3-Bridging is possible in **A**, as is reflected in the formation of the cyclopropane derivative **105**. In **B** and **D** a similar through-space interaction is prevented due to the 1,3-*diaxial*-effect and/or the 1,3-*peri*-effect (*vide supra*). The large

difference in reactivity between **40** as compared with **66** and **67** can therefore not be attributed to TSI.

6.3 Concluding Remarks

The product composition in the reactions of the mesylates **40**, **66**, and **67** is strongly dependent on the steric consequences of alkyl substituents at C_4. When repulsive steric interactions are absent or small as in intermediate **A** derived from **40**, homofragmentation can occur. In this case, the participating σ-bonds are properly aligned (W-like arrangement) to approach the homohyperconjugatively stabilized transition state. In the intermediates **B** and **D** derived from **66** and **67**, respectively, the σ-relays diverge from the ideal W-like arrangement as a result of which homohyperconjugation becomes less important and other reaction pathways (elimination, 1,3–H, and 1,2–Me shifts) are followed.
Alkyl substituents at C_4 have also a great impact on the reaction rate of these compounds. Introduction of one inductively electron-donating substituent at C_4 leads to an increase in reaction rate, despite the slight deviation of the "W" arrangement (compare the reaction rates of the mesylates **40** and **66**). This result is in good agreement with theoretical predictions for carbocationic processes.[17,19,20] Two alkyl substituents at C_4, as in mesylate **67**, distorts the "W" arrangement appreciably as a result of which the increase in reaction rate is less pronounced but still evident.

6.4 Experimental Section

General.[21] Compounds **41**, **105**, and **108** have been fully characterized before.[1]

Reactions of Mesylates 40, 66, and 67 with Sodium *tert*-Amylate. General Procedure. All reactions were carried out on 0.20–0.50 mmol of mesylate at a concentration of *ca.* 0.1 M in dry benzene. These solutions were degassed and refluxed under an Ar atmosphere. *Ca.* 5 equiv of sodium *tert*-amylate (3.2 M in toluene) was added at once, *via* syringe, to the refluxing solution of the mesylate. Unless otherwise indicated, the reaction mixture was heated at reflux temperature for 2 min, quenched with precooled saturated aqueous NH_4Cl, and then quickly cooled to 0 °C. The mixture was vigorously stirred for 20 min, followed by extraction with ten 15-mL portions of CH_2Cl_2. The combined organic layers were dried and evaporated to afford the crude reaction product. Product ratios, yields, and pure compounds were obtained by chromatographical techniques.

a. The general procedure was employed by using 0.100 g (0..25 mmol) of **40**. Workup and flash chromatography (1:1 petroleum ether (bp 40–60 °C)/EtOAc) afforded 0.015 g (20%) of a 7:1:2 mixture of **41**, **108**, and **105**, respectively. Also 0.080 g (80%) of unreacted **40** was isolated.

b. The general procedure was employed by using 0.214 g (0.51 mmol) of **66**. Workup and flash chromatography (5:1 petroleum ether (bp 40–60 °C)/EtOAc) afforded 0.154 g of a mixture of at least four compounds and 0.012 g (6%) of unreacted **66**. Repeated column chromatography (250:1 petroleum ether (bp 40–60 °C)/EtOAc) of the mixture (0.154 g) gave in order of elution 0.053 g (32%) of **125**, 0.025 g of an unidentified mixture of at least four products according to GC and NMR, 0.056 g (34%) of **123**, and 0.020 g (12%) of **124**. The spectroscopic data of **123–125** are shown below.

(1α,4α,4aα,8β,8aβ)-4-[(*tert*-Butyldimethylsilyl)oxy]-1,2,3,4,4a,5,8,8a-octahydro-1,4a,8-trimethyl-1-naphthalenol (123): ^{1}H NMR (200 MHz) δ 0.03 (m, 6 H), 0.81–1.35 (m, 3 H), 0.88 (s, 9 H), 1.00 (s, 3 H), 1.40–1.76 (m, 4 H), 1.41 (s, 3 H), 1.81–2.16 (m, 3 H), 1.99 (s, 3 H), 3.23 (dd, J = 4.1, 11.4 Hz, 1 H), 5.45 (br s, 1 H); ^{13}C NMR (50 MHz) δ –5.06 (q), –4.12 (q), 11.80 (q), 17.85 (s), 22.81 (t), 25.27 (3q), 25.65 (q), 26.82 (t), 33.19 (q), 35.10 (t), 39.59 (s), 41.87 (t), 52.92 (d), 71.92 (s), 78.49 (d), 126.25 (d), 132.98 (s); MS m/z (relative intensity) 324 (M^+, <0.1), 309 (4), 176 (0.5), 267 (17), 252 (62), 215 (15), 175 (100), 150 (24), 120 (31), 75 (35); calcd for $C_{15}H_{27}O_2Si$ (M^+) m/z 267.1780, found m/z 267.1785.

(1α,4α,4aα,8β,8aβ)-4-[(*tert*-Butyldimethylsilyl)oxy]-1,2,3,4,4a,5,6,8a-octahydro-1,4a,8-trimethyl-1-naphthalenol (124): ^{1}H NMR (200 MHz) δ 0.02 (s, 3 H) 0.03 (s, 3 H), 0.87 (s, 9 H), 0.95–1.30 (m, 2 H), 1.02 (d, J = 0.6 Hz, 3 H), 1.20 (d, J = 5.4 Hz, 3 H), 1.28 (s, 3 H), 1.41–2.11 (m, 6 H), 2.39 (m, $W_{1/2}$ = 27 Hz, 1 H), 3.23 (dd, J = 4.1, 11.5 Hz, 1 H), 5.50 (m, 2 H); ^{13}C NMR (50 MHz) δ –5.06 (q), –4.12 (q), 13.55 (q), 17.83 (s), 23.96 (q), 25.63 (3q), 27.07 (t), 29.28 (d), 33.30 (q), 35.10 (t), 39.93 (t), 39.93 (s), 40.63 (t), 53.79 (d), 71.28 (s), 79.22 (d), 122.73 (d), 134.70 (d); MS m/z (relative intensity) 309 (M^+–15, <0.1), 267 (29), 252 (12), 175 (100), 160 (21), 119 (45), 75 (35); calcd for $C_{15}H_{27}O_2Si$ (M^+) m/z 267.1780, found m/z 267.1780.

(1α,4α,4aα,8β,8aα)-4-[(*tert*-Butyldimethylsilyl)oxy]octahydro-1,4a,8-trimethyl-2(3*H*)-naphthaleno[1,2-*b*]oxirane (125): ^{1}H NMR (C_6D_6, 200 MHz) δ 0.08 (s, 3 H) 0.09 (s, 3 H), 0.86 (d, J = 7.1 Hz, 3 H), 0.99–1.96 (m, 11 H), 1.02 (s, 9 H), 1.18 (s, 3 H), 1.34 (s, 3 H), 3.23 (dd, J = 3.1, 11.27 Hz, 1 H); ^{13}C NMR (C_6D_6, 50 MHz) δ –5.23 (q), –4.27 (q), 14.93 (q), 17.80 (s), 19.71 (2q), 25.58 (3q), 25.58 (t), 27.00 (t), 27.00 (d), 31.22 (t), 33.27 (t), 33.73 (t), 39.29 (s), 63.07 (s), 65.56 (s), 77.31 (d); MS m/z (relative intensity) 324 (M^+, <0.1), 309 (1), 267 (100), 175 (48), 166 (42), 143 (26), 120 (28), 77 (44); calcd for $C_{15}H_{27}O_2Si$ (M^+) m/z 267.1780, found m/z 267.1783.

c. The general procedure was employed by using 0.100 g (0.23 mmol) of **67**. Workup and flash chromatography (100:1 petroleum ether (bp 40–60 °C)/EtOAc) gave 0.011 g (11%) of unreacted **67** and 0.068 g (87 %) of **(1α,4α,4aα,7β,8aβ)-4-[(*tert*-Butyldimethylsily)oxy]octahydro-1,4a,7-trimethyl-8-methylene-(7*H*)-1-naphthalenol (126)**: ^{1}H NMR (200 MHz) δ 0.03 (s, 3 H) 0.04 (s, 3 H), 0.87 (s, 9 H), 0.92–1.91 (m, 9 H), 0.96 (s, 3 H), 1.05 (d, J = 7.2 Hz, 3 H), 1.27 (s, 3 H), 2.05 (br s, 1 H), 2.50 (m, $W_{1/2}$ = 12 Hz, 1 H), 3.33 (dd, J = 4.1, 11.5 Hz, 1 H), 5.08 (br s, 1 H), 5.16 (br s, 1 H); ^{13}C NMR (50 MHz) δ –5.03 (q), –4.08 (q), 12.92 (q), 17.83 (s), 18.50 (q), 25.63 (3q), 26.54 (t), 28.90 (t), 29.08 (q), 35.27 (t), 40.89 (t), 40.89 (d), 42.69 (s), 50.12 (d), 71.43 (s), 80.04 (d), 110.24 (t), 149.46 (s); MS m/z (relative intensity) 338 (M^+, <0.1), 323

(0.3), 281 (11), 189 (100), 147 (14), 120 (15), 76 (31); calcd for $C_{16}H_{29}O_2Si$ (M^+–57) *m/z* 281.1937, found *m/z* 281.1937.

6.5 References and Notes

(1) See chapter 3.

(2) See chapter 4.

(3) Paddon-Row, M. N. *Acc. Chem. Res.* **1982**, *15*, 245-251.

(4) Hoffmann, R. *Acc. Chem. Res.* **1971**, *4*, 1-9.

(5) Jordan, K. D.; Paddon-Row, M. N. *Chem. Rev.* **1992**, *92*, 395-410 and references cited therein.

(6) For structural assignments see chapter 3.

(7) GC analysis of the crude reaction mixture revealed the presence (15 %) of at least four other products. The identity of these compounds could not be established.

(8) (a) Gonzalez, A. G.; Galindo, A.; Mansilla, H.; Gutierrez, A. *Phytochemistry* **1981**, *20*, 2367-2369.
(b) Moreau, S.; Biguet, J.; Lablache-Combier, A.; Baert, F.; Foulon, M.; Delfosse, C. *Tetrahedron* **1980**, *36*, 2989-2997.

(9) (a) Adcock, W.; Kok, G. B. *J. Org. Chem.* **1987**, *52*, 356-364.
(b) Grob, C. A.; Gründel, M.; Sawlewicz, P. *Helv. Chim. Acta* **1988**, *71*, 1502-1507.
(c) Lambert, J. B.; Salvador, L. A.; So, J.-H. *Organometallics* **1993**, *12*, 697-703.

(10) The Newman projections were drawn based on full geometry optimizations by means of the MNDO (modified neglect of diatomic overlap) method. See: Dewar, M. J. S.; Thiel, W. *J. Am. Chem. Soc.* **1977**, *99*, 4899-4907.

(11) Shibata, T.; Ohkura, T.; Shimizu, N.; Inayama, S. *Heterocycles* **1986**, *24*, 893-896.

(12) (a) Tsuda, Y.; Kashiwaba, N.; Hori, T. *Chem. Pharm. Bull.* **1983**, *31*, 1073-1078.
(b) Tsuda, Y.; Kashiwaba, N.; Iitaka, Y. *Chem. Pharm. Bull.* **1983**, *31*, 1370-1373.
(c) Tsuda, Y.; Kiuchi, F. *Chem. Pharm. Bull.* **1984**, *32*, 4806-4832.

(13) Collins, C. J. *Chem. Soc. Rev.* **1975**, *4*, 251-262.

(14) Sorensen, T. S.; Whitworth, S. M. *J. Am. Chem. Soc.* **1990**, *112*, 6647-6651.

(15) Jenniskens, L. H. D.; Wijnberg, J. B. P. A; de Groot, A. *J. Org. Chem.* **1991**, *56*, 6585-6591.

(16) Jensen, F. R.; Smart, B. E. *J. Am. Chem. Soc.* **1969**, *91*, 5686-5689.

(17) (a) Traylor, T. G.; Hanstein, W.; Berwin, H. J.; Clinton, N. A.; Brown, R. S. *J. Am. Chem. Soc.* **1971**, *93*, 5715-5725.
(b) Hartmann, G. D.; Traylor, T. G. *J. Am. Chem. Soc.* **1975**, *97*, 6147-6151.

(18) Fischer, W.; Grob, C. A.; von Sprecher, G.; Waldner, A. *Tetrahedron Lett.* **1979**, *21*, 1905-1908.

(19) Lenoir, D.; Apeloig, Y.; Arad, D.; Schleyer, P. v. R. *J. Org. Chem.* **1988**, *53*, 661-675.

(20) Grob, C. A. *Acc. Chem. Res.* **1983**, *16*, 426-431.

(21) For general experimental details, see: chapter 2. Lithium and sodium *tert*-amylate were prepared by the procedures described in reference 1.

Chapter 7

The Significance of TBI in the Desilylation Reaction of Some O-Silylated 1,4-Diol Monosulfonate Esters*

7.1 Introduction

As mentioned before, perhydronaphthalene-1,4-diol monosulfonate esters react smoothly upon treatment with sodium *tert*-amylate in refluxing benzene. The outcome of these reactions indicates that the primarily formed oxygen anion is electronically coupled with the sulfonate ester group. The lone-pair electrons of the alkoxide group interact through the four intervening σ-bonds with the electron-poor sulfonate ester bond. As a result of this through-bond orbital interaction[1] (TBI) the dissociation of the C–OSO_2R bond is facilitated.[2] The concept of TBI and TSI could be successfully applied to rationalize the reactivity of these compounds and the formation of all products that were found.[3] Although an impressive amount of indirect evidence, supporting the view that long-range orbital interactions play a dominant role in the reactions with sodium *tert*-amylate, was accumulated[4-6] we sought for a more direct way to demonstrate the importance of TBI for the chemical behavior of these compounds.

Just as the electron-donating alkoxide group can induce ionization of the remote sulfonate ester bond, the presence of a nucleofugal sulfonate ester group may influence the formation of the electron-rich alkoxide function. For example, the tertiary alcohol group in the compounds studied so far may be more acidic than the tertiary hydroxyl group in a corresponding compound in which the mesylate is replaced, *e.g.*, by a hydroxyl group.

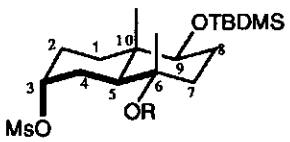

58 : R = H
106 : R = TMS

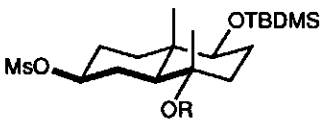

59 : R = H
107 : R = TMS

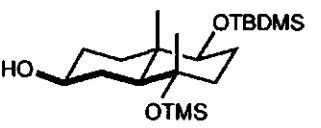

130

Chart 7.1

* This chapter will be part of a publication: Orrū, R. V. A.; Bastiaansen, P. M. F. M.; Wijnberg, J. B. P. A.; de Groot, A. *J. Org. Chem.* submitted.

At this point it should be recalled that the O-silylated mesylates **106** and **107** (Chart 7.1),[3] react fast upon treatment with tetrabutylammonium fluoride (TBAF) in refluxing benzene. Dependent on the orientation of the sulfonate ester group homofragmentation and/or β-elimination are the main reaction paths followed. However, at room temperature only desilylation takes place.

The susceptibility of the silyloxy group to the nucleophilic attack of a fluoride ion may be influenced by the remote nucleofugal mesylate group. As a result, the rate of desilylation of a compound without a mesylate group is expected to be (much) lower than the rate of desilylation of a compound with a remote mesylate group. Thus, the determination of the desilylation rate may provide a very direct method to detect long-range orbital interactions between the mesylate group and the silyloxy group in these cases.

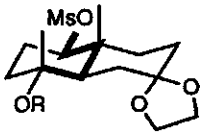

61: R = H
127: R = TMS

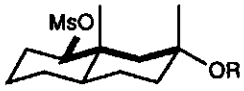

63 : R = H
128 : R = TMS

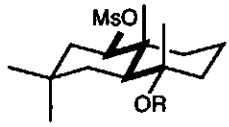

65: R = H
129: R = TMS

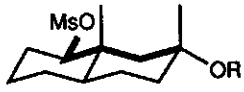

131

Chart 7.2

Therefore, we decided to synthesize the O-silylated mesylates **106, 107,** and **127–129** (Chart 7.1 and 7.2) which are structurally similar to the hydroxy mesylates **58, 59, 61, 63** and **65** studied in chapters 3 and 4. The rates of desilylation were determined conveniently and compared with the corresponding compounds that lack the mesylate functionality (compounds **130** and **131**). In this way quantitative kinetic data could be obtained. The results of these investigations are described in this chapter.

7.2 Results and Discussion

The silyl ethers **106**, **107**, and **127–129**, all with a mesylate group, were prepared in high yields by the reaction of the appropriate alcohols with TMSCl and hexamethyldisilazane (HMDS).[7]

For the synthesis of **130**, with a hydroxyl group instead of a mesylate group, the keto alcohol **71** was treated with TMSCl and HMDS in dry pyridine directly followed by reduction of the ketone function with $LiAlH_4$ in THF (Scheme 7.1).

Oxidation of the C_1-alcohol function in **84** with PDC, followed by silylation (TMSCl, HMDS) and reduction ($LiAlH_4$) afforded the silyl ether **131** in good yield (Scheme 7.1).

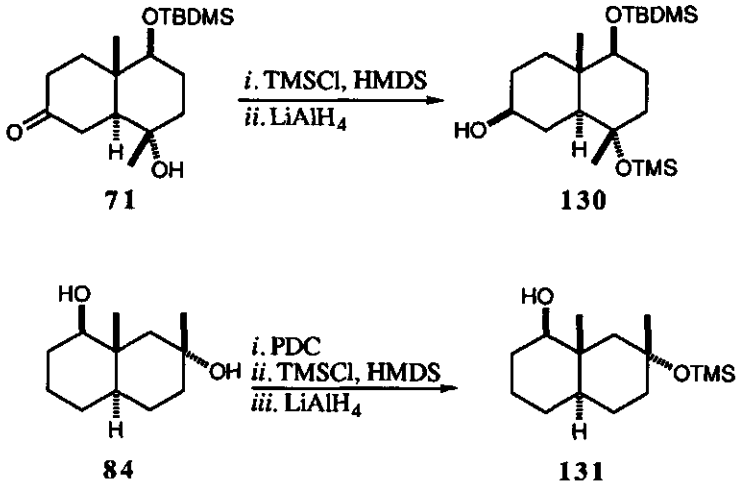

Scheme 7.1

Cleavage of the TMS-ether bond with tetrabutylammonium fluoride (TBAF) in acetonitrile at room temperature resulted in the corresponding alcohols.[8,9] No other products were detected. The desilylation reaction was studied at pseudo-first-order conditions; a ten-fold excess of TBAF was used in all reactions. The desilylation kinetics were followed by HPLC monitoring of the disappearance of the starting material.[10] The plots of the measured quantity of starting material (N)[11] as a function of time (t) gave straight lines (Figures 7.1 and 7.2) with good correlations. In this way the pseudo-first-order rate constants could be determined. Compound **129** reacted very fast with TBAF and therefore only estimated data could be obtained. Further details are given in the Experimental Section and the kinetics results are summarized in Table 7.1.

*Figure 7.1: Plots of the measured quantities (N) of the silyl ethers **106, 107, and 130** as a function of time (t).*

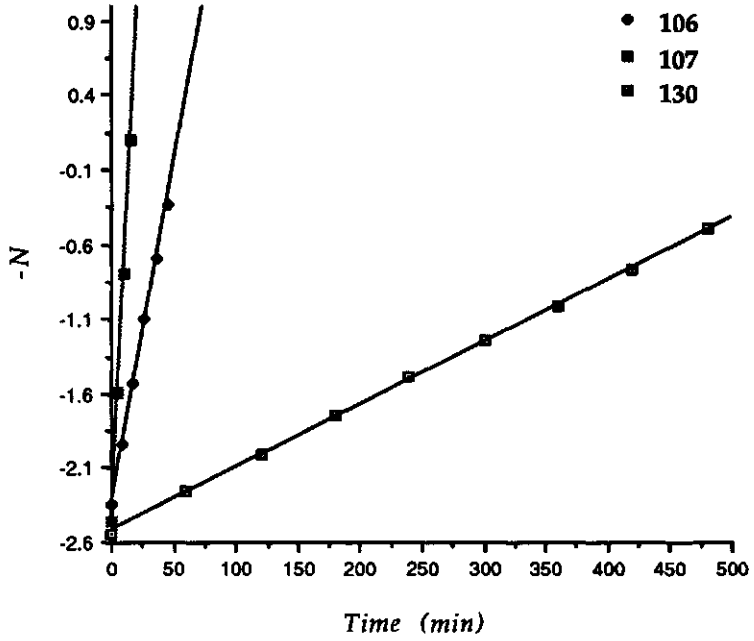

*Table 7.1. Rate constants[a] for desilylation of silyl ethers **106, 107, and 127–129** in acetonitrile at room temperature[b].*

entry	compound	k_{obs} [c]	r^2 [d]
1	**106**	4.19	0.997
2	**107**	17.3	0.999
3	**127**	3.15	0.999
4	**128**	6.10	0.998
5	**129**	>35 [e]	
6	**130**	0.515	0.996
7	**131**	0.474	0.999

[a] Pseudo-first-order rate constants (k_{obs}) for the average of two or more runs. [b] Reactions were performed at ambient temperatures (21–24 °C). [c] Units are 10^{-2} s^{-1}. [d] Worst correlation coefficient reported. [e] The reaction of **129** proceeded very fast and k_{obs} could not be detected accurately.

Figure 7.2: Plots of the measured quantities (N) of the silyl ethers 127, 128, and 131 as a function of time (t).

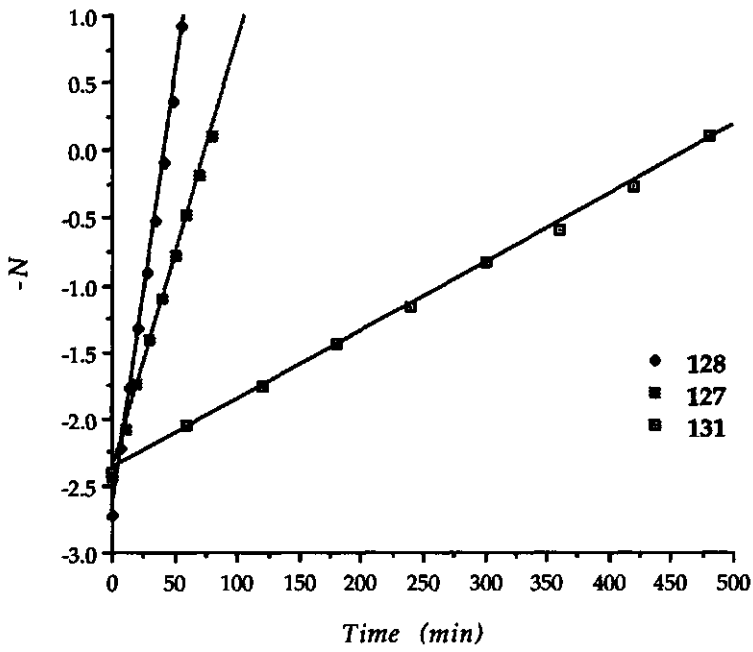

The entries 1–5 in Table 7.1 clearly show that the compounds bearing a mesylate group react considerably faster than the compounds **130** and **131** (entries 6 and 7, respectively). In order to obtain comparable data about the influence of the mesylate group on the rate of desilylation, the rate of a MsO-containing substrate (**106**, **107**, or **127–129**) was related to that of a corresponding HO-containing substrate (**130** or **131**). In this way relative rate constants (k_{rel}; Table 7.2) were obtained. The rates of the C_3 mesylates **106** and **107** are compared to the rate of the C_3 alcohol **130** (entries 1 and 2; k_{rel}, Table 7.2). The k_{rel} values for the compounds **127–129** were obtained by comparison of their desilylation rates with that of the alcohol **131** (entries 3–5; Table 7.2).

The rate enhancements as shown in Table 7.2 are significant for all the mesylates studied and confirm our assumption that a remote nucleofuge (like OMs) strongly affects the rate of desilylation of these compounds. In our opinion only an electronic interaction, transmitted *via* the σ-bonds connecting the mesylate and silyloxy group, can account sufficiently for the observed k_{rel} values.

Table 7.2. Rate ratios for mesylates 106, 107, and 127–128.

entry	k_{obs} ratio of	k_{rel}
1	**106 : 130**	8.14
2	**107 : 130**	33.6
3	**127 : 131**	6.65
4	**128 : 131**	12.9
5	**129 : 131**	>75

Steric effects are believed to play a minor role here. In all compounds the silyloxy group is equatorially oriented and points to the outskirts of the molecule. Furthermore, in all cases a 1,3-*diaxial* interaction is operating between the angular methyl group at C_{10} and the methyl group attached to the carbon atom to which the silyloxy group is attached. Finally, other bulky substituents in these molecules are spatially far removed from the reaction center. So, any possible steric influence of these groups on the rate of desilylation should be small. In this context it is noteworthy that the hydroxy compounds **130** and **131** react practically at the same rate upon treatment with TBAF (entries 6 and 7, respectively; Table 7.1). This observation supports the conclusion that steric effects play (if any) an indecisive role in the desilylation reaction of the compounds that were studied here.

The observed rate enhancements can be rationalized by assuming a long-range orbital interaction that couples the sulfonate ester group and the silyloxy group through the intervening three C–C single bonds. Due to the electronegative nature of oxygen and the electropositive nature of silicon, the Si–O bond is polarized with the (partly) negative charge on oxygen and the (partly) positive charge on silicon. This bond is therefore susceptible to nucleophilic attack at silicon.[12] Particularly, the attack by a fluoride ion is favored, since this would result in a strong Si–F bond. In the MsO-containing substrates **106**, **107**, and **127–129** the partly negative charge localized on the oxygen atom can be delocalized by an electronic interaction with the remote nucleofugal mesylate group. In the HO-containing compounds **130** and **131** a similar ground state interaction of the negative charge to the hydroxyl group is, at least, much less important. Delocalization of charge in the mesylates results in a weaker Si–O bond, making the silicon atom more susceptible for nucleophilic attack by the fluoride ion as compared to the alcohols. Hence, the rates of desilylation of the mesylates are enhanced relative to their hydroxyl analogues.

Furthermore, it is believed that due to the presence of empty *3d* orbitals in the silicon atom the nucleophile can attach itself to silicon before the leaving group (here the rest of the molecule) departs (Chart 7.3).[13] Coordination of the fluoride ion stretches the Si–O bond producing an increased negative charge on the leaving group.[14] So, in the transition state of the desilylation reaction even more negative charge will be localized at the oxygen atom. The activation energy for the desilylation reaction is lowered when the surplus of negative charge is stabilized. In other words, stabilization of the developing negative charge on the oxygen atom assists the departure of the leaving group.[15] In the MsO-containing substrates this stabilization is possible *via* σ-delocalization, in the HO-containing substrates not. As a result, the rates of desilylation for the mesylates **106, 107,** and **127–129** will be increased as compared to their respective hydroxyl analogues.

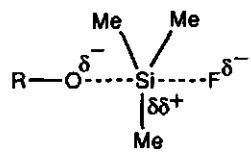

Chart 7.3

In conclusion, long-range electronic interactions (operating in the ground state, in the transition state, or in both) between the nucleofugal sulfonate ester group and the partly negative charge on the oxygen atom of the silyloxy group can account for the observed high rate ratios of these compounds.

Desilylation versus Heterolysis

At this point it should be realized that the previously described reactions of perhydronaphthalene-1,4-diol monosulfonate esters with sodium *tert*-amylate in refluxing benzene are rationalized in a similar way as the TBAF reactions.[16] In the sodium *tert*-amylate reactions the formation of an alcoholate function intramolecularly induces heterolysis of the sulfonate ester group *via* orbital interactions through the three intervening C–C single bonds. In other words, the initially formed negative charge at the oxygen atom couples with the nucleofugal mesylate group, just as was suggested above for the desilylation reactions. Due to this stabilizing interaction, the mesylate group splits off more easily in the *tert*-amylate reactions. As a result of the same stabilizing long-range orbital interaction, the cleavage of the Si–O bond occurs more easily in the TBAF reactions.

A further point of similarity between the sodium *tert*-amylate reactions and the TBAF reactions is that the order of the reactivities of the hydroxy mesylates and O-silylated mesylates, respectively, are the same. Figure 7.1 clearly shows that the equatorial mesylate **107** reacts faster than its α-isomer **106**. The k_{rel} value for **107** is about four times higher than the k_{rel} value for **106** (entries 1 and 2, respectively; Table 7.2). Likewise, the C_6–hydroxyl analogue **59** reacts somewhat faster than the C_6–hydroxyl analogue **58** upon treatment with sodium *tert*-amylate.[3] Furthermore, the silyloxy mesylate **129** reacts much faster than the silyloxy mesylates **127** and **128**. The k_{rel} value for **129** is at least five times higher than that of **128** and more than ten times higher than the k_{rel} value for **127** (entries 3–5; Table 7.2). The same order of reactivity was found for the corresponding hydroxy mesylates (**65**, **63**, and **61**, respectively) upon treament with sodium *tert*-amylate.[5]

The relative reactivities found for the base-induced reactions of the hydroxy mesylates are attributed to the different σ-relays in these compounds. It was demonstrated that transmission of TBI is highly favored when a W-like arrangement is operating between the electron donor and the electron acceptor function.[17,18] The hydroxy mesylates exhibiting such an optimal "all *trans*" arrangement of connecting σ-bonds react fast upon treatment with sodium *tert*-amylate, whereas deviation from this optimal geometry reduces the reactivity considerably.

At this point the reactivities of the O-silylated mesylates **106** and **107** (TBAF reactions) in comparison with the reactivities of the hydroxy mesylates **58** and **59** (sodium *tert*-amylate reactions) deserve some comment. The compounds **59** and **107** both having a W-like arrangement of the relaying σ-bonds react faster than their respective "sickle-relay" analogues **58** and **106**. However, the difference in reactivity between **106** and **107** is considerable (factor four) whereas the difference in reactivity between **58** and **59** is only modest. It has been shown that in processes which involve initial ionization of a leaving group, the cationic center is stabilized by delocalization of a neighboring σ-bond (σ-participation), provided that the alignment of the σ-bond and the (incipient) p orbital is favorable.[5,6] In the TBAF reactions of **106** and **107** no ionization of the mesylate group takes place and therefore no cationic center is generated at C_3. As a result, σ-participation does not play a very important role in the desilylation reactions. The difference in reactivity between **106** and **107** must therefore be attributed to the different σ-relays between the interacting functionalities. On the other hand, the mesylates **58** and **59** are believed to react *via* dipolar intermediates generated by the initial ionization of the mesylate group.[3] The cationic center at C_3 in the dipolar intermediate derived from **59** is stabilized by delocalization of the C_4–C_5 bond which is oriented antiperiplanar to the leaving group (**b**; Figure 7.3). However, it is known that C–H bonds can also stabilize effectively bordering carbocationic centers.[19] In the

initially formed dipolar intermediate derived from **58**, the axial C_4–H bond (**a**; Figure 7.3) is properly aligned and may stabilize the incipient carbocationic center at C_3. One should expect that **59** will react considerably faster than **58** because in **59** a "W" arrangement of the σ-relay is operating whereas in **58** this relay is sickle-like. The small difference in reactivity between both compounds must therefore be the result of an additional stabilization *via* σ-participation of C–H bond(s) in the dipolar intermediate derived from **58**.[20] Apparently, C–H hyperconjugation (**a**; Figure 7.3) can compete favorably with C–C hyperconjugation in these intermediates (**b**; Figure 7.3).

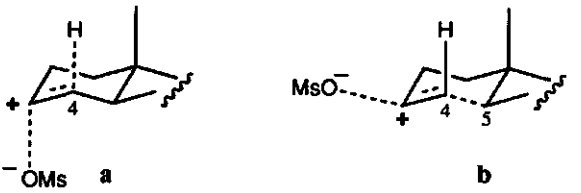

Figure 7.3: C–H hyperconjugation (a) and C–C hyperconjugation (b).

In conclusion, the differences in reactivity found for all the O-silylated mesylates studied in this chapter may be attributed to different σ-relays. The compounds in which a "W" arrangement of σ-bonds is present between the mesylate group and the silyloxy group react much faster upon treatment with TBAF than the corresponding mesylates with a deviation from the optimal arrangement of the σ-relay (see k_{obs} of **107** *versus* **106** and **129** *versus* **127** or **128**, respectively; Table 7.1).

In the reactions of the hydroxy mesylates with an optimal "all *trans*" geometry of the relaying σ-bonds, TBI is always accompanied by TSI.[5] When at the same time the inductivity is high, homohyperconjugation[21-23] may be operating. Through-space interaction (1,3-bridging) can completely determine the outcome of the reaction (*e.g.*, homofragmentation), but the contribution of TSI to the reactivity of these compounds is only modest. However, this conclusion was based on indirect evidence, since it is quite impossible to distinguish between TBI and TSI in the *tert*-amylate reactions of compounds with a "W" arrangement of the relaying σ-bonds. However, it is known that a decrease of inductivity leads to less bridging.[24] A diminished electron-donating ability of the alkoxide group results in a decrease of inductivity and the through-space interaction is diminished. For example, replacement of Na^+ by Li^+ as counterion in the reactions with *tert*-amylate results in a decrease of inductivity. The Li^+–O^- bond has a more covalent character than the Na^+–O^- bond.[25] As a result, the electron-donating ability of the alkoxide function with Li^+ as a counterion will be diminished and bridging becomes negligible.[3,5] In the initial state of the desilylation reaction

examined here, instead of an alkali metal counterion, a TMS group attached to oxygen *via* a real covalent bond is present. The resulting inductivities in these systems are, of course, very low. However, in the transition state of the desilylation reaction no "real" negative charge will be localized on the oxygen atom either. The formation of a pentacoordinated intermediate (Chart 7.3), is directly followed by a nucleophilic attack of water on the silicon atom.[13] Commercial TBAF sources exists as the trihydrate TBAF•$3H_2O$, so water is always in close vicinity.[26] The bond forming process toward silicon occurs simultaneously with the cleavage of the (elongated) Si–O bond, and a molecule of water donates a proton to the oxygen as the bond breaks.[27] Therefore, it is clear that the resulting inductivities in the transition state are also quite small. Consequently, TSI plays an indecisive role in the desilylation reactions. The long-range interaction between the mesylate group and the silyloxy group, whether operating in the ground state, transition state, or in both must be entirely attributed to a through-bond electronic coupling.

The results described in this chapter show nicely that electronic effects of distant substituents can exert a substantial influence on the reactivity of certain functional groups. It was demonstrated experimentally that σ-delocalization is an important phenomenon that can account for many processes in the chemistry of saturated organic compounds. The concept of TBI suffices not only to explain the reactivity of 1,4-diol monosulfonate esters under strongly basic conditions with *tert*-amylate in refluxing benzene, but also provides a rationale for the desilylation reactions of O-silylated mesylates.
Through-space effects do not play a very important role in the desilylation reactions. Therefore, these reactions may serve as an easy accessible chemical probe to study the chemical significance of through-bond orbital interactions in general.

7.3 Experimental Section

General. See chapter 2.

General Procedure for the Preparation of the Silyl Ethers 127-129.[28] To a solution (0.015-0.032 M) of the corresponding mesylates **61**, **63**, and **65** in dry pyridine were added *ca.* 10 equiv hexamethyldisilazane (HMDS) and TMSCl (*ca.* 7.5 equiv). The reaction mixture was stirred at rt and followed by TLC. At completion, the mixture was concentrated at reduced pressure. The remaining residue

was submitted directly to flash chromatography (3:1 petroleum ether (bp 40–60 °C)/EtOAc). By using this procedure the silylated mesylates **127-129** were prepared.

(4'aα,5'α,8'β,8'aβ)-Octahydro-4'a,8'-dimethyl-8'-[(trimethylsilyl)oxy]spiro[1,3-dioxolane-2,2'(1'*H*)-naphthalene]-5'-ol 5'-(Methanesulfonate) (127): yield 89%; ^{1}H NMR (C_6D_6, 200 MHz) δ 0.00 (s, 9 H), 0.68 (s, 3 H), 0.80 (s, 3 H), 1.26–2.01 (m, 11 H), 2.21 (s, 3 H), 3.41–3.62 (m, 4 H), 4.27 (dd, *J* = 5.7, 11.4 Hz, 1 H); ^{13}C NMR (C_6D_6, 50 MHz) δ 2.56 (3q), 12.96 (q), 22.99 (q), 26.78 (t), 30.21 (t), 30.89 (t), 37.57 (q), 38.28 (t), 38.44 (s), 40.35 (t), 50.39 (d), 63.78 (t), 64.07 (t), 74.08 (s), 88.82 (d), 109.08 (s); MS *m*/*z* (relative intensity) 391 (M^+–15, <0.1), 312 (53), 221 (18), 212 (59), 169 (15), 143 (88), 99 (100), 75 (41); calcd for $C_{17}H_{31}O_6SSi$ (M^+–15) *m*/*z* 391.1610, found *m*/*z* 391.1610.

(2α,4aα,8β,8aβ)-Decahydro-2,8a-dimethyl-2-[(trimethylsilyl)oxy]-8-naphthalenol 8-(Methanesulfonate) (128): yield 92%; ^{1}H NMR (C_6D_6, 200 MHz) δ 0.14 (s, 9 H), 0.58–1.83 (m, 12 H), 0.62 (s, 3 H), 1.17 (s, 3 H), 2.00 (d, *J* = 13.5 Hz, 1 H), 2.21 (s, 3 H), 4.17 (dd, *J* = 6.7, 12.7 Hz, 1 H); ^{13}C NMR (C_6D_6, 50 MHz) δ 2.83 (3q), 12.83 (q), 23.75 (t), 26.28 (t), 26.38 (t), 27.75 (t), 29.87 (q), 37.92 (q), 39.03 (s), 42.03 (t), 44.16 (d), 52.79 (t), 74.01 (s), 89.91 (d); MS *m*/*z* (relative intensity) 348 (M^+, 20), 269 (44), 163 (38), 143 (100), 110 (31), 75 (30); calcd for $C_{16}H_{32}O_4SSi$ (M^+) *m*/*z* 348.1790, found *m*/*z* 348.1786.

(1α,4aβ,5β,8aα)-Decahydro-1,4a,7,7-tetramethyl-1-[(trimethylsilyl)oxy]-5-naphthalenol 5-(Methanesulfonate) (129): yield 81%; ^{1}H NMR (C_6D_6, 200 MHz) δ 0.00 (s, 9 H), 0.74 (s, 3 H), 0.77 (s, 3 H), 0.82 (s, 3 H), 0.84–1.85 (m, 11 H), 1.00 (s, 3 H), 2.19 (s, 3 H), 4.32 (dd, *J* = 6.3, 11.4 Hz, 1 H); ^{13}C NMR (C_6D_6, 50 MHz) δ 2.52 (3q), 12.14 (q), 17.85 (t), 26.66 (q), 29.94 (q), 31.15 (s), 33.10 (q), 33.97 (t), 37.63 (t), 38.30 (q), 39.41 (s), 41.31 (2t), 47.97 (d), 74.79 (s), 87.88 (d); MS *m*/*z* (relative intensity) 376 (M^+, 10), 361 (16), 297 (39), 191 (27), 183 (43), 143 (100), 133 (92) 117 (27), 73 (55); calcd for $C_{18}H_{36}O_4SSi$ (M^+) *m*/*z* 376.2104, found *m*/*z* 376.2102.

Preparation of the Silyl Ethers 130 and 131. a. The above general procedure was employed by using 0.050 g (0.15 mmol) of **71**. After workup, the crude product (0.060 g) was dissolved in 20 mL of dry THF and cooled to 0 °C. To the solution was added 0.100 g (2.67 mmol) of $LiAlH_4$ and the reaction mixture was stirred at 0 °C for 15 min, after which time the reaction was carefully quenched with a small amount of saturated aqueous Na_2SO_4. The mixture was dried and evaporated. The resulting residue was flash chromatographed (10:1 petroleum ether (bp 40–60 °C)/EtOAc) to give 0.045 g (75%) of **130** as a clear oil.

(2α,4aα,5α,8β,8aβ)-5-[(*tert*-Butyldimethylsilyl)oxy]decahydro-4a,8-dimethyl-8-[(trimethylsilyl)oxy]-2-naphthalenol (130): ^{1}H NMR (C_6D_6, 200 MHz) δ 0.06 (s, 3 H), 0.09 (s, 3 H), 0.22 (s, 9 H), 0.92 (s, 3 H), 1.00 (s, 9 H), 1.24 (s, 3 H), 1.19–1.92 (m, 11 H), 2.25 (m, $W_{1/2}$ = 21 Hz, 1 H), 3.19 (dd, *J* = 3.9, 10.9 Hz, 1 H), 3.48 (m, $W_{1/2}$ = 30 Hz, 1 H); ^{13}C NMR (C_6D_6, 50 MHz) δ –4.97 (q), –4.16 (q), 2.68 (3q), 13.75 (q), 17.99 (s), 23.09 (q), 25.79 (3q), 29.38 (t), 30.70 (t), 31.27 (t), 39.25 (s), 39.85 (t), 41.12 (t), 51.56 (d), 71.35 (d), 74.92 (s), 79.97 (d); MS *m*/*z* (relative intensity) 385 (M^+–15, 1), 343 (42), 325 (70), 258 (46), 234 (54), 161 (89), 120 (21), 105 (15), 75 (100); calcd for $C_{21}H_{44}O_3Si_2$ (M^+–15) *m*/*z* 385.2594, found *m*/*z* 385.2593.

b. To a stirred solution of 0.12 g (0.61 mmol) of **84** in 50 mL of CH_2Cl_2 was added 0.600 g (1.59 mmol) of PDC. The mixture was stirred at rt for 20 h and then filtered through Celite. The filter cake was washed with three 20-mL portions of CH_2Cl_2 . The solvent was evaporated and the resulting residue

(0.090 g) was silylated according to the general procedure described above. After the usual workup, the crude oil (0.099 g) was treated with $LiAlH_4$ as described above. Workup and flash chromatography (10:1 petroleum ether (bp 40–60 °C)/EtOAc) yielded 0.099 g (60%) of the silyl alcohol **131**.

(1α,4aβ,7β,8aα)-Decahydro-7,8a-dimethyl-7-[(trimethylsilyl)oxy]-1-naphthalenol (131): ^1H NMR (C_6D_6, 200 MHz) δ 0.28 (s, 9 H), 0.80–1.85 (m, 13 H), 0.83 (s, 3 H), 1.22 (s, 3 H), 2.24 (dd, *J* = 2.2, 13.1 Hz, 1 H), 3.03 (dd, *J* = 4.6, 9.7 Hz, 1 H); ^{13}C NMR (C_6D_6, 50 MHz) δ 2.90 (3q), 12.22 (q), 24.30 (t), 26.75 (t), 27.00 (t), 29.91 (t), 29.91 (q), 39.49 (s), 42.39 (t), 44.19 (d), 53.36 (t), 74.57 (s), 80.09 (d); MS *m/z* (relative intensity) 270 (M^+, 17), 255 (7), 167 (20), 143 (100), 121 (4), 109 (9), 73 (30); calcd for $C_{15}H_{30}O_2Si$ (M^+) *m/z* 270.2015, found *m/z* 270.2013.

Kinetic Studies. The rate of disappearance of starting material (**106, 107,** and **127–131**) was followed by HPLC. The reactions were studied under the conditions at which [TBAF]>>[substrate], *i.e.*, pseudo-first-order conditions. The following procedure was adopted: to a solution of 1.5 mL of 0.0055 M of silyl ether in dry acetonitrile (in sealed ampules) was added 50 μL of 1.1 M of TBAF in THF at once, *via* syringe, and mixed thoroughly. The reaction was followed at ambient temperatures (21–24 °C) until at least 80% of the starting material was converted. No internal standard was required because of the highly reproducible injection volumes (± 1%) possible with an autosampler.

High Performance Liquid Chromatography. The HPLC equipment was a high precission pump, and a refractive index detector assembled with a 10 μL loop injection valve. The chromatography column (25 x 1/4 cm) was packed with 10 μm SPHERISORB ODS 2. Results were obtained by eluting with acetonitrile/water (isocratic, 80 or 95 % v/v) at a column temperature of 26 °C. The solvent mixture was degassed prior to elution (flow rate = 1 mL/min). Injections of 10 μL ± 0.1 μL were performed with an autosampler, manipulated according to the manufacturers instructions for chromatographic applications.

7.4 References and Notes

(1) Hoffmann, R. *Acc. Chem. Res.* **1971**, *4*, 1-9.

(2) Gleiter, R.; Stohrer, W.-D.; Hoffmann, R. *Helv. Chim. Acta* **1972**, *55*, 893-906.

(3) See chapter 3.

(4) Paddon-Row, M. N.; Jordan, K. D. In *Modern Models of Bonding and Delocalization*; J. F. Liebman and A. Greenberg, Eds.; VCH publishers: New York, **1988**; chapter 3.

(5) See chapter 4.

(6) See chapter 6.

(7) Langer, S. H.; Connell, S.; Wendler, I. *J. Org. Chem.* **1958**, *23*, 50-58.

(8) Corey, E. J.; Venkateswarlu, A. *J. Am. Chem. Soc.* **1972**, *94*, 6190-6191.

(9) For general properties of some tetraalkylammonium fluorides see: Christe, K. O.; Wilson, W. W.; Wilson, R. D.; Bau, R.; Feng, J. *J. Am. Chem. Soc.* **1990**, *112*, 7619-7625.
(10) Bentley, T. W.; Gream, G. E. *J. Org. Chem.* **1985**, *50*, 1776-1778.
(11) N=ln[substrate]; The [substrate] was derived conveniently from the peak height.
(12) Colvin, E. In *Silicon in Organic Synthesis*; Butterworth and Co publishers: London, **1981**, p 5.
(13) Corriu, R. J. P. *Pure Appl. Chem.* **1988**, *60*, 99-106.
(14) Corriu, R. J. P.; Perz, R.; Reye, C. *Tetrahedron* **1983**, *39*, 999-1009.
(15) Dietze, P. E. *J. Org. Chem.* **1992**, *57*, 6843-6847.
(16) See references 3 and 5.
(17) Paddon-Row, M. N. *Acc. Chem. Res.* **1982**, *15*, 245-251.
(18) Jordan, K. D.; Paddon-Row, M. N. *Chem. Rev.* **1992**, *92*, 395-410 and references cited therein.
(19) Cieplak, A. S.; Tait, B. D.; Johnson C. R. *J. Am. Chem. Soc.* **1989**, *111*, 8447-8462 and references cited therein.
(20) C–H hyperconjugation is only possible in compound **58**, all other compounds studied in this thesis, have an equatorial mesylate group and C–H hyperconjugation is prevented.
(21) See chapter 5.
(22) Adcock, W.; Kok, G. B. *J. Org. Chem.* **1987**, *52*, 356-364.
(23) Grob, C. A.; Gründel, M.; Sawlewicz, P. *Helv. Chim. Acta* **1988**, *71*, 1502-1507.
(24) Grob, C. A. *Acc. Chem. Res.* **1983**, *16*, 426-431.
(25) Paquette, L. A.; Gilday, J. P. *J. Org. Chem.* **1988**, *53*, 4972-4978.
(26) Ko, S. Y.; Malik, M.; Dickinson, A. F. *J. Org. Chem.* **1994**, *59*, 2570-2576.
(27) Dietze, P. E. *J. Org. Chem.* **1993**, *58*, 5653-5662.
(28) The silyl ethers **106** and **107** were prepared following previously described procedures.[3]

Chapter 8

Concluding Remarks and Outlook

8.1 General

The interaction of orbitals over an intervening σ-framework, first systemized by Hoffmann *et al*,[1] proved to be an useful concept to account for all of the experimental results presented in the previous chapters.

Carbocations are established to form the optimal situation to study TBI, because strong electron demand tends to magnify the orbital interactions. By the same token, electron-donating substituents capable of receiving positive charge also bring about enhanced long-range effects. Consequently, the stimulating effect of strong donors such as O^- on carbocation production is probably the best match to investigate the chemical consequences of orbital interactions mediated *via* a saturated σ-bridge.

The conditions chosen in this investigation are perfect for this purpose. It was demonstrated that perhydronaphthalene-1,4-diol monosulfonate esters react smoothly upon treatment with sodium *tert*-amylate in refluxing benzene. The apolar medium prevents the generation of a carbocationic center *via* solvolysis of the sulfonate ester bond. Furthermore, nucleophilic displacement of the mesylate by the non-nucleophilic *tert*-amylate ion is not very likely. The strong base serves to deprotonate the tertiary hydroxyl group of the substrate, thus generating primarily an oxygen anion, just as in the Wharton reaction[2]. The lone-pair electrons of the alkoxide group interact through the four intervening σ-bonds with the electron-poor sulfonate ester bond and facilitate its dissociation. It must be emphasized that without an O^- no reactions take place at all (Chapter 3). So, under the prevailing reaction conditions the strong electron-donating oxygen anion assists in the production of a carbocationic center *via* TBI over four σ-bonds.

The extent of this σ-delocalization together with phenomena connected with the stabilization of carbocations, like σ-participation[3] or homohyperconjugation[4], determine the overall and relative reactivity of the compounds that were studied. In addition, typical carbocationic processes such as, (homo)fragmentation, rearrangement, and β-elimination determine the product outcome of these reactions.

8.2 Reactivity

The extent of TBI depends particularly on the geometry of the σ-bonds connecting the interacting functionalities. As predicted theoretically, a W-like configuration of the σ-relay highly favors the transmission of TBI.[5] This finds expression in very fast reactions of compounds in which a "W" arrangement of the relaying σ-bonds is operating (structure I; Chart 8.1). The deviation of the "W" arrangement in the sickle-like structures II and III makes TBI more difficult, thereby reducing the reactivity of such compounds (Chapter 4). These results are consistent with the "*trans* rule", which predicts that the extent of orbital interactions through σ-bonds is maximized for an "all *trans*" arrangement of the relaying saturated carbon chain.[5]

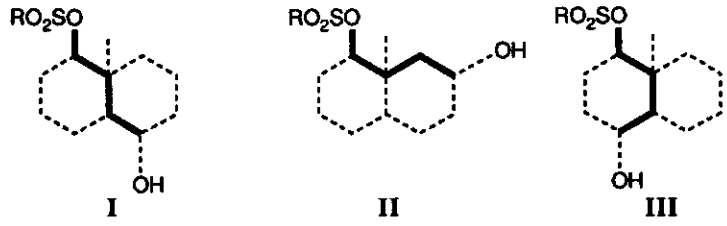

Chart 8.1

Closely related to this stabilizing TBI effect are σ-participation, 1,3-bridging, and homohyperconjugation which are frequently applied in carbocation chemistry to account for the stabilization of (incipient) carbocationic centers.

σ-Participation is effective whenever a neighboring σ-bond is oriented coplanar with the p orbital of the developing carbocation (or antiperiplanar to the leaving group in the starting product).[6] As a consequence, an electronic delocalization of the electron-pair of that σ-bond with the incipient cation is possible. This should strongly influence the formation and reactivity of the resulting carbocationic species. Electron-donating substituents, such as oxygen anions, enlarge the electron density of the participating C_γ–C_β bond *via* TBI and stimulate σ-participation resulting in a more facile ionization of the mesylate group (Figure 8.1).[7]

σ-Participation predicts that inductively donating substituents R, like CH_3, at a position β to the leaving group have an accelerating effect on the formation of the carbocationic center.[8] Our experiments showed clearly that compounds with a tertiary or quaternary C_β atom react considerably faster than compounds with a secondary C_β atom (Chapter 6).

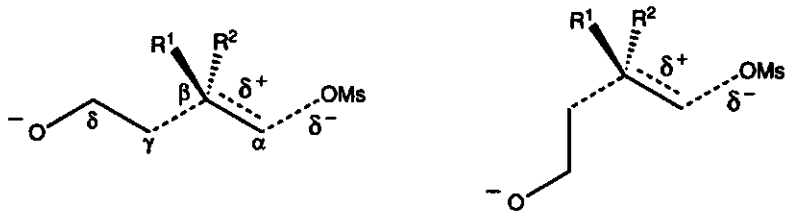

Figure 8.1: σ-Participation.

Bridging is believed to be attended with σ-participation,[3,7] however, the length or angles around the participating σ-bond are not altered appreciably by σ-participation.[8] From this it follows that although bridged intermediates may occur, 1,3-bridging alone does not attribute to the overall stabilization of a developing cation (Chapters 4 and 6). It should be noted that σ-participation may also be operative in compounds with a sickle-like geometry of the σ-relay provided the C_γ–C_β bond is oriented antiperiplanar to the sulfonate ester (Figure 8.1) (Chapter 4).

When inductivity[9] is strong and a perfect "W" arrangement of σ-bonds connects the electron demanding center with the electron-donating substituent, a very strong stabilizing interaction may be the result. This is often referred to as homohyperconjugation.[4]

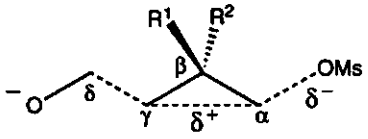

Figure 8.2: Homohyperconjugation.

The oxygen anion donates electrons to the C_γ–C_β bond by a through-bond inductive mechanism, thus attenuating the electron density of this bond and its ability to participate in the ionization process. At the same time the back lobe of the C_γ–C_δ–O^- bond is enlarged and interacts, through-space, with the developing p orbital at C_α (Figure 8.2). However, it should be emphasized that the magnitude of homohyperconjugation depends very critically on the conformation of the relaying σ-bonds, the order of substitution at C_β, and the electron-donating ability of the oxygen anion (Chapters 3, 4, and 6).

In conclusion, stabilization of the incipient carbocationic center *via* σ-participation or homohyperconjugation may account for the relative reactivities of

perhydronaphthalene-1,4-diol monosulfonate esters. However, long-range orbital interactions through σ-bonds (TBI) greatly influences the extent of both stabilizing interactions. The extent of TBI, in turn, is determined by the inductivity of the system and the geometry of the relaying σ-bonds, and accounts greatly for the overall reactivity of the compounds that were studied. The interplay of σ-participation, homohyperconjugation, and TBI can be described in a generalized way as depicted in Figure 8.3.

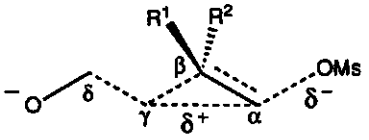

Figure 8.3: Combination of TBI, homohyperconjugation, and σ-participation.

The Desilylation Reaction

The desilylation reaction of O-silylated 1,4-diol monosulfonate esters is rationalized satisfactory when through-bond orbital interactions are invoked (Chapter 7). The compounds in which σ-delocalization is diminished react very slowly upon treatment with TBAF. On the other hand, the compounds in which a "W" arrangement of σ-bonds is present between the mesylate and silyloxy group react fast under the same conditions. Just as is the case in the *tert*-amylate reactions.
Electronic effects of distant substituents can have a significant effect on the reactivity in general of certain functional groups. TBI is a an important phenomenon that can account for many processes in the chemistry of saturated organic compounds.

8.3 Product Formation

The dipolar intermediates, which are initially formed in the reactions with *tert*-amylate, undergo typical carbocationic processes like rearrangement, β-elimination, H- or Me-shifts, and (homo)fragmentation. Each process is discussed briefly in the following subsections.

8.3.1 Rearrangement

The initially formed secondary carbocationic species will undergo rearrangement when more stable tertiary ions are the result.

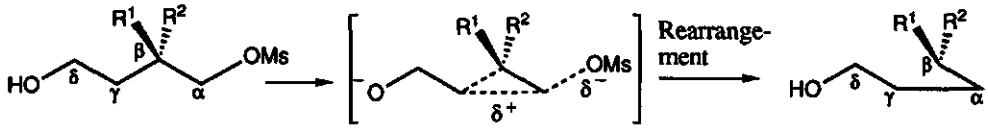

Scheme 8.1

In other words, only when the β carbon atom is quaternary, rearrangement is feasible. Bridged ions are likely intermediates on the rearrangement path (Scheme 8.1).[3]
A prerequisite for the occurrence of rearrangement is that the C_γ–C_β bond and the leaving group have the proper antiperiplanar relationship. On the other hand, the geometry of the σ-relay is not very important for the rearrangement process, since in compounds possesing a W-like arrangement as well as in compounds with a sickle-like arrangement, rearrangement is observed (Chapter 4).

8.3.2 β-Elimination

When no bordering C–C single bond is oriented properly for rearrangement, elimination of a β proton can be an alternative pathway (Scheme 8.2). Intermolecular, as well as intramolecular elimination has been observed (Chapter 3). Intramolecular elimination is favored when the oxygen anion, the β proton and the mesylate group are properly aligned (see Scheme 8.2), otherwise the intermolecular process will become more important. It is noteworthy that the dissociation of the leaving group may be assisted by C–H hyperconjugation (σ-participation of a C–H σ-bond) whenever this bond is oriented coplanar with the p orbital of the incipient carbocation.[10]

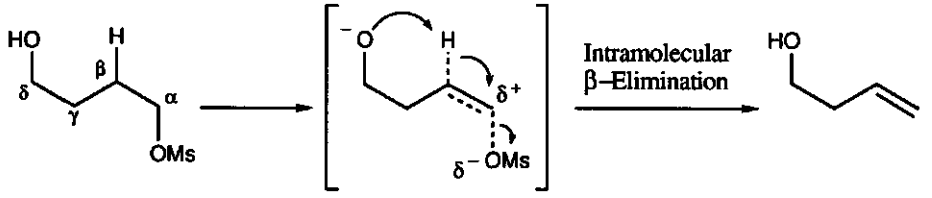

Scheme 8.2

8.3.3 Hydride- and Methyl Shifts

Products formed *via* a 1,2-H, 1,3-H, or a 1,2-Me shifts have also been detected (Chapters 3 and 6). When the associated mesylate group and the shifting hydrogen atom or methyl group are oriented in an *anti*-fashion these processes are not unlikely.

This is the case when the resulting carbocation is more stable than the initially formed secondary one and when other processes, like rearrangement (*vide supra*) or homofragmentation (*vide infra*), are stereoelectronically not favored.

8.3.4 Homofragmentation

Homofragmentation occurs only with the operating σ-relay being W-like. Furthermore, the electron-donating ability of the oxygen anion must be high. The formation of a cyclopropane moiety (Scheme 8.3) can only occur if the back lobe of the polarized C_γ–C_δ–O^- bond is large enough, and in a proper position for dorsal C-participation in the ionization process of the leaving group. Only when inductivity is high and the geometry of the intervening carbon chain is "all *trans*", these conditions are met (Chapters 3 and 4). The homohyperconjugative effect (*vide supra*) will ultimately lead to C_γ–C_α bond formation with simultaneous breaking of the C_γ–C_δ bond, *i.e.*, homofragmentation. At this point it should be emphasized that only minor deviations from the ideal "W" arrangement of the σ-relay prevents homohyperconjugation and thereby the homofragmentation process (Chapter 6).

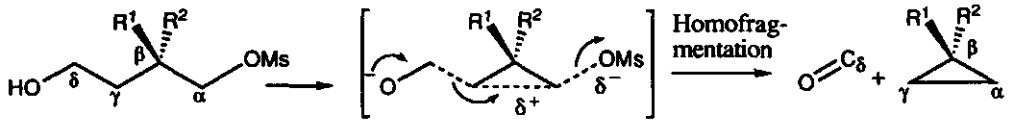

Scheme 8.3

8.4 Outlook

Combination of the special stereoelectronic features connected with TBI (and TSI) with the concepts of σ-participation and homohyperconjugation provides a very workable theory. The stereochemical and stereoelectronic requirements for the reactions of perhydronaphthalene 1,4-diol monosulfonate esters upon treatment with strong non-nucleophilic base in refluxing apolar media are now well established. In addition, the results obtained from the desilylation reactions described in Chapter 7 can also be explained when TBI is invoked, which demonstrates the general utility of the theory.

As for the applicability in synthesis, the rearrangement and β-elimination reaction have already been applied in the total syntheses of sesquiterpenes.[11] The rearrangement was used in the total synthesis of (±)-*epi*-nardol (**52** in Scheme 8.4).[11a]

Rearrangement in combination with β-elimination has been used in the total synthesis of the natural sesquiterpene (±)-alloaromadendrane-4α,10α-diol (55 in Scheme 8.5).[11b]

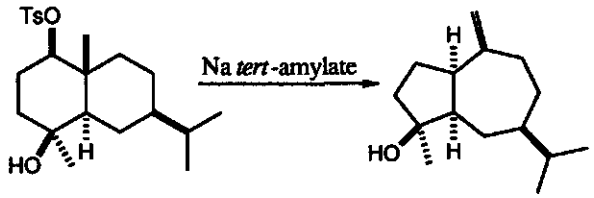

51 52

Scheme 8.4

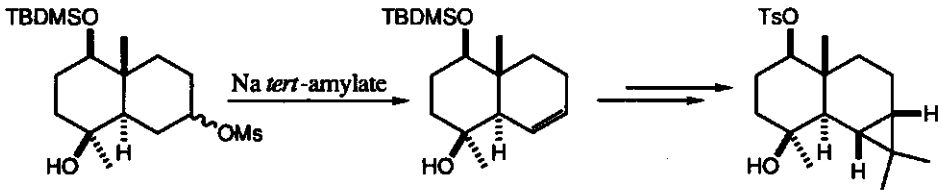

39 and/or 40 41 53

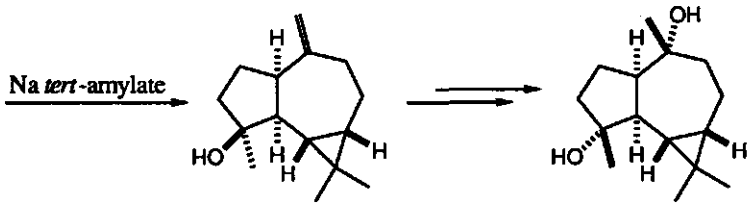

54 55

Scheme 8.5

Application of the homofragmentation reaction is currently under investigation. Several natural products possess fused cyclopropane rings. Homofragmentation of suitable substrates possessing the desired conformation of relaying σ-bonds may be a successful approach to synthesize such compounds. It is promising that processes similar to homofragmentation are thought to occur in the biosynthesis of compounds with a fused cyclopropane ring.[12] For example, waitziacuminone is, most likely formed by a proton-catalyzed homofragmentation reaction of spathulenol (Scheme

8.6).[13] We can thus look forward to many more applications of TBI-induced reactions in the synthesis of natural products.

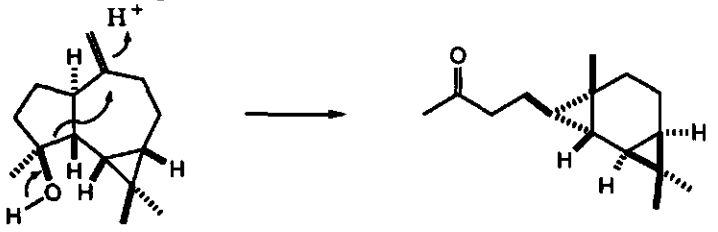

Spathulenol Waitziacuminone

Scheme 8.6

8.5 References and Notes

(1) (a) Hoffmann, R.; Imamura, A.; Hehre, W. J. *J. Am. Chem. Soc.* **1968**, *90*, 1499-1509.
(b) Hoffmann, R. *Acc. Chem. Res.* **1971**, *4*, 1-9.

(2) (a) Wharton, P. S. *J. Org. Chem.* **1961**, *26*, 4781-4782.
(b) Wharton, P. S.; Hiegel, G. A. *J. Org. Chem.* **1965**, *30*, 3254-3257.

(3) First proposed by: Winstein, S.; Trifan, D. *J. Am. Chem. Soc*, **1952**, *74*, 1147-1160.

(4) (a) Adcock, W.; Kok, G. B. *J. Org. Chem.* **1987**, *52*, 356-364.
(b) Grob, C. A.; Gründel, M.; Sawlewicz, P. *Helv. Chim. Acta* **1988**, *71*, 1502-1507.
(c) Lambert, J. B.; Salvador, L. A.; So, J.-H. *Organometallics* **1993**, *12*, 697-703.

(5) (a) Paddon-Row, M. N.; Jordan, K. D. In *Modern Models of Bonding and Delocalization*; J. F. Liebman and A. Greenberg, Eds.; VCH publishers: New York, **1988**; chapter 3.
(b) Paddon-Row, M. N. *Acc. Chem. Res.* **1982**, *15*, 245-251.

(6) Jensen, F. R.; Smart, B. E. *J. Am. Chem. Soc.* **1969**, *91*, 5686-5689.

(7) Lenoir, D.; Apeloig, Y.; Arad, D.; Schleyer, P. v. R. *J. Org. Chem.* **1988**, *53*, 661-675.

(8) (a) Traylor, T. G.; Hanstein, W.; Berwin, H. J.; Clinton, N. A.; Brown, R. S. *J. Am. Chem. Soc.* **1971**, *93*, 5715-5725.
(b) Hartmann, G. D.; Traylor, T. G. *J. Am. Chem. Soc.* **1975**, *97*, 6147-6151.

(9) The strength with which the inductive effect is transmitted to the reaction center: Grob, C. A. *Acc. Chem. Res.* **1983**, *16*, 426-431.

(10) Cieplak, A. S.; Tait, B. D.; Johnson C. R. *J. Am. Chem. Soc.* **1989**, *111*, 8447-8462 and references cited therein.

(11) See chapter 1, pp 18-19. For further details see: (a) Wijnberg, J. B. P. A.; Jenniskens, L. H. D.; Brunekreef, G. A.; de Groot, A. *J. Org. Chem.* **1990**, *55*, 941-948.
(b) Jenniskens, L. H. D.; Wijnberg, J. B. P. A; de Groot, A. *Ibid.* **1991**, *56*, 6585-6591.

(12) For example see: Sakui, N.; Kuroyanagi, M.; Ishitobi, Y.; Sato, M.; Ueno, A. *Phytochemistry*, **1992**, *31*, 143-147.

(13) Jakupovic, J.; Schuster, A.; Bohlmann, F.; King, R. M.; Haegi, L. *Phytochemistry*, **1989**, *28*, 1943-1948.

Summary

In this thesis the base-induced reactions of perhydronaphthalene-1,4-diol monosulfonate esters are described. These compounds undergo smoothly, typical carbocationic processes upon treatment with sodium *tert*-amylate in refluxing benzene. The product outcome, product ratio, and (relative) rate of these reactions is satisfactorily explained when through-bond orbital interactions (TBI) over four σ-bonds are invoked. In order to gather more detailed information about the basic stereochemical and stereoelectronic principles underlying these processes, synthetical organic, computational, and kinetic investigations were undertaken.

Most experimental studies on TBI have focussed on its spectroscopic manifestations and are reviewed repeatedly. On the other hand, there are relatively few reviews on the chemical consequences of TBI over three or more σ-bonds. A number of illustrative examples of chemical reactions in which long-range orbital interactions are believed to play an essential role are discussed in chapter 1. In the same chapter also attention is drawn to the synthetic utility of some of these reactions.

In chapter 2 the syntheses of the mesylates **39, 40,** and **58-67** are described. The compounds **39, 40, 58,** and **59** are prepared in order to investigate how the orientation of the sulfonate ester group in combination with the orientation of the tertiary hydroxyl group determines the outcome and rate of their reactions with sodium *tert*-amylate. The results of these investigations are described in chapter 3. It was found that an equatorial sulfonate ester group favors homofragmentation leading to the cyclopropane derivative **105**. In case of an axial sulfonate ester group β-elimination, which strongly depends on the stereochemistry of the tertiary deprotonated hydroxyl group, is the main reaction path. In the chapter 3 the synthesis of the O-silylated mesylates **106** and **107** is also described. These compounds show no reaction at all upon treatment with strong base. On the other hand, fast reactions are observed when **106** and **107** are treated with TBAF. Generation of an alcoholate is crucial for the observed reactions. Homofragmentation and an internal return reaction with inversion of configuration of the mesylate group in the axial mesylates **39** and **58** is explained by assuming a 1,3-bridged intermediate carbocation.

The mesylates **60–65** are prepared (Chapter 2) to determine the influence of the geometry of the relaying σ-bonds on the reactions with sodium *tert*-amylate. In chapter 4 the results of these studies are described in detail. An alcoholate function intramolecularly induces heterolysis of the sulfonate ester group in an apolar solvent *via* orbital interactions through three intervening C–C single bonds. It is shown that

the reactivity of the compounds **60–65** is only affected by the relative position of the hydroxyl function to the sulfonate ester group and not by the orientation of the hydroxyl group. The two chief pathways by which these compounds react are rearrangement (**60**, **62**, and **63**) and homofragmentation (**64** and **65**). Stereoelectronic effects play a dominant role here, except in compound **61** where steric factors primarily determine the reactivity and product outcome (ether formation). Homofragmentation is much faster than rearrangement and is only possible when a 1,3-bridged through-space interaction accompanies TBI. The extent of TBI as well as the product composition is strongly determined by the σ-relay of the four σ-bonds between the electron donor (alcoholate) and the electron acceptor (sulfonate ester bond). These results are consistent with the "*trans* rule", which is in line with predictions from theoretical models regarding TBI.

The product outcome, product ratio, and relative rate of the base-induced reactions of perhydronaphthalene-1,4-diol monosulfonate esters described in chapter 4 are satisfactorily explained with the concept of TBI. However, the conclusions are all based on empirical results. In chapter 5 the results of semi-empirical calculations, using the MNDO method, performed on model systems are presented. In this way a more detailed understanding of the stereoelectronic features underlying the homofragmentation and rearrangement reaction is obtained. The trends in the results of the MNDO simulations are the same as those found in the reactions of the compounds **60–65**. Whether rearrangement or homofragmentation takes place depends on the geometry of the σ-relay and the inductivity of the system. Cyclopropanoid bridged structures seem to be involved in the rearrangement process as well as in the homofragmentation process.

In order to explore the effects of the order of substitution of the carbon atom that borders the carbon atom to which the mesylate group is attached the compounds **40**, **66**, and **67** were synthesized. This subject is discussed in chapter 6. The product formation is strongly dependent on the steric consequences of alkyl substituents at β carbon atoms. Homofragmentation is highly favored when the repulsive steric interactions do not prevent a homohyperconjugatively stabilized transition state. This is only possible in an ideal "W" arrangement of the σ-relay (**40**). Due to the repulsive 1,3-*peri*-effect in **66**, and a combination of the 1,3-*peri*-effect and the 1,3-*diaxial*-effect in **67** the σ-relay diverges from the ideal "all *trans*" geometry as a result of which other reaction pathways (elimination, 1,3–H, and 1,2–Me shifts) are favored over homofragmentation. Introduction of inductively electron-donating substituents leads to an increase in reaction rate, despite the (slight) deviation of the "W" arrangement. It is concluded that although bridged ions are important intermediates

in the observed reaction paths, they are not decisive for the reactivity of these compounds.

The O-silylated mesylates **106** and **107** react fast upon treatment with TBAF in refluxing benzene (Chapter 3). At room temperature only desilylation takes place. To investigate the influence of a remote nucleofugal mesylate group on the rate of desilylation, apart from **106** and **107**, also the O-silylated compounds **127–131** are synthesized and treated with TBAF as is described in chapter 7. The rates of desilylation are determined conveniently by HPLC monitoring of the disappearance of the starting material. The desilylation rate of compounds with a mesylate group is much higher than the desilylation rate of corresponding compounds with a hydroxyl group instead (**130** and **131**). Furthermore, compounds having a "W" arrangement (**107** and **129**) of the relaying σ-bonds react considerably faster than their "sickle relay" analogs (**106**, **127**, and **128**). The results presented in this chapter show nicely that long-range electronic effects of distant substituents can exert a substantial influence on the reactivity of certain functional groups in general.

In conclusion, the concept of TBI offers a good explanation for the reactivity of the compounds studied throughout this thesis. The stereochemical and stereoelectronic requirements for the base-induced reactions of perhydronaphthalene-1,4-diol monosulfonate esters are now well established. The general utilitly of the concept of σ-delocalization and TBI in everyday chemistry is demonstrated.

Samenvatting

In dit proefschrift worden de base-geïnduceerde reacties van perhydronaftaleen-1,4-diol monosulfonaatesters beschreven. Deze verbindingen ondergaan gemakkelijk typisch carbokationachtige processen na behandeling met natrium*tert*-amylaat in refluxende benzeen. De produktvorming, produktverhouding, en (relatieve) snelheden van deze reacties worden goed verklaard met behulp van through-bond orbitaal interacties (TBI). Synthetisch organische, rekenkundige en kinetische studies werden uitgevoerd om meer informatie te verkrijgen over de stereochemische en stereoelectronische basisprincipes die ten grondslag liggen aan deze processen.
In de meeste experimentele studies naar TBI is de aandacht gericht op de spectroscopische gevolgen ervan. Herhaaldelijk zijn hiervan overzichten verschenen in de literatuur. Er zijn echter weinig overzichten verschenen die handelen over de chemische gevolgen van TBI. Ter illustratie wordt in hoofdstuk 1 wordt een aantal voorbeelden besproken van reacties waarvan wordt aangenomen dat orbitaal interacties over grote afstand een essentiële rol spelen. Tevens wordt de aandacht gevestigd op de bruikbaarheid van sommige van deze reacties in de organische synthese.
De synthese van de mesylaten **39**, **40** en **58–67** wordt beschreven in hoofdstuk 2. De verbindingen **39**, **40**, **58** en **59** zijn gemaakt om te onderzoeken op wat voor manier de oriëntatie van de sulfonaatestergroep, in combinatie met de oriëntatie van de tertiaire hydroxylgroep, de uitkomst en de snelheid van de reacties met natrium*tert*-amylaat bepaalt. De resultaten hiervan staan beschreven in hoofdstuk 3. Homofragmentatie leidt tot de cyclopropaanverbinding **105** en treedt op als de mesylaatgroep equatoriaal staat. Met een axiale mesylaatgroep vindt voornamelijk β-eliminatie plaats. Deze β-eliminatie is sterk afhankelijk van de stereochemie van de tertiaire hydroxylgroep. In hoofdstuk 3 wordt ook de synthese van de O-gesilyleerde mesylaten **106** en **107** beschreven. Deze verbindingen vertonen helemaal geen reactie als ze behandeld worden met sterke base. Worden ze echter behandeld met TBAF dan wordt een snelle reactie waargenomen. De vorming van een alcoholaatanion is cruciaal voor deze reacties. De homofragmentatie-reactie en de "internal return"-reactie met inversie van configuratie van de mesylaatgroep in **39** en **58** kunnen worden verklaard door een 1,3-gebrugd carbokation aan te nemen.
De mesylaten **60–65** zijn gesynthetiseerd (hoofdstuk 2) om de invloed van de geometrie van de σ-bindingen tussen de mesylaatgroep en de tertiaire hydroxylgroep te onderzoeken. In hoofdstuk 4 worden de resultaten van deze studies in detail

beschreven. Een alcoholaatfunctie induceert, intramoleculair, de heterolyse van de sulfonaatestergroep in een apolair oplosmiddel *via* orbitaal interacties over de drie tussenliggende enkele C–C bindingen. De reactiviteit van de verbindingen **60–65** wordt alleen beïnvloed door de relatieve positie van de hydroxylfunctie ten opzichte van de mesylaatgroep. De twee belangrijkste reactiepaden waarlangs deze verbindingen reageren zijn omlegging (**60, 62, en 63**) en homofragmentatie (**64 en 65**). Stereoelectronische factoren spelen een grote rol bij deze reacties, behalve bij verbinding **61** waarin voornamelijk sterische factoren de reactiviteit en produktvorming bepalen (ethervorming). De homofragmentatie-reactie verloopt veel sneller dan de omleggingsreactie en is alleen mogelijk indien een 1,3-gebrugde through-space interactie samengaat met TBI. Zowel de grootte van TBI als de produktsamenstelling worden sterk bepaald door de σ-relay van de vier σ-bindingen tussen de elektrondonor (alcoholaat) en de elektronacceptor (sulfonaatester binding. Deze resultaten zijn goed verenigbaar met de "*trans* regel" die wordt voorspeld door theoretische TBI-modellen.

De produktvorming, produktverhouding en relatieve snelheden van de base-geïnduceerde reacties van perhydronaftaleen-1,4-diol monosulfonaatesters, beschreven in hoofdstuk 4, zijn goed te verklaren met het TBI-concept. De conclusies zijn echter allemaal gebaseerd op empirische resultaten. In hoofdstuk 5 worden de resultaten van semi-empirische MNDO berekeningen, uitgevoerd aan modelsystemen, gepresenteerd. Op deze manier is een meer gedetailleerd begrip verkregen van de stereoelectronische principes die ten grondslag liggen aan de homofragmentatie- en de omleggingsreactie. De trends die naar voren komen uit de MNDO simulaties zijn dezelfde als die worden gevonden voor de chemische reacties van **60–65**. Of omlegging danwel homofragmentatie plaatsvindt hangt af van de geometrie van de σ-relay en de inductiviteit van het systeem. Cyclopropaanachtige structuren lijken te zijn betrokken bij het omleggingsproces maar ook bij het homofragmentatie proces.

Om de effecten van de substitutiegraad van het koolstofatoom naast het koolstofatoom waaraan de mesylaatgroep gebonden is te onderzoeken, zijn de verbindingen **40, 66** en **67** gesynthetiseerd (hoofdstuk 2). De resultaten van de reacties met natrium*tert*-amylaat worden besproken in hoofdstuk 6. De produktvorming is sterk afhankelijk van de sterische gevolgen van alkylsubstituenten aan de β-koolstof atomen. Het homofragmentatie proces wordt begunstigd als er geen sterische interacties zijn die een homohyperconjugatief gestabiliseerde overgangstoestand verhinderen. Dit is alleen mogelijk in een ideale "W"-geometrie van de σ-relay (**40**). Door het 1,3-*peri*-effect in **66** en een combinatie van het 1,3-*peri*-effect en het 1,3-*diaxiale*-effect in **67** wijkt in deze gevallen de σ-relay af van de ideale "all *trans*"-

geometrie. Als gevolg hiervan worden andere reactiepaden (eliminatie, 1,3-H en 1,2-Me shifts) begunstigd boven homofragmentatie. De aanwezigheid van inductief elektronenstuwende β-substituenten leidt echter ook tot een versnelling van de reactie ondanks de (kleine) afwijkingen van de "W"-geometrie. Ondanks dat gebrugde intermediairen belangrijk zijn in de waargenomen reactiepaden, spelen ze een ondergeschikte rol in de reactiviteit van dit soort verbindingen.

De O-gesilyleerde mesylaten **106** en **107** reageren snel na behandeling met TBAF in refluxende benzeen (hoofdstuk 3). Bij kamertemperatuur vindt alleen desilylering plaats. Om de invloed van een "verre" mesylaatgroep op de desilyleringssnelheid te onderzoeken zijn, behalve **106** en **107**, ook de O-gesilyleerde verbindingen **127–131** gesynthetiseerd en behandeld met TBAF. Dit wordt beschreven in hoofdstuk 7. De desilyleringssnelheden zijn eenvoudig bepaald door het verdwijnen van het uitgangsmateriaal te volgen met behulp van HPLC. De desilyleringssnelheid van de verbindingen met een mesylaatgroep is veel hoger dan de desilyleringssnelheid van de corresponderende verbindingen met een hydroxylgroep (**130** en **131**). Bovendien reageren de verbindingen met een "W"-geometrie (**107** en **129**) van de tussenliggende σ-bindingen sneller dan de "sickle"-geometrie analoga (**106, 127,** en **128**). De resultaten die gepresenteerd worden in dit hoofdstuk laten duidelijk zien dat electronische effecten van verre substituenten een substantiële invloed kunnen uitoefenen op de reactiviteit van andere substituenten.

Concluderend kan gezegd worden dat het TBI-concept goed de reactiviteit van de verbindingen, die in dit proefschrift bestudeerd zijn, verklaart. De stereochemische en stereoelectronische voorwaarden voor de base-geïnduceerde reacties van perhydronaftaleen-1,4-diol monosulfonaatesters zijn nu vastgesteld. Bovendien is de algemene bruikbaarheid van σ-delocalisatie en TBI in "alledaagse" chemie aangetoond.

Curriculum Vitae

Romano Vincenzo Antonio Orrū werd op 5 februari 1965 geboren te Heerlen als zoon van een Italiaanse mijnwerker en zijn Brabantse vrouw. In 1982 behaalde hij het diploma HAVO aan de R.K. School voor HAVO van het Coriovallum College te Heerlen. Twee jaar later behaalde hij het diploma Atheneum-B aan het R.K. Atheneum van hetzelfde college. Vanaf 1984 volgde hij de studie Moleculaire Wetenschappen aan de Landbouwuniversiteit te Wageningen. Afstudeervakken heeft hij verricht bij de werkgroep Analytische Chemie (dr. S. M. van der Kerk) en voor de vakgroep Organische Chemie (dr. J. B. P. A. Wijnberg) te Wageningen. De stageperiode werd doorgebracht bij het spectroscopisch laboratorium van de afdeling analytische chemie (dr. J.-R. Mellema) en bij de computational medicinal chemistry groep (dr. J. M. L. Pieters) van Organon te Oss. In maart 1990 werd het doctoraalexamen Moleculaire Wetenschappen, chemische- en fysisch-chemische oriëntatie, afgelegd. Van 1 februari 1990 tot 1 februari 1994 was hij als Onderzoeker In Opleiding verbonden aan de vakgroep Organische Chemie van de Landbouwuniversiteit Wageningen. Daar werd het in dit proefschrift beschreven onderzoek verricht onder leiding van dr. J. B. P. A. Wijnberg en prof. dr. Ae. de Groot.

Aantekeningen: